Synthesis and Evaluation of Specially Designed Polymeric Materials for the Removal of Metals and Metalloids in Low Level Concentrations

By

Abdul Nishad P
(CHEM01201004021)

BHABHA ATOMIC RESEARCH CENTRE

A thesis submitted to the
Board of Studies in Chemical Sciences

In partial fulfillment of requirements
for the Degree of
DOCTOR OF PHILOSOPHY
of

HOMI BHABHA NATIONAL INSTITUTE

August, 2016

Homi Bhabha National Institute

Recommendations of the Viva Voce Committee

As members of the Viva Voce Committee, we certify that we have read the dissertation prepared by ***Abdul Nishad P***, entitled ***'Synthesis and Evaluation of Specially Designed Polymeric Materials for the Removal of Metals and Metalloids in Low Level Concentrations'*** and recommend that it may be accepted as fulfilling the thesis requirement for the award of Degree of Doctor of Philosophy.

Chairman - Dr. S. Anthonysamy S. Anthonysamy **Date:** 17/3/17

Guide / Convener - Dr. S. Velmurugan **Date:** 17/03/17

Examiner - Dr. C.T. Aravindakumar **Date:** 17.3.2017

Member 1- Dr. N. Sivaraman N. Sivaraman **Date:** 17/3/2017

Member 2- Dr. S. Rangarajan **Date:** 17/3/2017

Member 3- Dr. M. P. Srinivasan M.P. Srinivasan **Date:** 17/3/2017

Final approval and acceptance of this thesis is contingent upon the candidate's submission of the final copies of the thesis to HBNI.

I/We hereby certify that I/we have read this thesis prepared under my/our direction and recommend that it may be accepted as fulfilling the thesis requirement.

Date: 17/03/2017

Place: Kalpakkam

Guide

STATEMENT BY AUTHOR

This dissertation has been submitted in partial fulfillment of requirements for an advanced degree at Homi Bhabha National Institute (HBNI) and is deposited in the Library to be made available to borrowers under rules of the HBNI.

Brief quotations from this dissertation are allowable without special permission, provided that accurate acknowledgement of source is made. Requests for permission for extended quotation from or reproduction of this manuscript in whole or in part may be granted by the Competent Authority of HBNI when in his or her judgment the proposed use of the material is in the interests of scholarship. In all other instances, however, permission must be obtained from the author.

(Abdul Nishad P)

DECLARATION

I, hereby declare that the investigation presented in the thesis has been carried out by me. The work is original and has not been submitted earlier as a whole or in part for a degree / diploma at this or any other Institution / University.

(Abdul Nishad P)

List of Publications Arising From the Thesis

Journal

1. Removal of Antimony over Nano Titania Impregnated – Epichlorohydrin Crosslinked Chitosan Beads from a Typical Decontamination Formulation, Padala Abdul Nishad, Anupkumar Bhaskarapillai, Sankaralingam Velmurugan, ***Nuclear Technology***, 197 (2017) 88-98
2. Towards finding an efficient sorbent for antimony: Comparative investigations on antimony removal properties of potential antimony sorbents, Padala Abdul Nishad, Anupkumar Bhaskarapillai, Sankaralingam Velmurugan, ***International Journal of Environmental Science and Technology*** (2016). doi:10.1007/s13762-016-1181-2
3. Nano-titania-crosslinked chitosan composite as a superior sorbent for antimony (III) and (V), Padala Abdul Nishad, Anupkumar Bhaskarapillai, Sankaralingam Velmurugan, ***Carbohydrate Polymers*** 108 (2014) 169–175
4. Cobalt (II) imprinted chitosan for selective removal of cobalt during nuclear reactor decontamination, Padala Abdul Nishad, Anupkumar Bhaskarapillai, Sankaralingam Velmurugan, Sevilimedu Veeravalli Narasimhan, ***Carbohydrate Polymers*** 87 (2012) 2690– 2696
5. Sorption behaviour of Co(II) and Cu(II) on chitosan in presence of nitrilotriacetic acid, Abdul Nishad Padala, Anupkumar Bhaskarapillai, Sankaralingam Velmurugan, Sevilimedu V. Narasimhan, ***Journal of Hazardous Materials*** 191 (2011) 110–117
6. Enhancing the sorption properties of nano titania-chitosan beads using epichlorohydrin as the crosslinker, Padala Abdul Nishad, Anupkumar Bhaskarapillai, Sankaralingam Velmurugan, ***Journal of Hazardous Materials*** *(Under Revision)*

International Conference/Symposium

1. Evaluation of the Suitability of a Titania - Biosorbent Composite for Use in Nuclear Reactor Decontaminations as Antimony Removal Agent, Padala Abdul Nishad, Anupkumar Bhaskarapillai, Sankaralingam Velmurugan*, 20th NPC International Conference (**NPC2016**), Brighton, United Kingdom - October 2-7, 2016 (Poster Presentation)

2. Antimony sorption properties of chitosan – nano TiO_2 composite beads, Padala Abdul Nishad*, Anupkumar Bhaskarapillai, Sankaralingam Velmurugan, Symposium on Water Chemistry and Corrosion in Nuclear Power Plants in Asia – 2015 (**AWC2015**), September 2 to 4, 2015, Anupuram, India (Poster Presentation).
3. Sorbents For Effective Removal Of Radioactive Antimony During Chemical Decontamination, Padala Abdul Nishad*, Anupkumar Bhaskarapillai, Sankaralingam Velmurugan, Nuclear Plant Chemistry Conference 2016 (**NPC2014**), October 26 to 31, 2014, Sapporo, Japan (Oral Presentation)
4. Experience Of Antimony Activity Deposition During Chemical Decontamination Of PHWRs And The Work To Mitigate The Deposition, Vinit Kumar Mittal, Santanu Bera, Abdul Nishad, Anupkumar Bhaskarapillai, S. V. Narasimhan and S. Velmurugan*, Water Chemistry and Corrosion in Nuclear Power Plants in Asia (**AWC2013**), October 14 to 17, 2013, Taichung, Taiwan (Oral Presentation)
5. Cobalt(II) Ion Imprinted Chitosan: Towards The Selective Removal Of Radiocobalt In Nuclear Industry; P. Abdul Nishad*, B. Anupkumar, S. Velmurugan and S.V. Narasimhan; **MACRO2010**, Frontiers of Polymers & Advanced Materials, December 15 to 17, 2010, New Delhi, India (Oral Presentation)

(Abdul Nishad P)

Dedicated to my teachers…

ACKNOWLEDGEMENTS

Apart from my efforts, this research work would not have been complete without the kind support and help of many people. I would like to extend my sincere thanks to all of them.

Firstly, I would like to express my sincere gratitude to my research guide Prof. S. Velmurugan for his constant supervision, continuous support, and motivation. His guidance helped me in all the time of this research work and writing of the thesis.

Besides my advisor, I would like to thank Prof. S. Anthonysamy (Chairman, Doctoral committee), Prof. N. Sivaraman, Dr. S. Rangarajan, and Dr. M.P. Srinivasan (Members, Doctoral committee) for their insightful comments, encouragement and valuable inputs which incented me to widen my research from various perspectives. I thank Dr. K.V.G Kutty (Ex-Chairman, Doctoral committee) for his valuable comments and support.

I am highly indebted to Dr. S.V. Narasimhan (Ex-Head, WSCD and Ex-member, Doctoral committee) for his kind support and granting me the permission to do P.hD.

I would like to place on record my special thanks to Dr. B. Anupkumar, for his constructive discussions, encouragements and critical review of the data and results embodied in this thesis. Without his guidance and persistent help this dissertation would not have been possible.

I would like to thank Dr. T.V.K. Mohan, Dr. V.P. Venugopal, Mr. Sinu Chandran, Dr. P. Chandrmohan, Mr V.S. Sathysheelan, Dr. V.K. Mittal, Mr. T. Saravanan, Dr. A.L. Rufus, Dr. H. Subramanian, Mr. Jayaram, Dr. Rajeshkumar, Dr. Hiren Joshi, Dr. Rachna, Ms. Padma S. Kumar, Dr. Puspalatha, Mr. P.J. George, Mr. A.C. Joshi and all other WSCD colleagues for their helps and support.

I would like to thank Dr. R. Venkata Krishnan, Mr. Madhavan, Dr. H. Seshadri for their helps and support.

I thank my friends Sudhir, Kiran, Nidhi, Debasis and Francis for the stimulating discussions and for all the fun we had during the research period.

I must thank my friends Jovin, Anuraj, Sabeena, Krishna Chandran, Anees, Illyas, Athira and all others for their care and affection that they showed to me.

I can't forget my wife Sarjil, my parents, all my teachers and well-wishers, who made me this achievement a possible, at this occasion and express my sincere gratitude for all of them.

Finally I thank the God almighty, most Gracious, most Compassionate.

CONTENTS

CONTENTS IN DETAIL

SYNOPSIS

I. Aim and Scope of the Work

Selective removal of metal ions is of economic and strategic importance to a large number of industries. Especially in nuclear industry, selective removal of the radioactive ions can lead to a large reduction in the volume of radioactive waste generated during power generation. This will eventually lead to better economics and wider acceptability of nuclear power. R& D on such types of selective materials are of importance and have gained wider attraction. Possibilities and economics of using such types of selective materials in nuclear industry have been reported and discussed elsewhere [1, 2].

Nuclear plant operators' worldwide aim towards reduced radiation field around the out of core surfaces of nuclear reactors to achieve reduced MAN-REM. Formation and deposition of the activated corrosion products is responsible for the radiation build up. The reduction of radiation field around the out of core surfaces is achieved through combination of preventive methods such as inhibiting the deposition of active ions over the out of core surfaces (through strict chemistry control) and cleaning protocols that involve the removal of already deposited activities through decontamination procedures. Dilute chemical decontamination (DCD) is one of the most successful and well accepted methods for the full system/component decontamination of the nuclear structural materials, especially under online conditions [3]. DCD campaigns on many Indian Pressurized Heavy Water Reactors (PHWRs) were successfully carried out using NAC formulation containing Nitrilotriacetic acid (NTA), Ascorbic acid and Citric acid [4]. The chemical formulation, when circulated through the coolant circuit, will dissolve the oxide layer present inside the coolant system surfaces along with the deposited activities, which are subsequently trapped in ion exchange columns. The process is carried out in a regenerative mode until the desired reduction in radiation field is obtained.

The plant data on various DCD campaigns showed ^{60}Co (whose physical quantity is at ppb or sub ppb level, but activity is in the order of curies) as the major contributor to the radionuclide inventory and the non-active iron (about 200 kg) as the major metal ion removed over the IX columns. A total quantity of about 6 to 7 Tons of IX resin is used in a typical decontamination campaign, and the radioactive ions are spread through all of these resin beds [4]. So, the selective removal of radioactive cobalt over special selective columns can reduce the active waste volume generated considerably due to the reduced physical quantity of the active ions. Such type of a Co(II) selective resin containing vinyl benzyl imino diacetic acid functional monomers, synthesized through metal ion imprinting technique and its demonstration under DCD conditions with complete exclusion of Fe(II) had been reported [2]. However, there are growing concerns about storage/disposal of organic resins used in nuclear reactors. Decomposability of sorbents, post-stripping of active ions, can play a major role in making the process more environmental friendly. Use of bio-degradable sorbents thus becomes a better option if they can match the sorption properties of the organic resins. Because of its natural abundance, versatility and high sorption capacities; chitosan and its derivatives have gained wide attention as effective biosorbents for the removal of various metal ions, including radioactive metal ions such as uranium [5,6]. Chitosan's resistance to radiolysis, and its applicability in the nuclear field, also has been investigated as early as in 1972 [7]. There are reports on the use of chitosan as a functional monomer in metal ion imprinting as well [8]. Presence of a large number of functional groups such as –NH_2 and –OH groups makes it a versatile material for ion imprinting. One of the objectives of this study is to modify the sorption properties of the biosorbent chitosan, through metal ion imprinting procedures, in order to make it suitable for the nuclear industry applications that demand selective sorption of Co(II) in presence of large excess Fe(II) under complexing conditions.

Some of the recent DCD campaigns of Indian PHWRs showed an increase in the radiation field on certain components around the out of core surfaces after the DCD process. This was attributed to the presence of active isotopes of antimony, which are released from the core into the coolant during shutdown and deposit on to the out of core surfaces without being removed over the cation resin bed during DCD [4, 9]. To circumvent this problem, either we should suppress the antimony deposition over the out of core surfaces during DCD using inhibitors or it has to be removed during (or prior to) decontamination using modified processes/sorbents. The low affinity of anion exchange resins for antimony, used during the H_2O_2 process applied for its prior removal, necessitates the use of a large quantity of the resin. Typically, to remove about 10 g of antimony it needs about 2 m^3 of the resin [10]. Thus, there exists a need for better antimony removing materials for use in the H_2O_2 process as well. Further, in the case of PHWRs, there is a scope for using such antimony selective materials that can be used during DCD campaigns without affecting the system chemistry.

The second objective of this study; finding better antimony sorbents, was primarily based on this aspect. Removal of antimony, considered to be an emerging contaminant in the ground waters, is of importance to the general drinking water treatment processes as well [11]. Sorbents developed for removing antimony may work well for arsenic as well. As it is considered to be a prominent ground water contaminant and considering the need for better arsenic removing materials, arsenic removal by the synthesized sorbents were also investigated.

II. Organisation of the Thesis

Chapter 1. Introduction

A general introduction to the topic is given in this chapter. Importance of operational water chemistry, formation and deposition of activated corrosion products, radiation field buildup around the out of core surfaces of nuclear reactors and decontamination of these surfaces using chemical formulations are detailed. Importance of IX columns used during DCD and the possibilities of improvement through the use of selective materials are discussed. Biosorbent chitosan and the metal ion imprinted polymers are introduced. Current status on the metal ion imprinting over chitosan was discussed with special reference to metal ions relevant to nuclear industry. The general properties, formation of activated corrosion products and removal strategies for the metal ions of interest, Cobalt and Antimony are also discussed.

Chapter 2. Experimental Details

Description of the general chemicals, procedures followed and details of the instruments utilized for the studies are given in this chapter. Procedures followed for the synthesis of Co(II)-ion imprinted chitosan and Nano TiO_2 impregnated epichlorohydrin crosslinked chitosan beads are detailed. Details on the sorption studies carried out under batch or column mode of operations, kinetic and equilibrium modeling of the sorption processes using general models reported in the literature are also described.

Chapter 3. Sorption Behavior of Chitosan

Studies on the removal of metal ions by chitosan, in presence of complexing agents used during dilute chemical decontamination campaigns, is limited. Investigations on the sorption of metal-ions along with complexants can give indications about the speciation and mechanisms involved in the metal ion sorption by chitosan from complexing media.

Removal of Co(II) by chitosan from Co(II)-NTA solutions, as NTA being a major component in the DCD formulation, is discussed in this chapter. Since most of the reported studies regarding the sorption of metal-ions by chitosan in presence of complexing agents were done with Cu(II) [12], sorption characteristics of Cu(II)-NTA over chitosan was also studied for comparison. Sorption of free and complexed metal ions, Co(II) and Cu(II) in presence and absence of Nitrilotriacetic acid (NTA), on the biosorbent chitosan was studied. Possibilities on the selective sorption of either of the metal-ions in the presence of the other have also been addressed. A detailed investigation on the role of pH on sorption of Co(II), Cu(II) and NTA was done. Significant change in selectivity of chitosan towards metal-ion uptake from NTA medium was observed with respect to change in pH. At pH 2.9, the uptake of cobalt was found to be more than that of copper, while the selectivity was reversed at pH 6.0.

Chapter 4. Cobalt (II) – Ion Imprinted Chitosan for the Selective Removal of Cobalt during Nuclear Reactor Decontamination

Molecular/metal ion imprinting has been reported widely for synthesizing selective sorbents for various molecules and metal ions [13]. These are highly crosslinked polymers synthesized in presence of a chosen molecule or metal ion as the template. The template is subsequently removed to get the molecularly/metal ion imprinted polymer. Selectivity of the biosorbent chitosan has been modified through metal ion imprinting technique for its potential application in nuclear industry. Synthesis of a Co(II) imprinted chitosan using epichlorohydrin as the crosslinker and evaluation of its sorption properties vis a vis to those of non-imprinted and raw chitosan have been reported in this chapter. The selective removal of Co(II) in presence of Fe(II), which is the major non-radioactive ion present in excess during decontamination, was studied. A reversal in selectivity was achieved through metal ion imprinting. The imprinted chitosan showed selective sorption of Co(II) over Fe(II), while the raw chitosan was selective to Fe(II) over Co(II). The retention of cobalt selectivity even from solutions having very low concentration of Co, and in presence of large excess of Fe(II), make the MIP as a promising sorbent to use in nuclear related applications.

Chapter 5. Removal of Antimony by Nano TiO_2 Impregnated-Epichlorohydrin Crosslinked Chitosan (TA-Cts) Beads and Other Potential Antimony Sorbents

Removal of antimony is a challenging task due to its presence in multi oxidation states under solution conditions and the low concentrations in which it is to be removed [14]. This chapter deals with the studies carried out in this regard. This chapter includes three sections. In the first section, sorption profiles and the sorption mechanisms associated with the removal of antimony in its two oxidation states (+3 and +5) have been investigated in detail through batch studies involving titania sorbents (RADEX® Sb-1000, nano TiO_2– special grade and AEROXIDE® TiO_2 P 25), a strong base anion resin (TULSION® A-33), a chelating resin (Amberlite® IRC-718), and a biosorbent (Chitosan). Significant sorption and associated change in solution pH were observed with all the sorbents, which revealed the nature of respective sorption equilibrium involved. The results have shown that Sb(V) is removed as its anionic species, while Sb(III) is removed either as an anionic species or as a cationic species according to the solution conditions and functional groups present in the sorbent. Among the six sorbents studied, titania based materials are seen to be more promising for antimony removal when both Sb(V) and Sb(III) are present in the solution, while anion resin was found to be better as a column material at relatively wider pH range for removal of antimony present as Sb(V).

In the second section; the excellent antimony sorption properties of titania based materials, reported in the previous section, were made useful in targeting large scale applications by synthesising a robust high performing sorbent for antimony, in the form of stable beads, using nano-TiO_2 and chitosan. The beads were characterized and studied for its antimony sorption properties. TA-Cts beads showed sorption characteristics similar to its parent compound nano titania in terms of uptake capacity and equilibrium pH of sorption, while the format was more suitable for column application unlike the parent nano-TiO_2. The sorbent exhibited complete sorption of antimony from aqueous solutions with antimony concentrations ranging from as low as 150 ppb to as high as 120 ppm. TA-Cts beads were shown to be stable and suitable for column mode operation.

In the third section; effect of composition on the physical and sorption properties of the TA-Cts beads was studied in detail. For this; TA-Cts beads having different ratio of nano TiO_2 and chitosan have been prepared and their solution and sorption properties were evaluated. Also, the effect of the crosslinker concentration, used during the synthesis, on the swelling and sorption properties of the Nano TiO_2-chitosan and Chitosan beads were also investigated in detail. Both swelling and antimony uptakes of the composite beads were found to decrease with increase in nano TiO_2 content (or decrease in chitosan content). The crosslinker, epichlorohydrin added was found to effect significant changes in physical and sorption properties of both the composite and chitosan beads. Antimony sorption was found to increase with increase in crosslinker amount added.

Chapter 6. Investigation on the Suitability of TA-Cts Beads for Antimony Removal during Nuclear Reactor Decontamination

Detailed studies on the radiation stability of the TA-Cts beads, its selectivity for other ions under NAC formulation conditions and the removal of antimony from typical DCD conditions, under batch and column conditions, over the TA-Cts beads had been reported in this chapter. Irradiation stability of the TA-Cts beads was studied up to a gamma dose of 50 kGy and compared with Tulsion® A33, the commercially used nuclear grade anion resin. Column performance of the TA-Cts beads, for removing antimony in presence of large excess of iron, was studied. Uptake of antimony, iron and NAC formulation over the TA-Cts beads were monitored under batch and column mode of operations. High antimony uptake, favorable selectivity and radiation stability that is comparable to that of commercial nuclear grade resins make the TA-Cts beads a potential antimony sorbent for the nuclear industry.

Chapter 7. Removal of Arsenic over the Nano TiO_2-Chitosan and Chitosan Beads

Arsenic contamination of ground water is a worldwide health problem and high Arsenic groundwater areas have been identified in all around the world [15]. Arsenic removal properties of the TA-Cts and the chitosan beads were studied and discussed in this chapter. Both chitosan and nano TiO_2-Chitosan beads were found to be effective in removal of As(V). TA-Cts beads were found to be the better option for complete removal of As(V) in comparison to crosslinked chitosan beads. The complete removal of As(V) even at an equilibrium pH conditions of 6.1 by the more titania containing beads project it an ideal solution for treating the ground water antimony contamination.

Chapter 8. Conclusions and Future Directions

A brief summary of the results and conclusions drawn based on the results and observations mentioned in the preceding chapters is presented in this chapter. Scope for future work in this area of research is also given.

III. Salient Findings and Conclusion

The study reveals the complexities involved and the possibilities in the removal of cobalt and antimony during dilute chemical decontaminations. The biosorbent chitosan, due to its ability to remove both metal ions and complexing agents, can act as a mixed bed resin. Selective removal of Co(II) by chitosan is possible through metal ion imprinting and by the careful selection of solution conditions. Nano titania based materials have good potential as antimony sorbents. It is possible to combine nano TiO_2 with chitosan without compromising on the former's sorption properties and with the added advantages of obtaining the sorbent in a format suitable for large scale column applications. Nano TiO_2 impregnated-epichlorohydrin crosslinked chitosan beads can be used for removing antimony during nuclear reactor decontaminations. The composition and the cross linker amount added play an important role in deciding the physical and sorption properties of the composite beads. The Nano TiO_2 – chitosan beads have good potential in general drinking water treatment processes as well due to its favourable arsenic sorption properties.

IV. References

1 P.-L. Frattini, D.-M. Wells, S.-E. Garcia, K. Richard, R. Asay, L. Yengoyan, *NPC 2012: Nuclear Plant Chemistry Conference, International Conference on Water Chemistry of Nuclear Reactor Systems*, France, **2012**.

2 A. Bhaskarapillai, N.V. Sevilimedu, B.r. Sellergren, *Industrial & Engineering Chemistry Research* 48 (2009) 3730.

3 H. Ocken, EPRI, Palo Alto, CA, TR-112352, **July 1999**.

4 S. Velmurugan, A.L. Rufus, V.S. Sathyaseelan, V.K. Mittal, S. Veena, S.V. Narasimhan, *Energy Procedia* 7 (**2011**) 645.

5 R.A.A. Muzzarelli, Carbohydrate Polymers 84 (**2011**) 54.

6 A.J. Varma, S.V. Deshpande, J.F. Kennedy, *Carbohydrate Polymer*s 55 (**2004**) 77.

7 R.A.A. Muzzarelli, O. Tubertini, *Journal of Radioanalytical Chemistry* 12 (**1972**) 431.

8 A.-H. Chen, C.-Y. Yang, C.-Y. Chen, C.-Y. Chen, C.-W. Chen, *Journal of Hazardous Materials* 163 (**2009**) 1068.

9 B.S. Tomar, S. Kumar, T.P. Chaturvedi, V.K. Manchanda, *IANCAS Bulletin* Vol. VII. No.2 (**2008**) 138.

10 D.G. Miller, D.A.Guzonas, R. Laporte, T.A. Dereski, R.A. Speranzini, *(AECL-11852, COG-97-472-I)*, AECL, Chalk River, Ontario, Canada, **1997**.

11 S.D. Richardson, T.A. Ternes, *Analytical Chemistry* 86 (**2014**) 2813.

12 R.-S. Juang, F.-C. Wu, R.-L. Tseng, *Water Research* 33 (**1999**) 2403.

13 B. Sellergren, *Molecularly Imprinted Polymers: Man-Made Mimics of Antibodies and their Application in Analytical Chemistry*, Elsevier Science, **2000**.

14 M. Filella, N. Belzile, Y.-W. Chen, *Earth-Science Reviews* 57 (**2002**) 125.

15 P.L. Smedley, D.G. Kinniburgh, *Applied Geochemistry* 17 (**2002**) 517.

LIST OF FIGURES

LIST OF TABLES

LIST OF ABBREVIATIONS AND SYMBOLS

µ	Micro
AIBN	Azobisisobutyronitrile
ALARA	As Low As Reasonably Achievable
AR	Analytical Reagent
BDL	Below Detectable Limit
C_0	Initial concentration
C_e	Equilibrium concentration
Cts-Epi	Epichlorohydrin crosslinked Chitosan
D	True swollen density or Specific gravity of swollen beads
DCD	Dilute Chemical Decontamination
DDW	Double Distilled Water
EAC	EDTA-Ascorbic acid-Citric acid
EC	Electron Capture
EDTA	Ethylenediaminetetraacetic acid
EGDMA	Ethylene glycol dimethacrylate
EPRI	Electric Power Research Institute
ESR	Equilibrium Swelling Ratio
EWC	Equilibrium Water Content
F_3O_4	Magnetite
FBR	Fast Breeder Reactor
GR	Guaranteed Reagent
ICP-AES	Inductively Coupled Plasma-Atomic Emission Spectrometer
IF	Imprinting Factor
IPN	Interpenetrating Polymer Network
KAPS	Kakrapar Atomic Power Station
K_D	Distribution Constant

MIP	Metal ion imprinted Polymer
MWe	Megawatt electric
NAC	NTA-Ascorbic acid-Citric acid
NAPS	Narora Atomic Power Station
NIP	Non Imprinted Polymer
NTA	Nitrilotriacetic acid
PHT	Primary Heat Transport
PHWR	Pressurised Heavy Water Reactor
ppb	Parts Per Billion
ppm	Parts per million
PWR	Pressurised Water Reactor
pZc	Point of Zero Charge
q_e	Uptake Capacity at equilibrium
q_t	Uptake Capacity at time t
$t_{1/2}$	Half-life
TA-Cts or TA-Cts-Epi	Nano Titania Impregnated-Epichlorohydrin Crosslinked Chitosan
TTPL	Travancore Titanium Products Limited
UPW	Ultra-Pure Water
V/V	Volume by Volume
VVER	Vodo-Vodyanoi Energetichesky Reaktor
W/W	Weight by Weight
WHO	World Health Organization
β	Beta
γ	Gamma

Chapter 1. INTRODUCTION

1.1 Nuclear Energy in India

Nuclear energy plays significant role in the development of the nation. Nuclear energy contributes to about 2% of the all India installed capacity (in MW) of power stations and a many fold increase in contribution of nuclear energy towards the supplied electrical energy by 2050 is expected. India has a three stage nuclear energy programme. In the first stage, natural uranium fuelled Pressurised Heavy Water Reactors (PHWR) generate electricity, and also produces plutonium-239 as a by-product. The second stage reactors are Fast Breeder Reactors (FBR) which use a mixed oxide fuel containing plutonium-239. FBR breed Pu-239 (from U-238) and U-233 (from the thorium blanket provided in the reactors). The Third stage aims to use the U-233 produced by the FBRs as the fuel for power generation. The three stage programme has been envisaged to attain self-sustainability in fissile nuclear fuel using the abundant thorium reserves of India. As of now, 18 PHWRs (540 MWe X 2, 220 MWe X 14, 200 MWe X 1, 100 MWe X 1), two BWRs (Boiling Water Reactors, 160 MWe X 2) and two VVER (Vodo-Vodyanoi Energetichesky Reaktor-Pressurised Water Reactor (PWR), 1000 MWe X 2) are in operation. Four PHWRs (700 MWe X 4) plus one second stage FBR (500 MWe) are under construction. PHWRs form the main stay of Indian nuclear energy power programme. These are horizontal pressure tube type reactors which use natural uranium as the fuel, and heavy water (D_2O) as the coolant and moderator.

1.2 Role of Chemistry in Nuclear Technology

Chemistry plays a pivotal role in nuclear industry; starting from the fuel fabrication (mining and extraction) to post treatment (reprocessing and waste management of the spent fuels) through operation of the nuclear power plants. Chemistry in the operation of nuclear power plants mainly deals with the reactor water chemistry of different cooling systems. Corrosion of the structural materials is one of the major issues faced by all types of power reactors including thermal powered ones. Optimum reactor water chemistry targets:

(i) Decreased corrosion (structural material integrity and plant life extension)
(ii) Minimum corrosion product deposits over pressure tubes and other surfaces (heat transfer efficiency and fuel integrity)
(iii) Minimum radiation field around the out of core surfaces (Nuclear reactor specific issue)

Unlike thermal power plants; nuclear powered ones have an additional risk in terms of radiation exposure. Hence, operational water chemistry becomes more important in the case of nuclear powered reactors for reducing the corrosion as well as radiation field. Safe operation and plant life extension necessitates strict chemistry control of the various heat transport systems of the power plants. In total, reactor water chemistry programmes gives information and provides support in;

(i) Reactivity control of the reactors
(ii) Ensuring and protecting the integrity of the materials and fuel used in the reactors
(iii) Reducing the hazardous radiation exposure to the occupational workers and
(iv) Reducing or minimizing the amount of hazardous waste generated during the operation

The major structural materials used in the Primary Heat Transport (PHT) systems of PHWRs [1] are;

(i) Carbon steel as the feeders and headers of the primary coolant system

(ii) Incoloy-800 (alloy containing 30 - 35% Ni, 19 - 23% Cr, 0.10% C (max.), 0.15 – 0.60% Al, 0.15 – 0.60% Ti, and remaining Fe (39.5% min.)) or Monel-400 (alloy containing 28 – 34% Cu, 2.0% Mn (max.), 2.5% Fe (max.), 0.3% C (max.), 0.5% Si (max.), 0.024% S (max.), and remaining Ni (63.0% min.)) as steam generator tubing and

(iii) Zr-Nb alloy (2.4 - 2.8% Nb, 1200 -1400 ppm O, 100 ppm Hf, and rest of Zr) or Zircaloy-2 (contain 1.2-1.7% - Sn, 0.07 - 0.2% Fe, 0.05 - 0.15% Cr, 0.03 – 0.08% Ni, 1200-1400 ppm O, 100 ppm Hf, and rest of Zr) as the pressure tube and fuel clad materials

Heavy water is used as the primary coolant and moderator. The heavy water primary coolant was maintained at an apparent pH of 10 - 10.5 with LiOH and a hydrogen concentration of 3-10 ml/kg with hydrogen gas injection. The temperature of the primary coolant ranges from 249 - 293 ^{O}C with a pressure as high as 8.5 MPa. The high temperature coolant interaction with the structural material leads to the corrosion of these structural materials. Corrosion and deposition of these corrosion products of the structural materials leads to the formation of oxide layers like Fe_3O_4, Nickel Ferrites or Chromites, ZrO_2 etc., on their surfaces. Normally two types of oxide layers were observed, one adherent inner layer next to the base metal formed *in-situ* by the corrosion of the base metal by high temperature coolant interactions and a loose outer layer formed by the precipitation and deposition of the dissolved metals and crud particles present in the recirculating water. In the case of PHWRs, a protective magnetite (Fe_3O_4) layer is formed over the carbon steel surfaces through the hot conditioning process [2].

1.3 Activated Corrosion Products and Radiation Field Build Up

Structural materials on interaction with the coolant at high temperature undergo corrosion leading to the formation of metal hydroxide/oxy-hydroxide/oxide corrosion products. They may remain in dissolved or in suspended particulate form, of sub-micron size, in the coolant system until it gets deposited back on the system surfaces or removed by purification systems. These corrosion products get activated by the neutron flux when they pass through the core. Presence of atoms/ions with high neutron capture cross-sections like ^{59}Co, ^{58}Fe, ^{123}Sb aggravates this problem. These atoms either come as constituents in the alloys or as an impurity in the materials used. The major activated corrosion products found in the PHT system of reactors along with their formation, decay half-lives and gamma energies are given in Table 1.1. These activated corrosion products remain trapped on the oxide layer lattices. With their fairly long half-lives and gamma ray activity, they increase the radiation field around the out of core surfaces and contribute significantly to the absorbed radiation dose of the working personnel.

Table 1.1. Major activated corrosion products found in primary coolant circuits of NPPs

Formation	Half life	Gamma energy (MeV)
^{59}Co (n,γ) ^{60}Co	5.3 years	1.17 & 1.33
^{58}Fe (n, γ) ^{59}Fe	44.5 days	1.10 & 1.29
^{54}Fe (n,p) ^{54}Mn	312 days	0.83
^{50}Cr (n, γ) ^{51}Cr	27.7 days	0.32
^{58}Ni (n,p) ^{58}Co	70.9 days	0.81
^{123}Sb (n, γ) ^{124}Sb	60 days	0.60 & 1.69

1.4 Decontamination of Deposited Activities

Any unwanted radioactivity on a surface is called as a contamination and the process which removes and transfers this activity to a place where it can be contained/controlled is termed as decontamination. Decontaminations are carried out to reduce/minimise the radiation field and for the practice of ALARA (As Low As Reasonably Achievable). ALARA guideline is practiced to minimise the dose received by the working personnel after taking care of the operational and economic constraints into account.

Decontamination can be of mechanical, electrical or chemical methods. Electrical may be of electropolishing (anodic) or electrolytic cleaning (cathodic) types [3]. Mechanical includes processes such as scrubbing (using brushes or even a grit) and washing (with an air or water jet) etc. Chemical decontamination utilises certain chemical formulations that can dissolve and keep these activities in solution till their removal over ion exchange columns. Full system decontaminations were generally obtained using chemical means. Major advantage is that; the process (or formulation) can be applied as ex-situ (for smaller components) or as circulation in-situ (for internal surfaces of pipes and components). Formulation used may be concentrated (3-10%, mostly used while decommissioning of the NPPs) or diluted (less than 1%, used for routine decontaminations).

1.5 Dilute Chemical Decontamination (DCD)

In dilute chemical decontamination (DCD) campaigns; chemical formulations are circulated through the system to dissolve the surface oxide layers (*adherent protective inner layers*) present over the contaminated metal surfaces and thereby release the trapped radionuclides. These dissolved metals and radionuclides are removed over cation exchange resins, in a formulation regenerative mode, and the particulate materials are removed by filtration. The decontamination is terminated after valving out the cation bed and valving in the mixed bed. The normal reactor water chemistry is then restored. A schematic of the DCD process is given in Fig. 1.1.

A number of formulations, depending upon the type of the reactor and the surface oxide layer present, have been used for decontaminating different types of reactors all around the world [3]. Table 1.2 gives an account of the different chemical decontamination techniques along with the formulations utilised for the purpose.

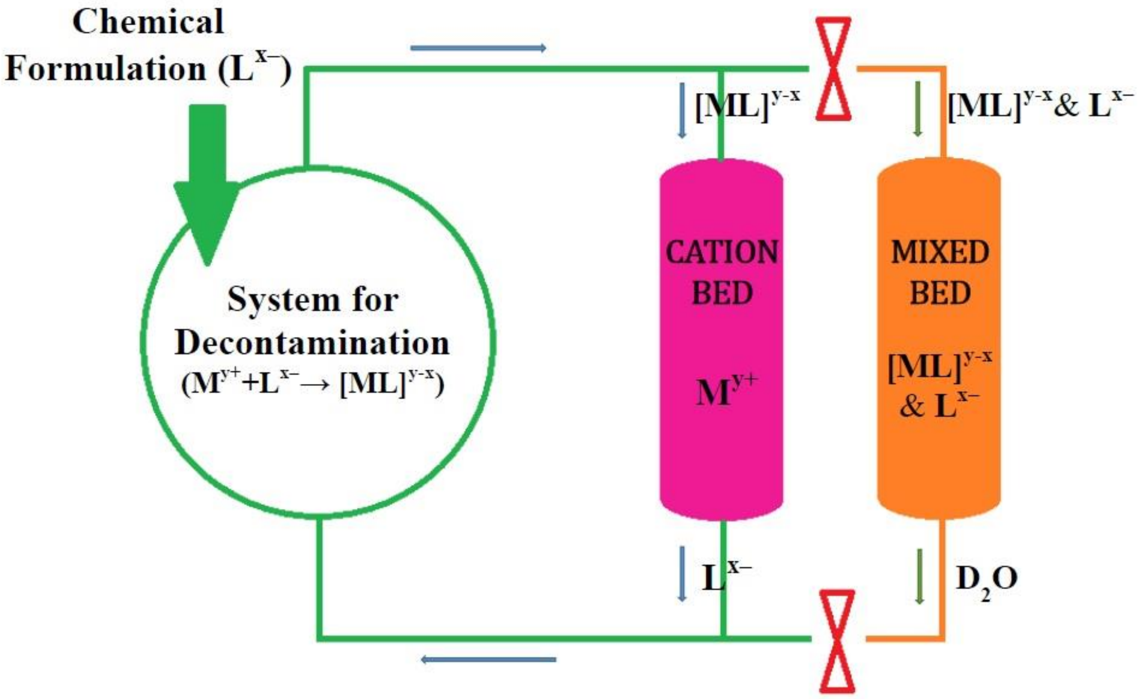

Figure 1.1. Schematic of the dilute chemical decontamination process

Table 1.2. Decontamination techniques and the chemical formulations used

Decontamination Technique	**Chemical Formulation**
CAN-DECON	Oxalic acid, Citric acid & EDTA
CAN-DEREM	Citric acid & EDTA
CITROX	Citric acid & Oxalic acid
Chemical Oxidation Reduction Decontamination (CORD)	Permanganic acid and Oxalic acid
Low Oxidation state Metal Ion (LOMI)	Vanadous formate and Sodium picolinate
EAC	EDTA, Ascorbic acid & Citric acid
NAC	NTA, Ascorbic acid & Citric acid

In Indian scenario, currently, a formulation containing Nitrilotriacetic acid (NTA)-Ascorbic acid-Citric acid combination (NAC) is used for the decontamination of the nuclear reactors (PHWRs). Strong acid cation resin (microporous) is used for the regeneration of the exhausted formulation and a mixed bed (containing strong base anion and strong base cation in 2:1 ratio) for the removal of the formulation along with the residual dissolved metals/complexes. The steps involved in the decontamination using NAC formulation are:

(i) Oxide dissolution: acid dissolution of the oxide aided by base metal or external reducing agents

$$Fe_3O_4 + 8\,H^+ + Fe\ (\text{or } 2e^-) \rightarrow 4\,Fe^{2+} + 4\,H_2O \qquad (1.1)$$

(ii) Complexation of the dissolved metal ions by the chelating agents

$$Fe^{2+} + NTA^{3-}\ (\text{or citrate}) \leftrightarrow [Fe\text{-}NTA]^- \qquad (1.2)$$

(iii) Regeneration of the formulation over cation exchange column

$$[Fe\text{-}NTA]^- + 2\,R\text{–}SO_3H \leftrightarrow (R\text{–}SO_3)_2Fe + NTA^{3-} + 2\,H^+ \qquad (1.3)$$

(iv) Removal of the formulation and metal complexes over the mixed bed (containing strong acid cation and strong base anion IX)

$$3\,R_4N^+OH^- + NTA^{3-} \leftrightarrow (R_4N)_3NTA + 3\,OH^- \qquad (1.4)$$

$$R_4N^+OH^- + [Fe\text{-}NTA]^- \leftrightarrow [R_4N^+(Fe\text{-}NTA)^-] + OH^- \qquad (1.5)$$

1.6 Need for the Specially Designed Materials for the Selective Removal of Radioactive Ions

The primary heat transport systems of Indian PHWRs were decontaminated eleven times using EAC or NAC formulations [4]. Decontamination factors ranging from 2 to 15 were obtained on different system surfaces. During decontamination campaigns typically 200 to 300 kg of iron along with 35 to 300 curies of total activity was removed from the systems and sorbed over the IX columns. About 7 m^3 of active solid waste in the form of spent ion exchange resins are generated during a typical decontamination campaign [4]. This active waste needs special treatment or waste disposal procedures. As far as the physical quantity is concerned; the non-active iron constitutes a major share of the total metal ions that are removed over these columns. But on the activity point of view; the major share comes from ions such as ^{60}Co, whose physical quantity is very less (ppb or sub ppb level) and is spread over the large volume of spent resins. So, selective removal of these active ions such as ^{60}Co, in presence of the large excess of non-active ions such as iron, can lead to a large reduction in the final active waste volume generated in each process. The active waste volume can be reduced considerably by using selective sorbents, which would enable segregation of active ions from the excess non-active ions [5]. Such segregation can make the decontamination process more economical and environment friendly. Moreover selective materials or processes can be used for effective decontamination of plant sites and the surrounding area during decommissioning under regular or accidental conditions. Table 1.3 gives a summary of the available/practiced separation techniques utilised for the purpose of removing general metal ions/pollutants from different streams.

1.7 Sorption and Ion Exchange Materials

Sorption was defined [6] as “the process by which a substance (sorbate) is sorbed (adsorbed or absorbed) on or in another substance (sorbent)”. It describes a process in which atoms, molecules or ions are getting attached or associated with a solid phase. Sorption comprises both absorption and adsorption. Absorption is a bulk (three dimensional) phenomena while adsorption is limited to the surface (two dimensional). Since a proper distinction between adsorption and absorption is not possible in most of the systems, especially in those involving natural systems, the term sorption is generally used. Sorption can include ion exchange process as well, where an ion is getting replaced for another during the process. Ion-exchange materials or resins can be considered as a special class of sorption materials by considering their vast range of availability and applicability. Sorption processes or ion-exchange processes have the advantage of direct utilisation of them in industrial applications without much operational difficulties.

Table 1.3. Separation techniques

Technique	Features
Precipitation	• Precipitating the metals as hydroxides or sulphides • Based on solubility product of the metal hydroxides/sulphides • Presence of complexing agents (e.g., EDTA) hinders precipitation
Adsorption	• Surface phenomenon • The intermolecular forces of attraction acting may be: (a) Physical - van der Waals' and electrostatic bonds, reversible and non-site specific interactions (b) Chemical – Ionic or covalent bonds, irreversible and site specific interactions
Coagulation and flocculation	• Mostly used in acidic drainage and high-density sludge treatments • Coagulation: Consolidation of smaller metal precipitate particles into larger metal precipitate particles (called flocs) – by using Al or Fe salts • Flocculants: Enhances the floc by making it heavier and more stable - by using mineral or synthetic type materials
Electrowinning	• Electrodeposition of metals from their solutions
Solvent extraction	• Based on solubility distribution between the aqueous and organic phases • Highly dependent upon parameters such as pH, nature of solvent, ratio of extractant to solvent, temperature
Membrane processes	• Use of a thin barrier capable of perm-selective mass transport • Based on particle size range and driving force it may be called as: microfiltration, ultrafiltration, nanofiltration, reverse osmosis and dialysis

Sorption processes may happen over a gaseous-solid interface; where a gas (sorbate) is sorbed over a solid (sorbent), or a liquid-solid interface; where a liquid (sorbate) is sorbed over a solid (sorbent). The intermolecular forces of attraction acting between the sorbent and the sorbate can be either weak as physical forces or involve formation of chemical bonding. Physical sorptions (or *physisorption*) occur through weak van der Waals' forces of attraction (such as dipole-dipole interactions, dispersion forces, induction forces etc.) and so the associated heat of sorption is generally below 50 kJ.mol^{-1}. While chemical sorption (or *chemisorption*) occur through ionic or chemical bonds and the associated heat of sorption is generally greater than 50 kJ.mol^{-1}.

There are broad varieties of sorption materials, and rich literature exists on the subject. A general classification of sorbent materials is of the natural or synthetic types (Fig. 1.2). Another classification of sorption materials may of the type of conventional and non-conventional sorbents [7]. Conventional materials include commercial activated carbons, organic ion exchange resins and commercial inorganic materials such as silica gel, activated alumina etc. Non-conventional sorbent materials includes sorbents derived from agricultural and industrial solid wastes (e.g., cotton waste, saw dust, fly ash etc.), natural inorganic materials (e.g., clays), natural or modified natural organic materials (e.g., cellulose and alginates), biosorbents (e.g., chitin and chitosan), and other sorbents like cyclodextrins, calixarenes, graphenes etc.

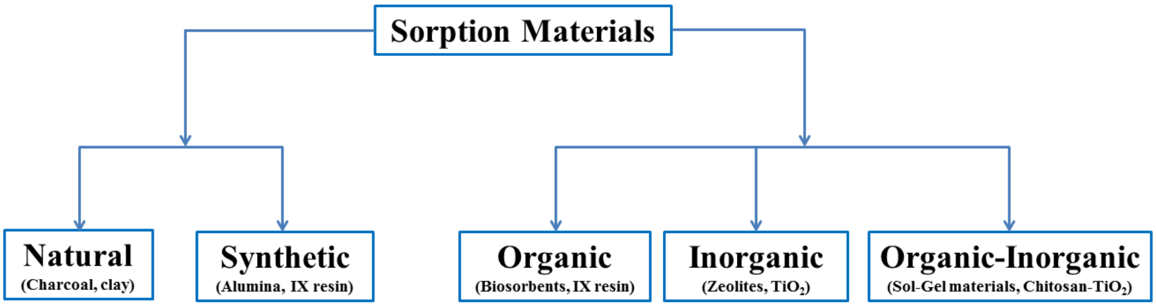

Figure 1.2. General classification of sorbents

1.8 Biosorbents

Biosorption can be defined as the passive, and metabolically-independent physico-chemical process by which certain materials of biological origin bind, and concentrate metal ions or organic compounds from aqueous solutions [8]. The binding may be through absorption, adsorption, ion exchange, surface complexation or precipitation. Bioaccumulation, a close analogue to biosorption, differs in the use of living biomass for the treatment (active and metabolically dependent) and the intracellular accumulation of the pollutants inside the living cells [9]. Many biosorbents have been successfully used to remove or concentrate metal ions even from their very dilute solutions [10]. Presence of functional groups such as carboxylic, hydroxyl, amine, sulphate and phosphate are responsible for their binding properties [11]. A wide spectrum of materials originating from different kinds of bacteria, fungi and algae biomass has been evaluated as biosorbents [12]. Waste materials from various food and agricultural industries also have been studied for their metal ion removal capabilities [13, 14].

1.9 Chitosan

Chitin/chitosan are the second most abundant biopolymers present in the nature after cellulose [15]. These are natural polysaccharides present in the crustacean shells. Chemically chitin consists of β-(1-4) linked N-acetyl-D-glucosamine units (Fig. 1.3a). Deacetylation of chitin will give the more versatile form chitosan, which contains randomly distributed β-(1-4)-linked D-glucosamine and N-acetyl-D-glucosamine units (Fig. 1.3b). Degree of de-acetylation of chitosan plays an important role in the final properties of the biopolymer and chitin with de-acetylation degree ranging from 60 to 100% is normally classified as chitosan. Chitosan has been widely studied for the removal of various types of pollutants such as heavy metals [16], dyes [17] and other industrial effluents [18].

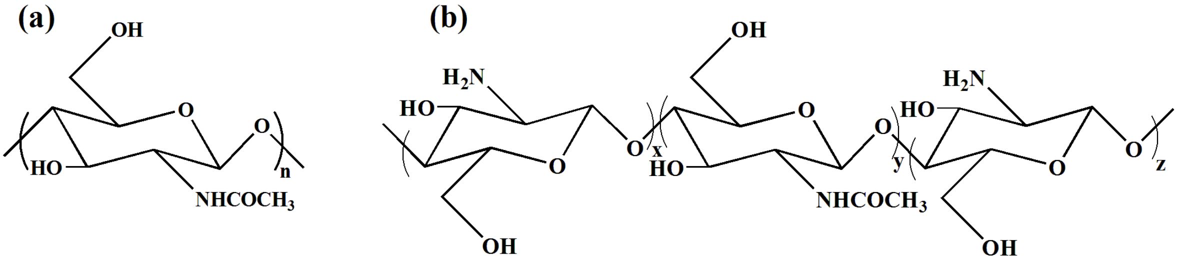

Figure 1.3. Chemical structures of (a) Chitin and (b) Chitosan

Extraction of chitin from the crustacean shells can be carried out either by chemical or by biological means [19]. A general schematic of the chemical process is given in Fig. 1.4.

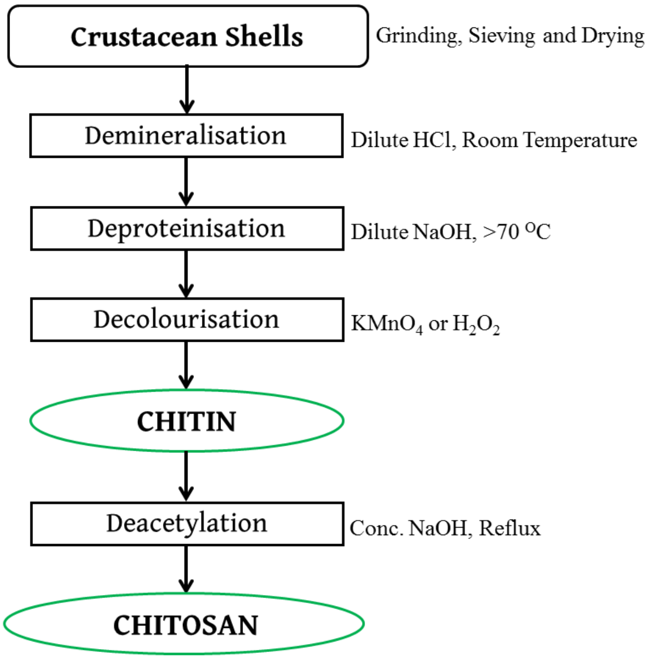

Figure 1.4. Schematic of the chitosan extraction from crustacean shells

1.10 Selectivity in Sorption Materials

Selective removal of a particular metal ion of interest in presence of other ions had gained much interest - both in terms of recovery (such as from the ore) and removal (such as from waste effluents). Selective removal of metal ions finds applications in; (i) Removal of drinking water pollutants such as arsenic in presence of other competing anions like sulphate and phosphates [20], (ii) Separation and isolation of metal ions such as Ni, Cr etc. from metallurgical point of view, (iii) Extraction of noble metals such as platinum and gold [21], (iv) To check and solve the heavy metal pollution of drinking water and treatment of industrial effluents [22], (v) Separation of radionuclides such as ^{137}Cs, ^{90}Sr and ^{60}Co from nuclear waste solution etc.

Selective removal of metal ions in presence of other competing ions will make the process more economic and widely accepted. Especially, in nuclear industry, metal ions like Cs, Sr and Co have gained much importance because of their presence in very low level (physical) quantities but high on associated radioactivity level. Selective removal of these active ions will lead to reduction of the active waste volume that needs special treatments as compared to the non-active waste. A number of selective sorbents and processes are being developed and tested with this objective. The selectivity in regular IX resins depends upon the hydrated ionic radius (smaller the hydrated ion radius, greater the affinity) and effective nuclear charge (higher the charge, higher the affinity) [23]. Introduction of chelating resins (that contain chelating functional groups for complexing the metal ions), with high selectivity for particular ions, had made it possible to design resins with preferred orders of selectivity for specific applications [24, 25]. The metal-ligand interactions and the complex stability determine the selectivity in these resins. Access to sorbent materials with selectivity for particular metal ion of interest was further enhanced with the introduction of metal ion imprinting technique. Metal ion imprinted polymers are prepared by freezing the metal-ligand complex geometry in a polymer matrix, using suitable crosslinkers. This will leads to enhancement in selectivity of the resin by limiting other unfavourable interactions. Metal ion imprinted polymers have opened a new class of materials with high degree of selectivity/specificity in the sorption materials available as of now.

1.11 Metal Ion/Molecularly Imprinted Polymers

The very idea of metal ion or molecularly imprinted polymers has got inspiration from the target specific interactions present in the nature; like enzyme-substrate rebinding. They are synthesised in such a way that target specific sites are created in a cross-linked polymer matrix by using template ions or molecules. The template binds the functional groups and protects it during crosslinking. The leaching out of the template ion or molecule from the crosslinked matrix, after crosslinking, leaves behind a favourable orientation of functional groups, inside the polymer matrix, for rebinding the template or its analogues (Fig. 1.5). A non-ion imprinted polymer is also prepared generally as a blank in the same manner as the imprinted polymer prepared (without the addition of the template) for comparison.

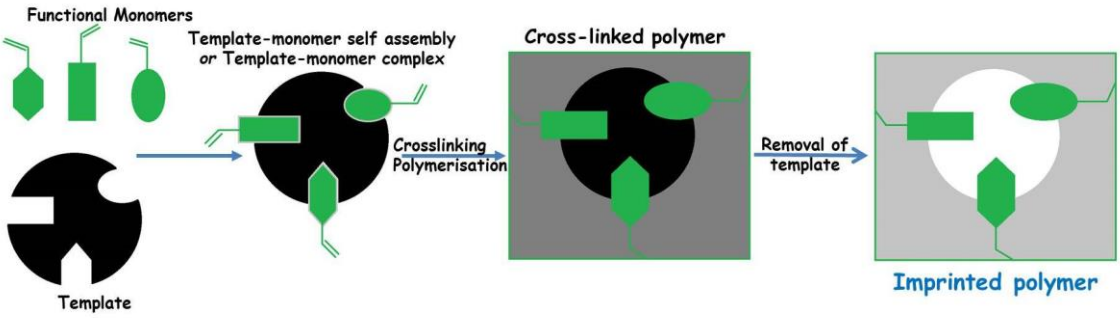

Figure 1.5. Schematic of the imprinting process

Rational design of imprinted polymers involves a correct choice of:

(i) Template: Can be a metal ion (in case of Metal-ion Imprinted Polymers) or a molecule (in case of Molecularly Imprinted Polymers). Templates have to be stable under polymerisation conditions and should have functional groups/charges suitable to interact with the functional monomers.

(ii) Functional Monomer: It should have a polymerisable moiety along with functional groups; that can bind the template in a reversible manner. The functional monomer-template complex has to be stable under polymerisation conditions with less number of unfavourable interactions.

(iii) Crosslinkers: It gives structural stability to the imprinted sites, decides the morphology of the imprinted polymer matrix and imparts mechanical stability to the imprinted polymer.

(iv) Initiators: Usually free radical generators like azobisisobutyronitrile (AIBN) or benzoyl peroxide, which can be decomposed easily either by photolysis or thermolysis, are used for initiating the polymerisation.

(v) Porogens: Sometimes added; to make the imprinted polymer macroporous and to increase the surface area and flow properties of the imprinted polymers.

The nature of functional monomer-template interaction, during synthesis and rebinding, is very crucial in deciding the sorption properties and selectivity of the imprinted polymers. Some of the reported template-monomer combinations and the associated interactions are given in Table 1.4.

Table 1.4. Functional monomer–template combinations utilised for imprinting: Different approaches

Functional monomer	**Template**	**Type of interaction**
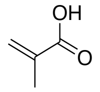 Methacrylic Acid	Atrazine [26]	Non-covalent: hydrogen bonds
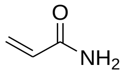 Acrylamide	Remazol Red 3BS [27]	Non-covalent: Electrostatic interaction between sulphonic acid and amine functional groups
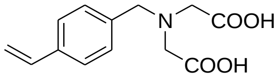 Vinylbenzyl-iminodiacetic acid	Co^{2+} [5]	Metal coordination: Chelation of the metal ion
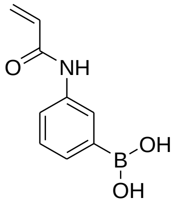 3-acrylamidophenylboronic acid	Mannose [28]	Covalent: Boronic ester bonds with diol functional groups present in mannose
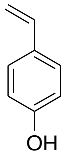 4-vinyl phenol	Cholesterol [29]	Semi-covalent: Covalent imprinting (Ester linkage and hydrolysis) and rebinding through hydrogen bonds

According to the functional monomer-template interactions involved, imprinting procedures are generally termed as;

1. Covalent Imprinting: It makes use of reversible covalent bonds such as boronic esters and Schiff bases, in synthesis of the functional monomer-template complex and rebinding of template analogues by the imprinted polymers. This approach

produces a better homogeneous population of binding sites with reduced non-specific sites inside the imprinted polymer matrix.

2. Non-covalent imprinting: This is the most widely utilised approach and makes use of interactions such as ionic, hydrogen bonds or other weak Van der Waals forces of attractions during synthesis of the functional monomer-template complex and in rebinding of the template analogues as well. Removal and rebinding of the templates are easy and fast; but there may be considerable non-specific interactions inside the polymer matrix.
3. Semi-covalent imprinting: This approach makes use of covalent Template-Monomer interactions during synthesis and non-covalent Template-Monomer interactions for rebinding.
4. Co-ordinate imprinting: Mainly utilised in the synthesis of metal-ion imprinted polymers; which make use of functional monomer (or ligand)-metal ion coordinate bonds during synthesis and rebinding.

Based on the synthetic approach, imprinting process can be classified into;

1. Two step synthesis: A polymerisable, template-functional monomer complex is prepared, isolated and purified, which is then subjected to crosslinking polymerisation.
2. One pot (*in-situ*) synthesis: Self-assembly or single pot approach: A pre-polymerization complex between template and functional monomer is formed in-situ and the crosslinking polymerisation is initiated in the same reaction vessel.

In cases wherein multiple template-functional monomer complexes may be formed, the first approach may be a necessity to ensure the formation of uniform binding sites. In cases where the template-functional monomer combination is known to form predominantly a single complex, the second option may be a better choice due to its simplicity.

Synthesis of imprinted polymers can be carried out using different polymerisation conditions such as bulk, suspension or emulsion polymerisation conditions and the properties of the final product largely depends upon the polymerisation technique followed.

(i) Bulk polymerisation: This is the most widely used polymerisation technique due to the simple procedure involved. There is a need for crushing or sieving of the imprinted polymers before template removal. There is no control over the physical form and there are difficulties associated with scaling up of the process.

(ii) Suspension or emulsion polymerisation: Imprinted polymers are directly prepared as micro/nano sized particles using this method in order to make it more suitable for intended applications [30, 31].

One of the major uses of suspension or emulsion polymerisations is in the surface template polymerisation; where imprinted sites are limited to the surface or very near to the surface of the polymer. This is achieved by attaching a template over an already present film/surface. It may be of a core shell type (like seeded emulsion [32] and molecularly imprinted nanoparticles [33]) or membrane type one [34].

1.12 Use of Metal Ion Imprinted Polymers in Nuclear Industry

Literature reports on metal ion imprinted polymers that are developed for the direct application in nuclear industry is very limited compared to the total number of literature available on metal ion imprinted polymers. The much studied metal ion in this regard is the uranyl (UO_2^{2+}) ion. There are a number of reports on the synthesis and utilisation of uranyl ion imprinted polymers for its determination and separation from sea water and other nuclear effluents [35-40]. A Co(II) imprinted polymer, synthesized using [N-(4-vinylbenzyl) imino] diacetic acid functional monomers, showed good selectivity for Co(II) against Fe(II), under strong complexing conditions and its use in DCD of NPPS, for the selective removal of active cobalt, was demonstrated [5]. Ion imprinted polymers for lanthanides and actinides such as Er, Lu, Ce, U and Th were also reported [41]. Some of the metal ion imprinted polymers reported; which may find relevance to the nuclear field was given in Table 1.5.

1.13 Ion Imprinted Polymers Using the Biosorbent Chitosan

There are a number of reports on the use of chitosan as a functional monomer in metal ion imprinting [47]. Presence of a large number of functional groups such as $-\mathrm{NH_2}$ and $-\mathrm{OH}$ groups makes it a versatile material for ion imprinting. Both modified and unmodified chitosan had been used as the functional polymer for imprinting. Modified forms include the functionalised derivatives of chitosan and its composites with other inorganic materials such as Fe_3O_4 [48] and TiO_2 [49]. Imprinted polymers using unmodified chitosan as the functional polymer have been prepared for various metal ions such as Cu(II) [50, 51], Zn(II) [50, 51], Ni(II) [50, 51], Pb(II) [50, 51] Ca(II) [52, 53] etc. Metal ions such as Sr(II) [54], Pb(II) [55, 56], Au(III) [57], Mo(VI) [58], Ni(II) [59], Cu(II) [59] etc., had been used for imprinting over the functionalised chitosan as well. Imprinted chitosans prepared in the form of composites with other inorganic oxides have been reported for metal ions such as U(VI) [60], As(III) [61], Ce(III) [62], Ni(II) [49, 63], Cu(II) [64], Pb(II) [65] etc. The current interest in imprinted polymers using chitosan is moving from the use of raw chitosan to modified chitosan with the perspective of dual applicability such as metal ion removal together with photo catalytic degradation of organic pollutants [49] or fast and simple post treatment such as magnetic separation [48]. Some of the reports on ion imprinted polymers prepared with chitosan and their metal uptake capacities are given in Table No. 1.6.

Table 1.5. Ion imprinted polymers which may find relevance to the nuclear industry

Metal ion	**Imprinting System:** EGDMA (Crosslinker) and AIBN (Radical initiator)	**Features**	**Ref.**
Cs	Functional monomer: Methacrylic acid Dibenzo-24-crown-8 ether (Selective crown ether)	Precipitation Polymerisation. Maximum adsorption capacity: MIP- 50 mg.g^{-1}, NIP-15.3 mg.g^{-1}. Preconcentration Factor: 100 (pH 9.0)	[42]
Th(IV)	Functional monomer: N,N′-bis(3-allyl salicylidene)o-phenylenediamine, Modified magnetic Fe_3O_4 particle, Tetraethyl orthosilicate, 3-Aminopropyltriethoxysilane and maleic anhydride (for preparing the vinyl functionalized $Fe_3O_4@SiO_2-NH_2$ core)	Surface imprinting Technique. Uptake capacity (pH 4.5): MIP - 42.54, NIP - 14.10 mg.g^{-1}. Relative selectivity coefficient values (MIP/NIP): Th(IV)/La(III) : 82.2 Th(IV)/Ce(III) : 93.1 Th(IV)/Nd(III) : 21.0 Th(IV)/U(VI) : 62.4	[43]
Ru(III)	Functional monomers: Methacrylic acid or acrylamide Template: Ru(III) 2-thiobarbituric acid complex	Solid phase extraction of Ru(III). Affinity for Ru(III) is more for methacrylic acid based IIP. Applicability over wide pH range.	[44]
Sr(II)	Functional monomer: Methylacrylic acid Chain transfer agent: S,S’-bis(α,α’-dimethyl-α’’-acetic acid) trithiocarbonate 3-(methacryloxyl) propyltrimethoxysilane modified graphene oxide (2D surface for ion imprinting)	Reversible Addition–Fragmentation chain Transfer (RAFT) polymerization with surface imprinting technique. Maximum adsorption capacity: MIP-145.77 mg.g^{-1}	[45]
Sb(III)	Monomer: Styrene Ligand: Ammonium pyrrolidine dithiocarbamate	Solid phase extraction of Sb(III). Maximum sorption capacity: IIP: 6.7 mg.g^{-1}. Enhancement factor: 232 Detection limit: 3.9 ng.L^{-1}	[46]

Table 1.6 Metal ion imprinted polymers using chitosan or modified chitosan

Functional monomer/ polymer system	**Metal ion**	**Cross linker**	**Uptake capacity / Results**	**Ref.**
Chitosan containing 8 –hydroxyquinoline moiety	U(VI)	Epichlorohydrin	MIP – 218 $mg.g^{-1}$ NIP – 136 $mg.g^{-1}$	[66]
Chitosan / polyvinyl alcohol blend	U(VI)	Ethylene glycol diglycidyl ether	MIP – 156 $mg.g^{-1}$ NIP – 129 $mg.g^{-1}$ (Langmuir)	[67]
Thiourea modified chitosan/TiO_2/Fe_3O_4 beads	Cd(II)	Gluteraldehyde and epichlorohydrin	MIP – 256.41 $mg.g^{-1}$ (Langmuir) 2,4-dichlorophenol degradation (98 %)	[68]
Chitosan	Ag(I)	Epichlorihydrin	MIP – ~120 $mg.g^{-1}$ NIP – ~90 $mg.g^{-1}$ Selectivity: Ag(I)/Cu(II) MIP – 4.21, NIP – 0.54	[69]
Chitosan/Fe_3O_4 microspheres	Cu(II)	Glutaraldehyde	MIP – 109.89 $mg.g^{-1}$ (Langmuir)	[70]
Chitosan/carbon nanotube composite and silica-coated nano Fe_3O_4	Gd(III)	Glutaraldehyde	MIP – 88 $mg.g^{-1}$ Selectivity coefficients: Gd^{3+}/La^{3+} – 3.50 Gd^{3+}/Ce^{3+} – 2.23	[48]
Interpenetrating Polymer Network (IPN) of methacrylic acid and chitosan	Pb(II)	Ethylene glycol dimethacrylate and tetraethyl orthosilicate	MI-IPN – 37.5 $mg.g^{-1}$ NI-IPN – 10.3 $mg.g^{-1}$	[71]

1.14 Cobalt

Cobalt belongs to the group 9 (d block elements) and period 4 of the periodic table. The electronic configuration is $[_{18}Ar]\ 3d^7\ 4s^2$. It exists in oxidation states of −3, −1, +1, +2, +3, +4, and +5. The most common oxidation states are +2 and +3. It finds use in the synthesis of strong magnets (such as ALNICO) and making of high performance or hard facing alloys (such as stellite) etc. Radiocobalt (^{60}Co) is used in the treatment of cancer and for the radiation sterilization of food and surgical items. The major ore of cobalt is the cobaltite (CoAsS) but it is generally obtained as a by-product of Nickel or Copper production industry. The stable isotope of cobalt is ^{59}Co with 100 % natural abundance.

^{60}Co and ^{58}Co are the two active isotopes of cobalt generally found in the coolant circuits of the nuclear reactors. ^{60}Co is produced by the (n, γ) reaction of the parent ^{59}Co, which comes mainly as an impurity in carbon steel, stainless steels, nickel alloys (0.02-0%) and as a constituent of hard facing alloys (50-70%) such as stellite. ^{59}Co has a thermal neutron capture cross-section of 37.18 barn and can easily undergo (n,γ) reaction to produce ^{60}Co, which has a half-life of 5.28 years and disintegrate to the stable ^{60}Ni through (β,γ) emission having high energy gamma rays of energy 1.17 and 1.33 MeV. ^{58}Co is produced through the (n,p) reaction of ^{58}Ni (68.27% natural abundance) and is favoured by the fast neutrons. The mean cross section for fission spectrum neutrons for the reaction is reported to be 111 ± 12 mb [72]. ^{58}Co has a half-life of 70.9 days and disintegrates to ^{58}Fe through electron capture (EC) and positron emission associated with the high energy gamma emission of 0.81 MeV. The decay modes of ^{60}Co (100% β emission to excited states of ^{60}Ni) and ^{58}Co (Electron Capture (85%) and Positron emission (15%) to excited states of ^{58}Fe) is shown in Fig. 1.6.

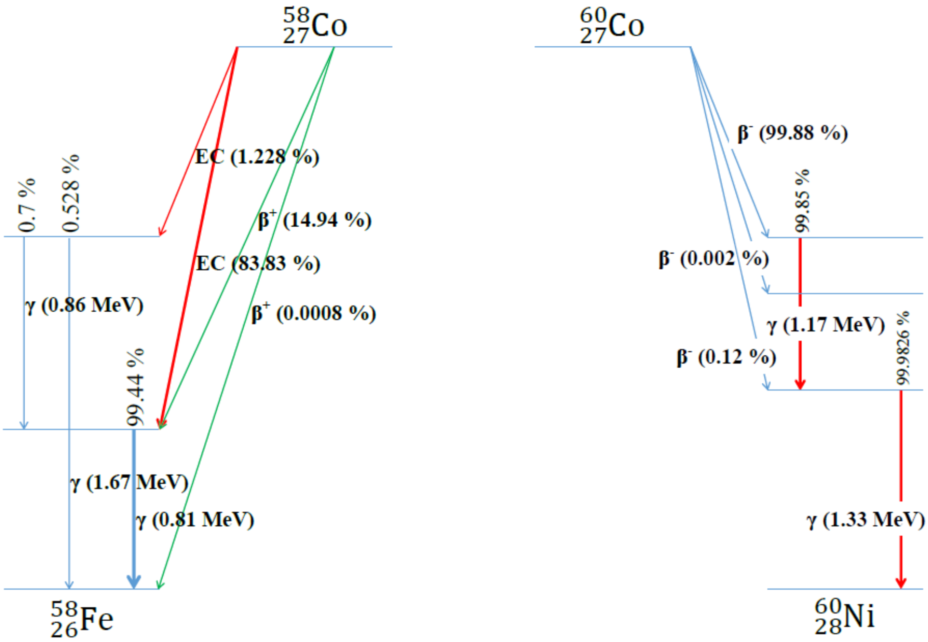

Figure 1.6. Decay schemes of ^{58}Co and ^{60}Co

In the initial stages of the operation of PWRs; ^{58}Co is the major concern because of its quicker build up and the larger source availability (from steam generator tubings). But, as the reactor ages ^{60}Co becomes more important (because of longer half-life) and both the isotopes together will contribute to a larger part of the total radioactive inventory. Moreover ^{60}Co contributes significantly to the radioactive inventory in comparison to the other nuclides [3]. So, any method which can selectively remove radio cobalt from other non-active ions, such as iron in case of DCD, will be of greater importance to the nuclear industry. Such type of an organic resin synthesis and its utilization, for removing Co(II) in presence of large excess of Fe(II) under DCD conditions, has been reported [5]. The results obtained during the studies predicted a significant reduction in the active waste volume generated during a typical DCD campaign where in regular ion exchange columns (without any specific selectivity) are used. Also, with the use of a cobalt sequestration resin (CoSeq™); during the nuclear plant's operating cycle as well as at plant outages, an EPRI study reported huge replacement power savings (of the order of \$500,000 to \$1 million per day) through improved worker safety (because of the reduced radiation fields and exposure) and lower electricity cost (due to reduced maintenance shutdowns) [73]. Modifying the selectivity of the biosorbent chitosan towards the selective removal of cobalt, during DCD canmpaigns, has been taken up with similar objectives.

1.15 Antimony

Antimony, a metalloid by nature, belongs to the subgroup 15 (Nitrogen family), period 5 of the periodic table of elements. The electronic configuration is $[_{36}\text{Kr}]\ 4d^{10}\ 5s^2\ 5p^3$. It has two stable isotopes; ^{121}Sb and ^{123}Sb with natural abundances 57.21 and 42.79 % respectively. Antimony can exist in various oxidation states (−III, 0, III, V) and generally found to exist in two oxidation states (III and V). Antimony occurs in nature mostly as its sulfide Sb_2S_3 (stibnite). Antimony find application in; electronics industry to make semiconductor devices such as infrared detectors and diodes, flame retarding additives, production of alloys and in treatment of certain tropical protozoan diseases such as leishmaniasis [74].

DCD campaigns on many Indian Pressurized Heavy Water Reactors (PHWRs) using the NAC formulation were successful and resulted in high decontamination factors [4]. But in some of the reactors; an increase in the radiation field was observed on certain components at the outer of core surfaces after the DCD process. This was attributed to the presence of active isotopes of antimony [75]. Antimony impregnated graphite seals are used in the coolant pumps of nuclear reactors. Due to the regular wear and tear of the same; antimony gets released into the coolant. Antimony is expected to be present either in elemental form or in +3 state due to the reducing conditions that prevail in the PHT system and may remain deposited over the clad surfaces (ZrO_2 over the Zircaloy surface) of the core under operating conditions. The inactive antimony (^{121}Sb &^{123}Sb; which have fairly good neutron absorption cross-sections of 5.75 & 3.8 barn respectively; 1 barn = 10^{-24} cm^2) that are deposited at the in core clad surfaces will get activated (to ^{122}Sb; $t_{1/2}$ 2.72 days and ^{124}Sb; $t_{1/2}$ 60.2 days) by the neutron flux present there [76]. The decay scheme for the ^{122}Sb and ^{124}Sb are given in Fig. 1.7. ^{125}Sb is another important active isotope of antimony, with a half-life of 2.76 years, which is formed as a fission product. The cumulative fission yields of ^{125}Sb are 0.034699 % (from ^{235}U) and 0.11332 % (from ^{239}Pu) [77].

During shutdown, the activated antimony deposits are released into the coolant, likely due to the ingress of oxygen, and deposits over the oxide layer present on the out of core surfaces [78]. Antimony removal over various iron oxides/hydroxides has been reported in the literature [79]. Such a kind of mobilization and re-deposition of active antimony was found to be responsible for the offset in the decontamination factor obtained by removing other activities such as ^{60}Co. To circumvent this problem, either suppress the antimony deposition over the outer core surfaces during regular chemical decontamination or remove it during (or prior to) the decontamination using modified processes/sorbents.

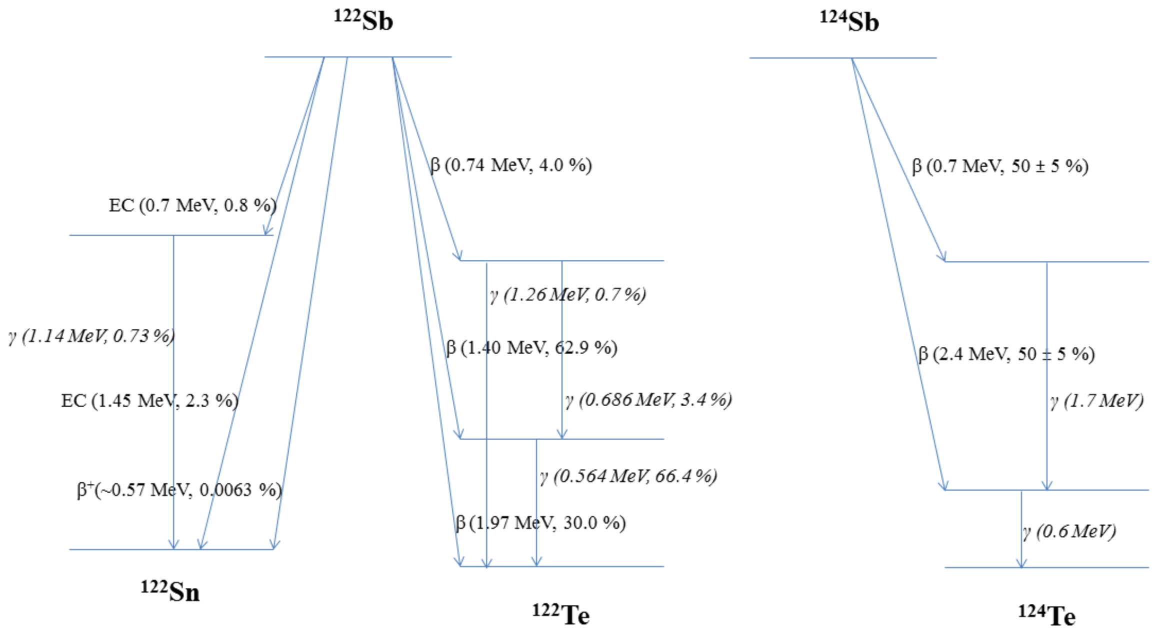

Figure 1.7. Decay schemes of ^{122}Sb and ^{124}Sb

The best method currently known for the removal of antimony activity, prior to regular decontamination, is the hydrogen peroxide process [3]. The process employs H_2O_2, an oxidising agent, which mobilises all the deposited antimony through oxidation which is then removed over anion resin beds. But, the low affinity of anion exchange resins for antimony necessitates the use of a large quantity of the resin. Typically, removal of about 10 g of antimony needs about 2 m^3 of the resin [80]. Thus, there exists a need for better antimony removing materials for use in the H_2O_2 process. This process, which was originally developed for PWRs, was also modified to be suitable for PHWRs [81]. The rate of disappearance of H_2O_2 in PHWRs during the process is high as compared to PWRs and an alternative reductive chemical process (using 100 ppm each of NTA, Citric acid and Rodine-92B at 85 ^{O}C) had been applied for the antimony removal in Narora Atomic Power Station Unit-2 (NAPS-2) and Kakrapar Atomic Power Station Unit -1 (KAPS-1). There was a considerable release and re-deposition of antimony at the out of core surfaces during the regular DCD process at KAPS-1, even after the applying the special antimony removal step (reductive chemical process) twice [82]. So the selective removal of antimony during the regular DCD process may be a better option. Moreover there is a better scope for using such antimony selective materials during DCD campaigns without affecting the system chemistry unlike the oxidizing H_2O_2 process. The major objective of finding better antimony sorbents for using under DCD conditions was primarily based on this aspect.

Chapter 2. EXPERIMENTAL DETAILS

2.1 Chemicals and Reagents Used

Chitosan (from shrimp shells with ≥75% deacetylation), Potassium hexahydroxo antimonate ($KSb(OH)_6$) and Chitosan (medium molecular weight, Brookfield viscosity 200-800 cP, 1 wt.% in 1% acetic acid, 25 °C, 75-85% deacetylated) were obtained from Sigma-Aldrich. RADEX® Sb-1000 and AEROXIDE® TiO_2 P 25 were provided as free samples by Graver Technologies USA and Evonik Industries AG, Hanau, Germany, respectively. Nano titania (as TiO_2 powder containing 17-18% moisture; 10-15 nm size, special grade) was obtained from Travancore Titanium Products Limited (TTPL), Trivandrum, India. Amberlite® IRC-718 (a chelating resin) and Nitrilotriacetic acid (A.R. grade) was obtained from HiMedia Laboratories Limited, India. Ascorbic acid (A.R. grade), sodium hydroxide (A.R grade) and $(NH_4)_2Fe(SO_4)_2$ were obtained from Ranbaxy fine chemicals Limited, India. $Co(NO)_3.6H_2O$ (G.R grade) and Potassium antimony (III) tartrate ($K_2Sb_2(C_4H_2O_6)_2$) were purchased from SD fine-chem, India. Epichlorohydrin (for synthesis), $Co(NO_3)_2.6H_2O$ (G.R. grade), Citric acid anhydrous (A.R. grade), Trisodium citrate (G.R grade) and nitrilotriacetic acid (G.R grade) were obtained from Loba Chemie, India. Sulphuric acid (98%, GR grade) was obtained from Merck India. $CuSO_4.5H_2O$ was obtained from Spunchem, India. $Na_2HAsO_4.7H_2O$ (A.R. grade) was obtained from Titan Biotech Ltd., India. All chemicals were used as such without further purification. The metal-ion/complexant solutions were prepared either in ultra-pure water (Sartorius arium®611) or in double distilled water, which used demineralised water as the feed.

2.2 Instrumental Details

Metal-ion concentrations were measured using an Inductively Coupled Plasma-Atomic Emission Spectrometer (ICP-AES, Ultima-2, Horiba Jovin Yvon, France). UV-Visible spectrometric analyses were made using a UV-Visible spectrophotometer (Evolution 500, UV-Visible Spectrophotometer). Raman spectra were recorded using a dispersive micro Raman Spectrometer (HR-800), Jobin Yvon, France. Argon ion laser, 514 of 785 nm, was focused using a 50X LD objective lens on sample surface with laser power of 0.5-1.0 mW. 1800 groves/mm grating was used with 15-30 sec data acquisition time. TOC measurements were done using a Total Organic Carbon analyser (TOC-VCSH, Shimadzu Corporation, Japan). Irradiation studies were done in a gamma chamber containing cobalt source with a dose rate of 5.852 kGy/h. Surface area (BET) measurements were done with nitrogen sorption (Thermoelectron, Sorptomatic 1990), while the pore size measurements were done using mercury porosimetry (Thermo Fischer Scientific). Solution pH measurements were done using a glass electrode. Bead size measurements were done using an electronic Vernier calliper (Mitu-toyo digimatic calliper).

2.2.1 Inductively Coupled Plasma - Atomic Emission Spectroscopy (ICP-AES)

Inductively coupled plasma atomic (or optical) emission spectroscopy (ICP-AES or ICP-OES) is an analytical technique used for the quantification of trace metals. It is a type of emission spectroscopy that uses the inductively coupled plasma as the source for excitation of the atoms. The temperature of the plasma ranges from 6000 to 10000 K. The excited atoms/ions de-excite into their ground state by emitting electromagnetic radiations of particular wavelengths characteristic to that element. The intensity of the emitted light will be proportional to the concentration of the element present in the sample.

ICP-AES system mainly consists of three systems namely, the sample introduction system, the plasma torch assembly and the spectrometer (Fig. 2.1). The sample introduction system consists of a peristaltic pump, Teflon tubings, a nebulizer, and a spray chamber. The liquid sample is pumped into the nebulizer (a concentric nebulizer made of glass is used for the studies) with the peristaltic pump and sample solution is sprayed into a cyclonic spray chamber. The nebulizer generates an aerosol mist in the spray chamber. The largest mist particles get settled (and go out as waste into the drain) and the finest mist particles (approximately 1 % of the total solution) will be swept vertically into the plasma torch assembly along with the argon gas. Plasma torch consists of three concentric tubes; (i) the outer tube made of quartz (used for passing the cooling argon; to protect the torch assembly) (ii) intermediate or auxiliary tube made of quartz (used to raise the plasma cone of the injector whenever necessary; for organic solutions) and the (iii) central injector tube made of alumina (used for the sample introduction into the plasma cone). A radiofrequency generator (of frequency 40.68 MHz) is used for producing and maintaining the plasma.

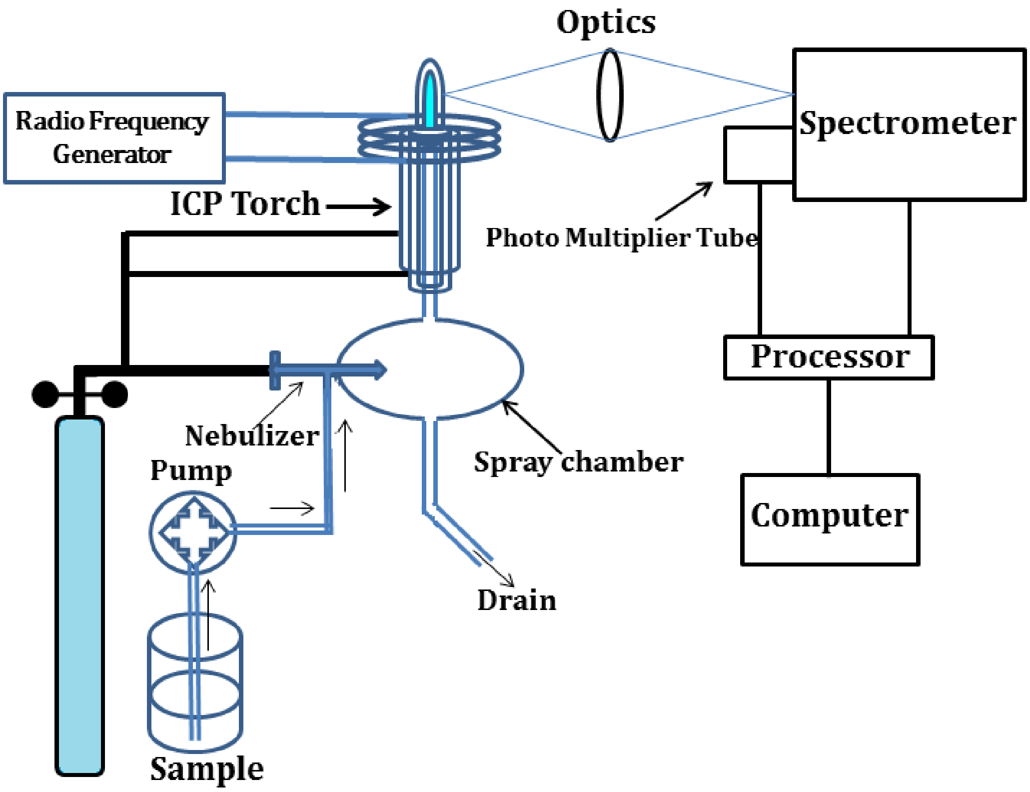

Figure 2.1.Schematic of the Inductively Coupled Plasma-Atomic Emission Spectrometer components

The sample introduced as the mist is atomised and then excited at the plasma (Fig. 2.2). The excited atoms will come to the ground state by emitting light rays (of discrete energy) characteristics to the element. The emitted light (or the plasma) is viewed horizontally (radial viewing) by an optical channel. The emitted light from the plasma is focused by a lens and passed through an entrance slit into the monochromator (sequential spectrometer).

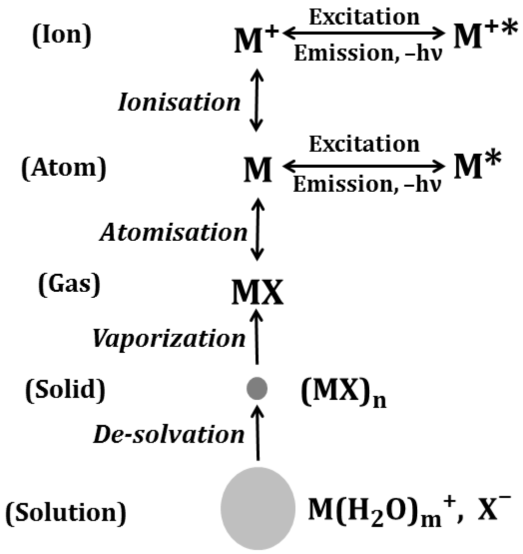

Figure 2.2. Processes happening for the sample injected into the inductively coupled plasma discharge

A collimator mirror is used for transmitting the entered light into the diffraction grating. The diffraction grating (2400 lines/mm, used in first/second order) will split the emitted light into its component colours (or wavelengths) and it is then transmitted to the detector through an exit slit using another mirror. The detector (photomultiplier tube) is fixed and rotation of the diffraction grating (sequentially) moves each wavelength into the detector. Photomultiplier tube will convert the emitted light into an electrical signal. It is a vacuum tube containing a photosensitive material called photocathode and it emits electrons when subjected to light. These photoelectrons are accelerated and multiplied over dyanodes (an electrode which serves as an electron multiplier through secondary emission). The current measured at the anode will be proportional to the intensity of the emitted light and the voltage applied across the dynodes, and is used for computing the concentration of the analyte in the sample by the system software through calibration.

2.3 Synthesis of Co(II) Imprinted Polymer

Co(II) imprinted chitosan was synthesized according to the reported literature procedure with some modifications [51]. Chitosan (from shrimp shells; 0.5 g, 2.33 mmol of -NH_2 for a 75% deacetylated chitosan) was dissolved in 25 mL acetic acid solution (3% v/v) with stirring on a magnetic stirrer. To this homogeneous solution, $Co(NO_3)_2.6H_2O$ (0.335 g, 1.157 mmol) was added and pH of the solution was raised to 6 by drop wise addition of 0.25 M aqueous NaOH solution under stirring. The precipitated Co(II) complexed chitosan gel was separated, washed with ultra-pure water, and transferred to a solution of epichlorohydrin (1.23 mL, 15.5 mmol). The crosslinking was initiated by increasing the solution pH to 11 with 0.25 M NaOH and the crosslinking reaction was continued for 24 h. The precipitate (polymer) was then separated, washed with ultra-pure water and dried in air. The complexed Co(II) from the dried polymer was removed by extraction with 1 M H_2SO_4 (100 mL). The polymer was then washed with excess water and treated with 0.05 M NaOH (50 mL) for regenerating the binding sites (-NH_2 groups in chitosan backbone). The polymer was again washed several times with ultra-pure water and ethanol, and dried under vacuum to obtain the metal ion (Co(II)) imprinted chitosan (MIP). A non-imprinted chitosan (NIP) was prepared in the same way as the MIP, but in the absence of the template ion (Co(II)). The NIP was also subjected to similar chemical treatments as the MIP to ensure identical preparation conditions.

2.4 Synthesis of the Nano Titania Impregnated Chitosan (TA-Cts) Beads

About 0.5 g of the chitosan (medium molecular weight) was dissolved in 20 mL of 3% acetic acid (v/v) solution. To this solution, nano titania (TTPL; 0.1 g) was added with stirring. The mixture was sonicated for 15 min followed by addition of the crosslinking agent epichlorohydrin (1 mL) with stirring. The resultant dispersion containing chitosan, TiO_2, and the crosslinking agent, was taken in a glass syringe (or using a peristaltic pump setup; Fig. 2.3) and dropped through a 22 gauge needle into a 0.25 M NaOH solution, under constant stirring, leading to formation of solid beads. The precipitated beads were left overnight to remain in the solution without stirring. The beads were separated, washed with ultra-pure water and dried overnight in an air oven at 50 ^{O}C. The dried beads were treated with 10 mL of 0.1 M HCl for 6 h in order to remove any un-reacted chitosan. The beads were further washed several times with ultra-pure water, and dried under vacuum. The purified dry beads thus obtained were used as the Nano TiO_2 impregnated-Epichlorohydrin crosslinked Chitosan (TA-Cts) composite beads for the sorption studies.

Figure 2.3. Setup used for preparing the chitosan (or TA-Cts) beads

2.5 Sorption Experiments

Sorption experiments were carried out in batch mode as well as in column mode.

2.5.1 Batch Sorption Studies

A fixed amount (g) of the sorbent was equilibrated with a fixed volume (L) of the metal ion solutions in a vial on a test tube rotator. The amount of metal-ion removed over the sorbent, at any time 't', was obtained either as uptake capacity (q_t, Eq. 2.1) or as percentage removal (%, Eq. 2.2)

$$q_t = \frac{(C_0 - C_t)}{W} \text{ x V} \qquad (2.1)$$

$$\text{Percentage Removal} = \frac{(C_0 - C_t)}{C_0} \times 100 \qquad (2.2)$$

Where, C_0 and C_t are the initial and final (at time't') liquid phase concentrations (mol.L^{-1}) of metal-ions respectively; V is the volume of the solution (L) and W is the weight (g) of the sorbent used.

Imprinting factor (I.F), which is a measure of the selectivity induced by the metal ion imprinting over the polymer, was obtained as

$$\text{I.F.} = {}^{Q_{MIP}}\!/_{Q_{NIP}} \qquad (2.3)$$

Where, Q_i is the ratio of the capacities for the imprinted ion, say Co(II), to the competitor ion, say Fe(II), on equilibration of the sorbent (MIP or NIP) with a solution containing both the ions (Eq. 2.4)

$$Q_i = {}^{q_{Co(II)}}\!/_{q_{Fe(II)}} \qquad (2.4)$$

2.5.1.1 *Distribution Constant or Partition ratio (K_D) and Selectivity*

Distribution Constant or Partition ratio [83] is defined as "The ratio of the concentration of a substance in a single definite form, A, in the extract to its concentration in the same form in the other phase at equilibrium".

For Co(II) sorption by the sorbent chitosan, it can be defined as the ratio of the concentration of Co(II) in sorbent chitosan to the Co(II) concentration of the solution at equilibrium. Unit is $L.Kg^{-1}$

$$K_D^{Co(II)} = \frac{[Co(II)]_{Sorbent}}{[Co(II)]_{Solution}} \qquad (2.5)$$

Selectivity of the sorbent for a particular metal ion over another ion can be derived as the ratio of their respective distribution constants.

$$k_{Co(II)/Cu(II)} = \frac{K_D^{Co(II)}}{K_D^{Cu(II)}} \qquad (2.6)$$

2.5.2 Equilibrium Modelling of Sorption

There are many mathematical models available in the literature for describing the adsorption equilibrium [84]. The most widely employed ones are the Freundlich and Langmuir isotherm models. These models are helpful in comparison and selection of the sorbents. Langmuir isotherm is based on a theoretical model which assumes monolayer adsorption over an energetically and structurally homogeneous adsorbent surface with no interactions between the sorbed species at the adjacent sites. Langmuir isotherm is represented by Eq. 2.5.

$$q_e = Q^0 \frac{bC_e}{1+bC_e} \qquad (2.5)$$

The linearised form of Langmuir adsorption isotherm is given as

$$\frac{C_e}{q_e} = \frac{1}{Q^0 b} + \frac{1}{Q^0} C_e \qquad (2.6)$$

Where, q_e is the amount of solute sorbed (mmol.g^{-1}) and C_e, the equilibrium concentration of the solute in the solution (mmol.L^{-1}). The Langmuir parameters are given as Q^0, the maximum monolayer adosprtion capacity (μmol.g^{-1}) and b, a coefficient related to the affinity between the solute and the sorbent [85]. A plot of $\frac{C_e}{q_e}$ vs C_e will give a line of slope $\frac{1}{Q^0}$ and intercept at $\frac{1}{Q^0 b}$.

Freundlich isotherm equation is an empirical model described by Eq. 2.7. It does not indicate a finite uptake capacity as it does not account for adsorbent saturation; and it can be associated with both heterogeneous and multilayer adsorptions.

$$q_e = K_F C_e^{1/n} \qquad (2.7)$$

Where, Freundlich parameters are given as K_F (L.Kg^{-1}) and 1/n (dimensionless). The linearised form is given as

$$\log q_e = \log K_F + \frac{1}{n} \log C_e \qquad (2.8)$$

A plot of $\log q_e$ vs $\log C_e$ will give a straight line of slope 1/n and intercept at $\log K_F$.

2.5.3 Sorption Studies under Flow Conditions: Column Mode

Column studies were carried out using a glass column fitted with a Teflon stopper. A small amount of glass wool was packed at the end of the column over which, the sorbent was filled. The bed volume and the height of the column obtained were noted. Metal ion solutions were passed through the sorbent column in once through mode at fixed flow rates using a peristaltic pump. Schematic of the sorption studies done in column mode is given in Fig. 2.4

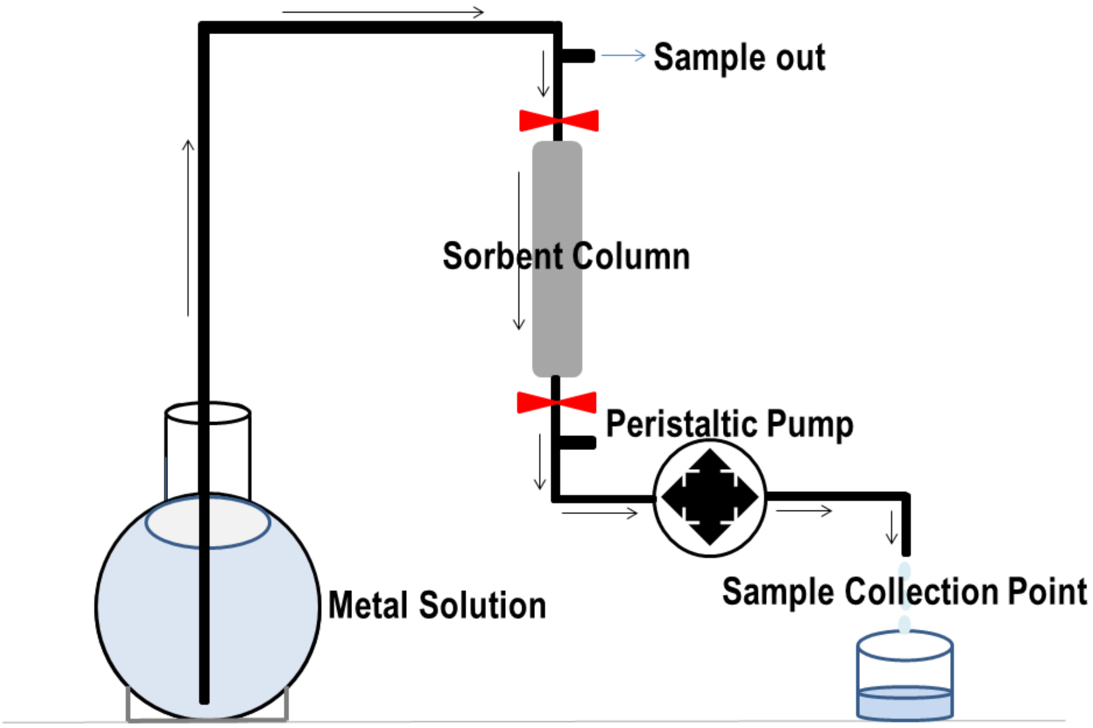

Figure 2.4. Schematic of the column studies

2.5.3.1 Theoretical Models for Sorbent Behaviour in Column Mode

Thomas model [86] and Yoon-Nelson model [87] are the general and widely used theoretical models to describe the column performance [88-90]. Both models were derived based on some assumptions with some limitations [89]. Thomas model helps to obtain the operational parameters for maximum (Thomas) adsorption capacity, q_T and the Thomas rate constant, K_T.

Linearized forms[88] of Thomas model and Yoon-Nelson models are given in Eq.2.9 and Eq. 2.10.

$$\ln\left(\frac{C_0}{C_t} - 1\right) = \frac{K_T q_t W}{F} - K_T C_0 t \qquad (2.9)$$

$$\ln\left(\frac{C_t}{C_0 - C_t}\right) = K_{YN}t - K_{YN}\tau \tag{2.10}$$

Where C_0 and C_t are, respectively, the influent (or initial) and effluent analyte concentrations (mg L^{-1}), K_T is the Thomas rate constant (mL mg^{-1} min^{-1}), q_T is the maximum adsorption capacity (mg g^{-1}) obtained by Thomas model, K_{YN} is the Yoon-Nelson rate constant (L min^{-1}), τ is the time required for 50 % sorbate breakthrough (min.), W is the weight of the sorbent used for column filling, F is the flow rate (mL $min.^{-1}$) at which the analyte solution is passing, V is the volume of the analyte solution passed at sampling time, t.

2.5.4 Kinetic Modelling of Sorption

The sorption profile and the rate limiting steps in the adsorption processes can be investigated using kinetic models. The pseudo first and second-order kinetic models are the commonly used kinetic models to investigate the solid/liquid adsorptions by fitting the experimental data with the kinetic expressions.

The linearised form of the integrated pseudo first order rate equation (Lagergren) is given by the Eq. 2.11 [91] and the plot $\log(q_e - q_t)$ vs t will give a straight line for the adsorption processes that follow the pseudo first order kinetic rate equation.

$$\log(q_e - q_t) = \log(q_e) - \frac{K_1}{2.303}t \tag{2.11}$$

Where q_e and q_t correspond to the uptake capacities at equilibrium and at time t, respectively and K_1 ($min.^{-1}$) is the rate of sorption. The equilibrium sorption capacity, q_e, must be known for fitting the Eq. 2.11 with the experimental data. In many cases q_e may be unknown and specifically in the case of chemisorption, as it is relatively slow, the equilibrium may not have been attained. So the pseudo first order kinetic equation may not fit well with the experimental data for the whole period [92].

The linearised form of the integrated pseudo second order rate equation is given by the Eq. 2.12 [91] and the plot $\frac{t}{q_t}$ vs t will give a straight line for the adsorption processes that follow the pseudo second order kinetic rate equation.

$$\frac{t}{q_t} = \frac{1}{K_2 q_e^2} + \frac{1}{q_e} t \qquad (2.12)$$

Where q_e and q_t correspond to the uptake capacities at equilibrium and at time t, respectively, and K_2 (g. mg^{-1}. $min.^{-1}$) corresponds to the rate constant of adsorption.

2.6 Swelling Studies

Swelling parameters of the sorbents are reported as Equilibrium Swelling Ratio *(ESR)* (Eq. 2.13) and Equilibrium Water Content *(EWC)* (Eq. 2.14) [93]. For this, a known weight (dry) of the sorbent beads was equilibrated with ultra-pure water (as swelling agent). The swollen beads were then separated and the surface water was removed by blotting with filter paper. The weights of the swollen beads were recorded and the swelling parameters were computed using these weights.

$$\text{ESR} = \frac{W_s - W_d}{W_d} \qquad (2.13)$$

$$\text{EWC} = \frac{W_e - W_d}{W_e} \qquad (2.14)$$

Where; W_s, W_d and W_e are the weights of the TA-Cts beads at swollen, dry and at the equilibrium swollen state respectively.

True swollen density or specific gravity of the swollen TA-Cts beads were determined using simple density bottle method [94] and it is given as Eq. 2.15.

$$D = (\frac{W_s}{M_{eq}})d \tag{2.15}$$

Where W_s is the weight of the swollen beads, M_{eq} is the weight of water equivalent in volume of the swollen beads (i.e., difference (a-b) between the weights of (a) density bottle filled with water alone, and (b) density bottle filled with water and swollen beads) and d is the density of water.

2.7 Nitrilotriacetic acid (NTA) Estimation Using UV-Visible Spectrometry

Nitrilotriacetic acid concentrations were determined by the dual wave length method, modified for NTA, using a UV-Visible spectrophotometer [95]. NTA solutions were treated with excess of Fe(III) reagent solution in 1.1 M H_2SO_4 and its absorptions at 258 nm and 305 nm were monitored against water as the blank. Strength of the NTA solution can be obtained using Eq. 2.16.

$$\text{Strength of NTA (M)} = \frac{(A_{258} - (\alpha\, A_{305}))}{K} \text{ x Dilution Factor} \tag{2.16}$$

$$\alpha = \frac{A^0_{258}}{A^0_{305}} \tag{2.17}$$

Where A_{258} and A_{305} are the respective absorptions at 258 nm and 305 nm; A^0_{258} and A^0_{305} are the respective absorptions for the reagent blank, and K – a constant; was obtained as the slope of the linear plot of $(A_{258} - (\alpha\, A_{305})$ against the respective standard NTA solutions of known concentrations.

Chapter 3. SORPTION BEHAVIOUR OF CHITOSAN

3.1 Introduction

Chitosan and its derivatives have gained wide attention as effective biosorbents, because of the natural abundance and high sorption capacities, for the removal of various metal ions, including radioactive metal ions such as uranium, and other pollutants [96, 97]. Chitosan's resistance to radiolysis, and its applicability in the nuclear field, also has been investigated as early as in 1972 [98]. The complexing nature and chemical reactivity of the amine and hydroxyl functional groups of the chitosan make it a suitable sorbent for the removal of metal ions during dilute decontamination of nuclear reactors [99].

Studies on the removal of metal ions by chitosan in presence of complexing agents, which are used during dilute chemical decontamination campaigns, are limited. The most studied metal-ion in this regard is copper(II) [100-104]. Juang et al. studied the removal of Cu(II) from solutions containing chelating agents such as EDTA, citrate, tartaric acid and gluconate and the optimal pH ranges reported for Cu(II) adsorption, based on metal ion alone sorption results, are 3.1–4.2, 5.0–5.8, 5.0–6.0 and 5.2–5.8 with EDTA, citrate, tartarate and gluconate, respectively [100]. Lu et al. modelled the sorption of copper-citrate on chitosan through theoretical calculations to develop a mathematical model to predict the copper adsorptions at varying pH values and copper to citrate ratios [101]. But, in these studies, the sorption of the complexing ligands was not monitored and the conclusions were drawn based on the results obtained from the metal-ion sorption. Thus, the nature of metal-ion sorption - as complex or as free metal ion - on chitosan has not been addressed. Cu(II)-EDTA sorption on to chitosan and its regeneration through electrolysis was also reported wherein possible mechanisms for the uptake of Cu(II) and EDTA in acidic and alkaline conditions were discussed [104]. Similarly, Ni(II)-citrate sorption by chitosan and its subsequent regeneration through electrolysis for reuse was reported wherein both nickel and citrate uptakes were monitored [105]. However, reports on the sorption of the ligand Nitrilotriacetic Acid (NTA) and its metal-ion complexes by chitosan are limited; except for a report by Jeon et al.[106], on the effect of NTA on mercury-ion removal and the reports on the preparation of chitosan-NTA conjugate for application in drug delivery systems [107, 108].

Removal of metal ions e.g., Co(II), the major activity encountered during DCD of NPPs [4], using biosorbents like chitosan is gaining interest due to its ease of availability and versatility. Decomposability of sorbents, post-stripping of active ions, can play a major role in making the radioactive waste management process more environment friendly. Use of bio-degradable sorbents becomes a better option, in this regard, if they can match the sorption properties of the organic resins. Though there are many reports on sorption properties of chitosan towards various metal ions, studies regarding its use for the removal of cobalt and other radioactive nuclides is very limited compared to the general heavy metal pollutants. Liu et al. synthesized a surface grafted Co(II) imprinted polymer using chitosan for the selective removal of cobalt and studied its adsorption performances [109]. Sorption behaviour of ^{60}Co and $^{152+154}$Eu radionuclides onto chitosan derivatives was studied by Metwally et al. [110]. Also, Mizera et al. studied the sorption of Cs, Co and Eu on oxidized coals in mixture with chitosan using radiotracer method [111].

Investigations on sorption of metal-ions along with complexants can give indications about the speciation and mechanisms involved in the metal ion sorption from complexing media. In this context, it is important to understand the sorption properties of the biosorbent, chitosan, especially towards cobalt from complexing medium. Removal of Co(II) by chitosan from its Co(II)-NTA solutions, as NTA being a major component in the DCD formulation, is discussed in this chapter. Since most of the reported studies regarding the sorption of metal-ions in presence of complexing media were done with Cu(II), sorption characteristics of Cu(II) in presence of NTA was also studied for comparison with Co(II) sorption. Possibilities on the selective sorption of either of the metal-ions by chitosan in presence of other ions have also been addressed.

3.2 Experimental Details

3.2.1 Chemicals and Reagents

Chitosan from shrimp shells with ≥75% deacetylation, obtained from Sigma–Aldrich, was utilised for the sorption studies. NaOH (1 M) solution was added for the dissolution of NTA.

3.2.2 Sorption Experiments

All the sorption experiments were carried out in batch mode at room temperature by equilibrating a fixed amount of chitosan with a fixed volume of experimental solution. The adsorbent to solution ratio was maintained same in all the experiments unless specified otherwise. To study the variations in metal-ion and NTA concentrations, and solution pH, with time during sorption, respective 1:1 metal-NTA solutions (22.5 mL) were equilibrated with chitosan (0.15 g).

To study the effect of pH on equilibrium sorption of NTA and metal ions from their respective aqueous solutions: For metal ion alone studies; 120 mg of the chitosan was treated with 18 mL of the 15 mM solutions of Co(II) or Cu(II), and for NTA alone studies; 60 mg of chitosan was treated with 18 mL of the 8 mM solutions of NTA.

The solutions were kept under stirring with constant speed in all sorption experiments. During sorption, pH and concentrations were monitored at fixed time intervals. Metal-ion concentrations were estimated using an Inductively Coupled Plasma-Atomic Emission Spectrometer. NTA concentrations were determined, using the UV-Visible spectrophotometer, by the dual wave length method, modified for NTA estimation. A Hach (sension 378) pH meter was used for pH measurements.

3.3 Results and Discussions

There are numerous reports on the metal binding by chitosan of which only a few focussed on the mechanisms involved in the metal ion-chitosan interactions [97, 112]. It is reported that though the hydroxyl groups (at the C-3 position; Fig. 3.1(i)) on chitosan also can contribute to metal-ion sorption [113], the uptake of metal ions are mainly effected via coordination with the amine (–NH_2) groups on chitosan [114]. Sorption of metal ions by chitosan, from a solution containing complexing agents, involves interplay of different mechanisms.

3.3.1 Mechanisms of Metal Uptake by Chitosan

When a solution containing metal ions/ligands or both is equilibrated with chitosan, the sorption can occur through the following modes of interactions.

I. <u>Chelation:</u> Chelation of metal ions by the –NH_2 and –OH groups of the chitosan (Eq. 3.1). This mode of metal-ion sorption is favoured by the presence of non-protonated amine (–NH_2) groups and non-complexing environment in the solution.

$$\mathrm{M^{2+} + R - NH_2 \leftrightarrow M(R - NH_2)^{2+}} \qquad (3.1)$$

Where, ‘R’ is the chitosan backbone. This mode of sorption leads to reduction in just the metal-ion concentration in the solution. Two models, (i) Pendant model (Fig. 3.1(i)), where the metal ion was bound to the amine group in a pendant fashion, and (ii) bridge model (Fig. 3.1(ii)), where the metal ion chelates with several amine groups from the same chain (intramolecular) or from different chains of chitosan (intermolecular), have been proposed for the metal removal through chelation [112].

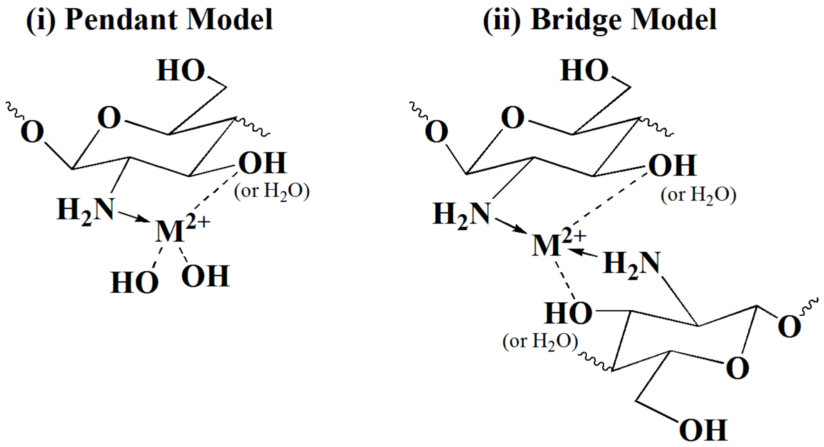

(i) Pendant Model

(ii) Bridge Model

Figure 3.1. Metal chelation by chitosan: (i) Pendant model and (ii) Bridge model

II. <u>Electrostatic attraction:</u> Chitosan can act as a weak base and is protonated in acidic solutions. pKa of chitosan, which mainly depends upon the degree of deacetylation, normally ranges between 6.2 and 6.7. Chitosan, with 87% deacetylation, is reported to have a pKa close to 6.5 [115]. In a solution containing complexing agents, protonated amine groups of the chitosan (i.e.,NH_3^+, Eq. 3.2) can sorb the negatively charged metal-ion complexes (i.e.,$[ML_x]^{n-}$, e.g., Eq. 3.3) through electrostatic attraction (Eq. 3.4). That is, protonation of amine groups leads to the uptake of anionic complexes and repulsion of free metal cations.

$$H^+ + RNH_2 \leftrightarrow (RNH_3)^+ \qquad (3.2)$$

$$Co^{2+} + H_3NTA \leftrightarrow [CoNTA]^- + 3H^+ \qquad (3.3)$$

$$(RNH_3)^+ + [ML]^{n-} \leftrightarrow [RNH_3 - ML]^{(n-1)-} \qquad (3.4)$$

This mode of sorption leads to reduction in both metal-ion and ligand concentrations in the solution.

III. Amide bond formation: This type of interaction is possible in solutions containing ligands with carboxylic acid functionalities. Covalent bond formation between the carboxylic groups of the ligands and –NH_2 group of the chitosan under favourable conditions leads to the sorption of ligand. Amide bond formation between EDTA and chitosan in acidic pH conditions was proved using FT-IR studies by Gylinè et al. [104]. This can result in the formation of an iminodiacetic acid group (or imino-monoacetic acid group if two –NH_2 groups are involved to yield diamide) linked to chitosan backbone [107]. The amide bond formation between chitosan and NTA is shown in Figure 3.2. This mode of sorption leads to reduced ligand concentration in solution. However, it is to be noted that the resultant iminoacidic groups are efficient metal chelating agents which can in turn complex with the free metal ions present in the solution thereby leading to further metal-ion sorption subject to the pH conditions as applicable.

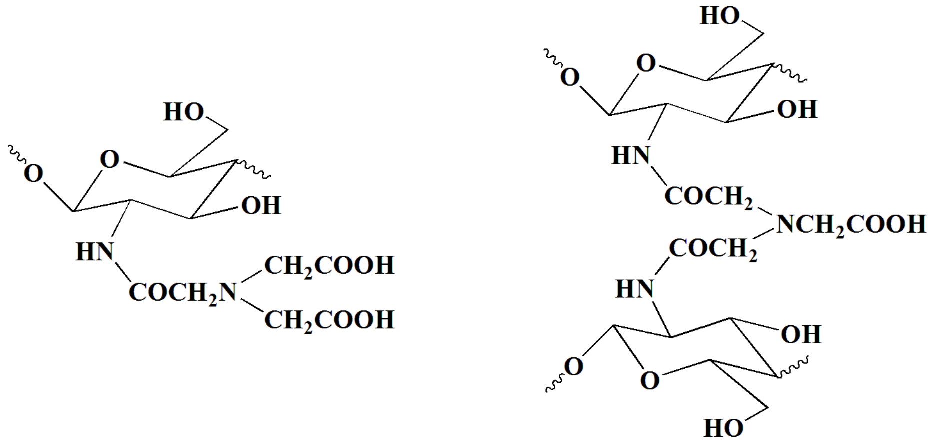

Figure 3.2. Amide bond formation between chitosan and NTA: Chitosan-NTA derivatives

The fraction of sorption occur through each mode is decided by a combination of factors such as the solution pH, stability of the complexes involved and the concentration of the various species present in solution. For example, the reactions (3.1) and (3.2) compete during equilibration of chitosan with a metal-ion solution in weekly acidic media. Such a complex interplay of different types of interactions involved in the sorption behaviour of chitosan, in presence and absence of complexing agent NTA, was studied in detail and the results are discussed here.

3.3.2 Sorption of Metal Ions by Chitosan from Complexing and Non-Complexing Solutions

Sorption capacities of chitosan for Co(II) and Cu(II), under different solution conditions like complexing and non-complexing solutions, were found out by batch studies with different solutions of metal ions. A 0.1 g of the chitosan was equilibrated with 15 mL of the solutions for the study and the results obtained are given in Table 3.1.

Table 3.1. Metal ion sorption by chitosan from complexing and non-complexing solutions: Uptake capacities and equilibrium pH obtained

Test Solution	**Metal Uptake**		**pH**	
	(µmol.g^{-1})	(%)	Initial	Equilibrium
14.30 mM Co(II) solution	282	13.6	5.5	6.0
13.78 mM Co(II) in 15 mM Acetate Solution	191	9.3	4.5	5.8
14.40 mM Co(II) 15 mM Citrate solution	1264	62.0	3.4	5.4
13.91 mM Co(II) in 15 mM NTA solution	366	18.6	2.7	6.3
14.51 mM Cu(II) solution	1918	92.0	4.5	5.7
14.30 mM Cu(II) in 15 mM Acetate solution	1699	80.2	4.3	4.7
14.37 mM Cu(II) in 15 mM Citrate solution	1813	88.8	3.1	4.3
14.68 mM Cu(II) in 15 mM NTA solution	840	39.0	2.6	6.8

Chitosan showed selectivity towards Cu(II) compared to Co(II). Uptake capacities were found to be affected by the solution nature, and the solution pH were found to shift towards neutral range on equilibration. The highest metal uptake was observed with Co(II)-citrate and Cu(II) solutions. The difference in uptake capacities obtained for Co(II) for complexing and non-complexing solutions indicated the interplay of different mechanisms. The decrease in sorption of Cu(II) from the non-complexing solutions acetate and water (non-buffered) solutions indicated the importance of equilibrium pH. NTA was chosen as the complexing agent to investigate the interplay of different kinds of interactions in the chitosan sorption, as it is the main constituent of the NAC formulation utilised for DCD.

3.3.3 Effect of Contact Time on Uptake of Metal-ions and NTA from Metal-NTA Solutions

Variations in metal-ion and NTA concentrations and solution pH with time during sorption were studied by equilibrating a 1:1 metal-NTA solution (22.5 mL) with chitosan (0.15 g).

3.3.3.1 Co(II) – NTA Case

The results obtained for the sorption studies using solution containing 14.1 mM Co(II) and 17.4 mM NTA are plotted in Fig. 3.3(a). It shows a sharp increase of Co(II) and NTA sorption, which then attains saturation, indicating the fast attainment of equilibrium. The increase in pH is due to the abstraction of free protons present in water by the amine groups of the chitosan. The increase in pH continued until equilibrium was attained. The rate of change in pH was very fast and comparable to that of Co(II)/NTA uptake by chitosan. Hence, the pH also reached a plateau on saturation. Protonation of the amine groups in chitosan enhances the sorption of the anionic complex, while it reduces the uptake of positively charged free metal ions. These two competitive (sorption modes I & II) processes play an important role in the sorption of metal ions and charged metal complexes from solutions containing metal ions and chelating agents. The uptake of Co(II) was seen to be comparatively more than NTA. This may be due to sorption of metal ions by both mode I (chelation) and mode II (electrostatic attraction of anionic Co-NTA species), whereas the uptake of NTA is, probably, only as its cobalt complex and not as free NTA.

3.3.3.2 Cu(II) –NTA Case

The results obtained for the sorption studies using solution containing 14.7 mM Cu(II) and 16.9 mM NTA was plotted in Fig. 3.3(b). In the case of Cu(II)-NTA solution; the sorption attained equilibrium quickly in a similar fashion to Co(II)-NTA. But, unlike as in the case of Co(II)-NTA, Cu(II) and NTA were sorbed in a 1:1 ratio which implied that the sorption was predominantly as negatively charged complex, $[\text{CuNTA}]^-$;(mode II). Since Cu(II) forms comparatively more stable complexes with NTA (Table 3.2), the chitosan amine groups may not be able to compete with NTA for the Cu(II) ions. Speciation studies using Visual MINTEQ (Version 2.61) indicated a higher fraction of Cu(II) being present as $[\text{CuNTA}]^-$, than Co(II) as $[\text{CoNTA}]^-$ in the lower pH values with the conditions provided.

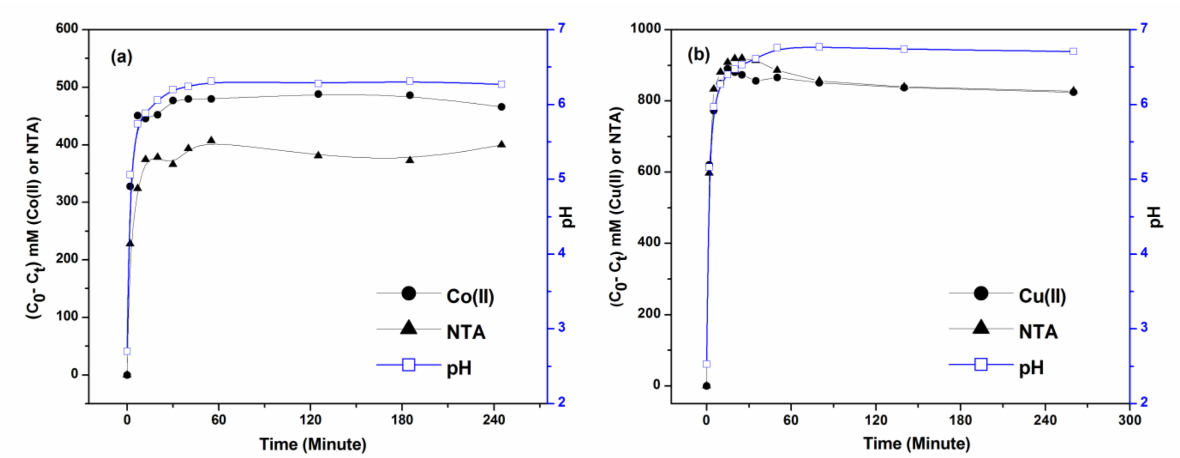

Figure 3.3. Effect of contact time on uptake of metal and NTA from Metal-NTA solutions: Change in solution pH, metal and NTA uptake by chitosan with time from (a) Co-NTA and (b) Cu-NTA solutions

3.3.4 Effect of pH on Equilibrium Uptake of Metal and NTA from Metal-NTA Solutions

To study the variation of the metal-ion and NTA uptake capacities with respect to pH; a 1:1 Metal-NTA solution was used in all the experiments. A constant pH (within ±0.3 during initial stages of sorption and ±0.1 towards the end) was maintained throughout the sorption experiments by adding 1 M NaOH or 1 M H_2SO_4 solutions. The change in pH was rapid in initial stages and slow towards the equilibrium.

Attainment of stable pH condition was fast for the pH values of 2, 3 and 7 while slow for the pH values of 4, 5 and 6. All the reactions were carried out until the pH stabilized (i.e., no change in the pH for at least 2-3 hours) and sampled for the estimation of metal and NTA uptake.

Table 3.2.Stability constant values for the NTA complexes of Co(II) and Cu(II), from NIST database (NIST critically selected stability constants of metal complexes, version 8.0.)

Chelate acidity	**logK**
$H^+ + NTA^{3-} = HNTA^{2-}$	10.29
$H^+ + HNTA^{2-} = H_2NTA^-$	2.91
$H^+ + H_2NTA^- = H_3NTA$	2.01
$H^+ + H_3NTA = H_4NTA^+$	1.0
Metal Complexes	
$Na^+ + NTA^{3-} = NaNTA^{2-}$	1.86
$Co^{2+} + NTA^{3-} = CoNTA^-$	10.38
$Co^{2+} + 2\ NTA^{3-} = Co(NTA)_2^{4-}$	14.33
$Co^{2+} + NTA^{3-} + H_2O = Co(OH)NTA^{2-} + H^+$	10.80
$Cu^{2+} + NTA^{3-} = CuNTA^-$	13.0
$Cu^{2+} + 2\ NTA^{3-} = Cu(NTA)_2^{4-}$	17.4
$CuNTA^- + H^+ = CuHNTA$	1.6
$Cu^{2+} + NTA^{3-} + H_2O = Cu(OH)NTA^{2-} + H^+$	9.2

3.3.4.1 Co(II) - NTA Case

The uptake of both cobalt and NTA was found to be increasing with pH with two maxima, one at pH ca. 6 and the other at pH ca. 3 (Fig. 3.4(i)). Even though there was a change in the individual capacity values obtained for Co and NTA at each pH for different repetitions, the trend in the capacity variation with equilibrated pH remains the same. There was a change in ratio of cobalt and NTA sorbed at each pH range. Speciation calculations done using Visual MINTEQ showed the presence of free NTA at the lower pH regions, and under the conditions provided. Functional groups generated through the amide bond formation may be responsible for the lower sorption maxima at pH ca. 3 (sorption through mode III). The major presence of free metal ion and NTA (as shown by the speciation calculations) and the competition from the SO_4^{2-}, from the sulphuric acid added for pH adjustment, with the complexed $[\mathrm{Co}-\mathrm{NTA}]^-$ for the protonated amine groups may be responsible for the reduced sorption at pH 2. At lower pH, the counter anion SO_4^{2-} can compete with the anionic complex species for the protonated amine groups of the chitosan [115]. The higher sorption maxima, around pH 6, where the competition of SO_4^{2-} is minimum, could be through the electrostatic interactions between the complexed anion, $[\mathrm{Co}-\mathrm{NTA}]^-$, and protonated amine groups of chitosan (sorption through mode II). The decrease in sorption beyond this point, i.e., pH 7 is due to the reduced fraction (< 20%) of protonated $–NH_2$ groups in the chitosan [100]. As all the cobalt and NTA are present as $[\mathrm{Co}-\mathrm{NTA}]^-$, and the majority of the chitosan $–NH_2$ groups being in neutral form, the only possible way is the competitive sorption of Co(II) by the chitosan through mode I against complexation by free NTA in the solution. Hence, there was reduced sorption at this pH. The reduced pick up in the pH region 4–5 may be due to the reduced sorption via formation of amide bond and reduced availability of free NTA, which added to the competition from SO_4^{2-} to $[\mathrm{Co}\text{-}\mathrm{NTA}]^-$.

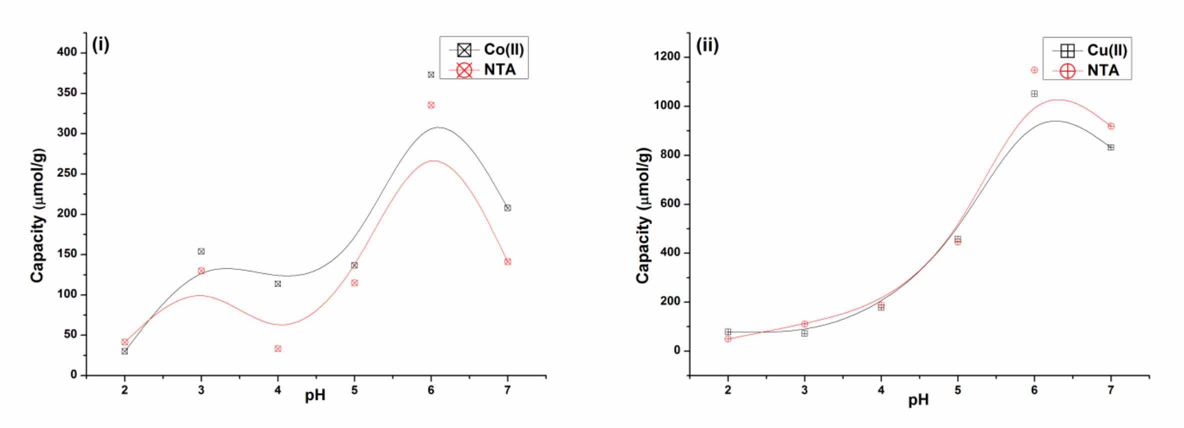

Figure 3.4. Effect of pH on equilibrium uptake of metal and NTA from Metal-NTA Solutions: Change in uptake capacities with pH for (i) Co(II)-NTA and (ii) Cu(II)-NTA

3.3.4.2 Cu(II) – NTA Case

The uptake of copper and NTA increased with increase in pH and gave a maximum sorption capacity near pH 6 (Fig. 3.4(ii)). The uptake of Cu(II) and NTA proceeded in a nearly 1:1 ratio, which implies that copper and NTA were taken as the Cu(II) –NTA complex (mode II). The very large log K values (Table. 3.1) for Cu(II) –NTA complexes makes it difficult for Cu(II) to be sorbed through mode I. Speciation studies also showed almost complete conversion of the Cu(II) to the complexed form even at lower pH conditions under the experimental conditions. This ensures uptake to be only as $[\mathrm{Cu\text{-}NTA}]^-$ complex. But, at pH 6 and beyond, due to availability of an excess amount of free $-NH_2$ groups, there can be sorption of free Cu^{2+} ions to some extent. Comparatively (as compared to in case of Co(II)–NTA) low fraction of the free NTA present in solution under the experimental conditions (as calculated using Visual MINTEQ) might have hindered the sorption mechanism through amide bond formation. These factors make the sorption at acidic pH less for Cu(II)–NTA than for Co(II)–NTA. But, as the pH is increased Cu(II) forms the anionic complex, $[\mathrm{Cu\text{-}NTA}]^-$, and the competition from SO_4^{2-} also decreases. This results in increased sorption trough mode II. Hence, the capacities increased with increase in pH. At these pH values (beyond 4), the Cu complex uptake was more than that of Co which is due to the well-known general higher preference for copper by the sorbent [116, 117]. The decrease in sorption capacity above pH 6 indicates that the interaction involved in the sorption of copper-NTA is an electrostatic one. The optimum pH range for $[\mathrm{Cu} - \mathrm{NTA}]^-$ sorption was found to be around pH 6, which is close to the pKa of chitosan's amine protonation [103].

The optimum pH range for obtaining the maximum uptake capacities was found to be the same for both Cu(II) and Co(II) in NTA medium. This implies that the optimum pH, for obtaining the maximum uptake, is mainly dependent on the nature of the ligand (NTA) and the chitosan functional group. The report by Juang et al. on the sorption of Cu from solutions containing different complexing agents, which reported different optimum pH range for different complexing agent solutions, also supports this argument [100].

3.3.5 Effect of pH on Equilibrium Sorption of Metal ions and NTA from Their Respective Aqueous Solutions

Variation in sorption capacities for Co(II), Cu(II) and NTA from their respective solutions on chitosan was also carried out for comparison.

3.3.5.1 Co and Cu Cases

In the case of metal-ion solutions, below pH 6.5, the metal-ions have to compete with H^+ ions for sorption by chitosan. At very low pH, the uptake capacity was found to be negligible and then increased with increase in pH (Fig. 3.5(i)). The uptake capacity for copper was found to be increasing rapidly along with the increase in pH as compared to cobalt. Chitosan was found to be more selective towards copper under all pH conditions as reported in earlier studies [116-118]. This observation is in accordance with the Irving-Williams series which gives the stability sequence of high spin octahedral metal complexes for the replacement of water by other ligands. The exothermic enthalpies reported by I.S. Lima et al. from calorimetric titration studies of metal-ion sorption on chitosan also support the higher sorption of copper [119].

3.3.5.2 NTA Case

For NTA sorption, an 8 mM aqueous solution of NTA was used. A dosage of 60 mg of chitosan per 18 mL of the NTA solution was used in all the experiments so that the number of sorption sites available in chitosan for the uptake of NTA was comparable with the conditions maintained in metal-ion/NTA complex studies. The results showed a sharp decrease in NTA sorption after pH 6 (Figure 3.5(ii)). The maximum sorption was found to be at around pH 4-5 where both the protonated amine groups and the anionic form of NTA ($HNTA^{2-}$) are in significant amount. The slightly reduced sorption at pH 3 may be, because of the competitive counter anions (SO_4^{2-}) and predominant presence of free NTA at this pH. Decrease in sorption capacity above pH 6, even though the fraction of anionic form of NTA increases, is because of the deprotonation of the amine groups. Navarro et al. had plotted the variation in protonation of the amine groups with change in pH [115]. Above pH 6.5 most of the amine groups will be in the –NH_2 form and hence the NTA uptake capacity decreases drastically above pH 6.

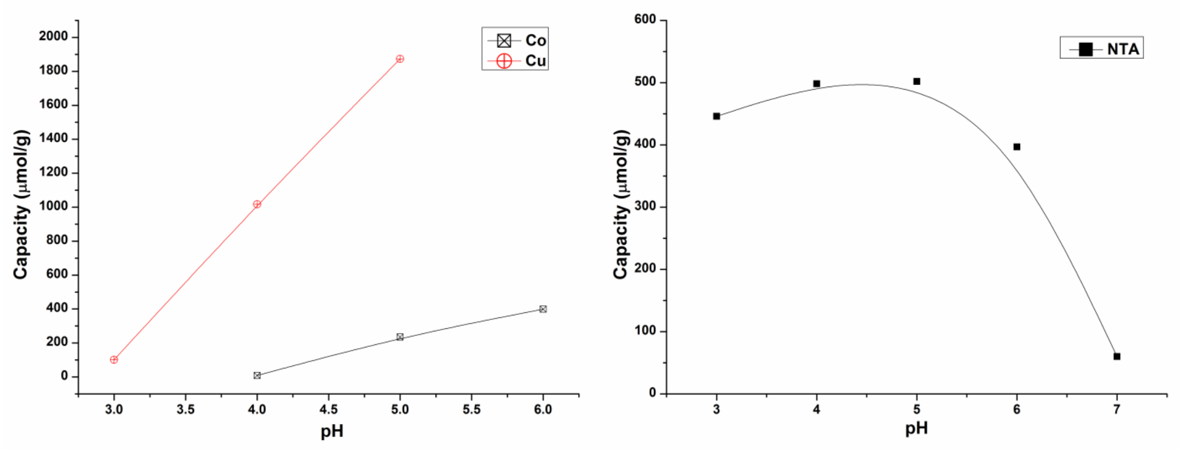

Figure 3.5. Effect of pH on equilibrium sorption of metal ions and NTA from their respective aqueous solutions: Change in uptake capacities with pH for (i) Co and Cu and (ii) NTA

It is interesting to note that the there is a drastic reduction in the NTA sorption beyond pH 6 (goes to near zero sorption at pH 7) for the NTA alone studies (Fig.3.5) as compared to the metal ion-NTA cases (Fig. 3.4). This observation may indicate the possibility of metal-ion assisted NTA sorption by chitosan's free –NH_2 groups over and above the other modes of sorption. The former occurs when the free (deprotonated) –NH_2 groups of the chitosan complex with the metal-ion/NTA complex in the solution by replacing the complexed water molecules. This mode of sorption is not available in NTA alone case and thereby leads to reduced sorption at higher pH as compared to metal-ion/NTA cases.

3.3.6 Equilibrium Modelling of Cobalt and NTA Sorptions: Adsorption Isotherms

Cobalt and NTA sorption (from their individual solutions) data were fitted with Langmuir and Freundlich sorption isotherm models (Eq. 2.6 and Eq. 2.8 respectively, section 2.5.2). Cobalt and NTA sorptions were found to be fitting in both Langmuir and Freundlich models in the concentration range of 0.083–0.82 mM for cobalt and 0.91–4.42 mM for NTA (Fig. 3.6 and 3.7). However, cobalt sorption in the concentration range of 0.82–50.72 mM was found to fit in Freundlich model alone (Fig. 3.7 b). The equilibrium pH for cobalt sorption was 6.0 (±0.2) and for NTA it was 5.9 (±0.2). The Langmuir and Freundlich parameters obtained from the plots were given in Table 3.3.

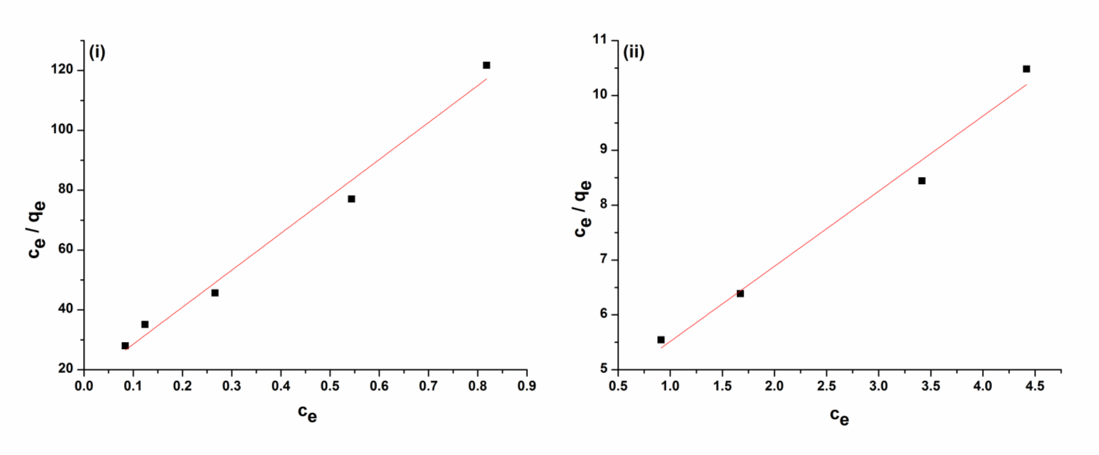

Figure 3.6. Langmuir plots for (i) Co(II) and (ii) NTA sorption over chitosan

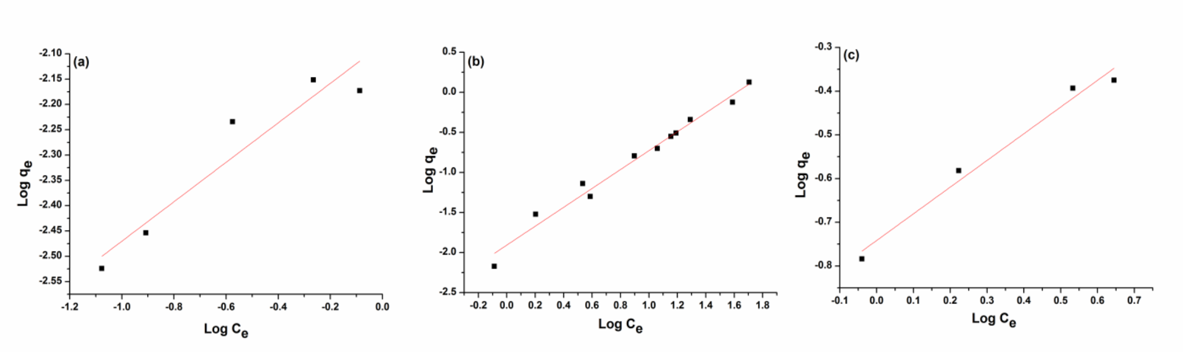

Figure 3.7. Freundlich plots for (a) Co(II); C_e: 0.083–0.82 mM, (b) Co(II); C_e: 0.82–50.72 mM and (c) NTA; C_e: 0.91–4.42 mM, sorption over chitosan

Table 3.3. Langmuir and Freundlich isotherm parameters for cobalt and NTA sorption

Sorbate	**Conc. range** (mM)	**Langmuir parameters**		**R^2** (Langmuir)	**Freundlich parameters**		**R^2** (Freundlich)
		Q^0 (µmol.g^{-1})	**b**		**K_F** (L.g^{-1})	**1/n**	
Co(II)	0.083 - 0.82	8.1	7.61	0.985	0.831 x 10^{-2}	0.39	0.910
	0.82 - 50.72	--	--	--	0.165 x 10^{-1}	1.08	0.987
NTA	0.91 - 4.42	730.1	0.33	0.983	0.181	0.61	0.980

3.3.7 Relative Metal-ion Sorption by Chitosan: Selectivity Variation with pH

The inherent capacity of chitosan for Cu(II) is known to be very high compared to other metal ions [117]. Earlier reports on the competitive sorption of metal cations on chitosan show that it will be difficult to separate other metal ions like Co(II) by chitosan sorption in presence of Cu(II) [120, 121]. However, the results discussed above on complexation of these metal ions with NTA and their subsequent sorption with chitosan indicate a possibility that the capacity, and hence the selectivity, of chitosan for metal cations can be varied by changing the equilibrium pH of the metal-complex solution. To investigate this possibility, competitive sorption study using Co(II) and Cu(II) together in NTA solution with a molar ratio 1:1:2 of Cu(II):Co(II):NTA was carried out. 0.12 g chitosan to 18 mL of the solution was used. The results (Table 3.4) showed that cobalt was preferentially sorbed at lower pH compared to copper. Equilibration time needed was found to be more at lower pH. During the equilibration, Cu(II) was sorbed initially and then slowly replaced by Co(II) before attaining equilibrium. Even though the pH of the solution stabilized within a short period, the metal-ion concentration in the solution varied, as was evident from the ICP-AES analysis carried out during the course of the sorption experiment. Solution concentration of Cu(II) increased in the solution while Co(II) decreased, due to desorption/sorption. While at higher pH (pH 6), time required for attaining the equilibrium was very less (less than 2 h), and the amount of copper sorbed was more (Table 3.4).

Table 3.4. Relative sorption of Co(II) and Cu(II) in NTA medium over chitosan: Selectivity variation with pH

$\mathbf{pH_{Eq.}}$	$\mathbf{t_{Eq.}}$ (h)	**Sorption Capacity** (μmol.g^{-1} of chitosan)			**Selectivity Coefficient** ($k_{Co/Cu}$)
		Co(II)	**Cu(II)**	**NTA**	
2.9	78	145	76	176	2.08
6.0	6	93	617	715	0.07

The reversal in selectivity is reflected clearly in the selectivity coefficient ($k_{Co/Cu}$) values obtained at these respective pH conditions as shown in Table 3.4. Ratio of the total metal-ion (Co(II) + Cu(II)) capacity to that of NTA was found to be 1:1 at pH 6, while at pH 2.9, a little more metal-ion sorbed chitosan was obtained. As Co(II) was sorbed more at pH 2.9, the difference in uptake of metal-ion and NTA was expected.

3.4 Conclusion

The biosorbent chitosan can be used for removing both metal ions and NTA from their solutions. Different mechanisms operate, according to the solution nature and pH, during the sorption of metal ions. In a non complexing solution, sorption of the metal-ions (Co and Cu) was found to increase with increase in pH while an optimum pH range was observed for their maximum uptake from complexing media. The optimum pH range seemed to be dependent on the nature of complexing agent and independent of the metal-ion used. The optimum pH range for NTA uptake from NTA solution was found to be around pH 5 and that for copper and cobalt sorption respectively from Cu(II)-NTA and Co(II)-NTA solutions was found to be around 6. Chitosan was found to be more selective towards copper in general. However, from metal ion-NTA solutions, sorption of Co(II) was found to be favoured at lower pH, whereas Cu(II) was favoured at higher pH. Change in selectivity with pH suggests that the mechanism involved in the sorption of metal ion-NTA complexes varies with pH and the speciation profile. Such variation of metal ion selectivity with pH can be utilised towards devising selective metal ion separations using chitosan.

Chapter 4. COBALT(II) – ION IMPRINTED CHITOSAN FOR SELECTIVE REMOVAL OF COBALT DURING NUCLEAR REACTOR DECONTAMINATION

4.1 Introduction

Sorption behaviour of chitosan in presence and absence of complexing agents such as NTA has been discussed in detail in the previous chapter. Various mechanisms that operate during the sorption processes and the selective removal of metal ions by the careful consideration of solution nature and pH also were discussed. Even though chitosan can act as a good sorbent under a wide range of conditions, its use in acidic solutions is limited because of its solubility in dilute organic and mineral acids (except H_2SO_4) [122]. Crosslinking of chitosan can reduce its solubility in dilute acids and also can impart improved physical and mechanical properties. However, crosslinking decreases the amount of complexing groups in chitosan, which are primarily responsible for the sorption, and thus negatively affects the uptake capacity of chitosan [123]. Such crosslinking, however, do not always lead to enhanced selectivity, whereas preparation of crosslinked chitosan through metal ion imprinting method can lead to enhanced selectivity towards the target ion of interest [51, 59, 124]. Molecular/metal ion imprinting has been reported widely for synthesizing selective sorbents for various molecules and metal ions [125]. These are highly crosslinked polymers synthesized in presence of a chosen molecule or metal ion as the template. The template is subsequently removed to get the molecularly/metal ion imprinted polymer (MIP).

The major contributor towards the radiation field build-up in PHWRs is the radioactive cobalt (^{60}Co and ^{58}Co). The main corroding surface in primary cooling water circuits of PHWRs is of carbon steel. Hence, the major amount of the metal ions removed during decontamination is the largely non-radioactive ferrous ions, while the physical quantity of radioactive metal ions is very minimal [4]. Use of conventional ion exchange resins for removing the metal ions generated during chemical decontamination campaigns leads to generation of large volume of radioactive waste because of the lack of selectivity. Selective removal of radioactive metal ions can lead to reduced volume of the radioactive resin waste generated. Synthesis and utilisation of a Co(II) ion imprinted polymer for such a use was reported earlier [5]. Designing biosorbents, with the ability to remove these radioactive ions selectively, can make the process more economical and environment friendly. We have attempted to alter the selectivity of chitosan by Co(II) imprinting in this context to make it usable in the DCD of NPPs.

Though there are reports on use of chitosan and cobalt imprinted chitosan for cobalt sorption, they do not address the selective removal of Co(II) in presence of large excess of Fe(II) from complexing medium [109, 126]. A Co(II)-ion imprinted chitosan using epichlorohydrin as the crosslinker was synthesised with this objective. Synthesis, and evaluation of the sorption properties of the Co(II)-ion imprinted chitosan vis a vis to those of non-imprinted and raw chitosan are discussed in this chapter. The applicability of the imprinted chitosan, under typical decontamination conditions in particular, was investigated in detail.

4.2 Experimental Details

4.2.1 Synthesis of the Co(II)-ion Imprinted and Non-ion Imprinted Chitosans

Synthesis of the Co(II)-ion imprinted and non-ion imprinted polymers had been discussed in the section 2.3. The scheme for the synthesis is given in Fig. 4.1.

4.2.2 Sorption Studies

To study the Co(II)-ion uptake by the sorbents (MIP, NIP and chitosan) from complexing (citrate and NTA) and non complexing conditions, batch sorption studies were carried out by equilibrating 20 mg of the sorbents with 2 mL of the respective solutions. Kinetic studies were done by equilibrating 100 mg of the MIP with 10 ml solution of 4 mM Co(II) in 50 mM citrate buffer (pH 4.8).

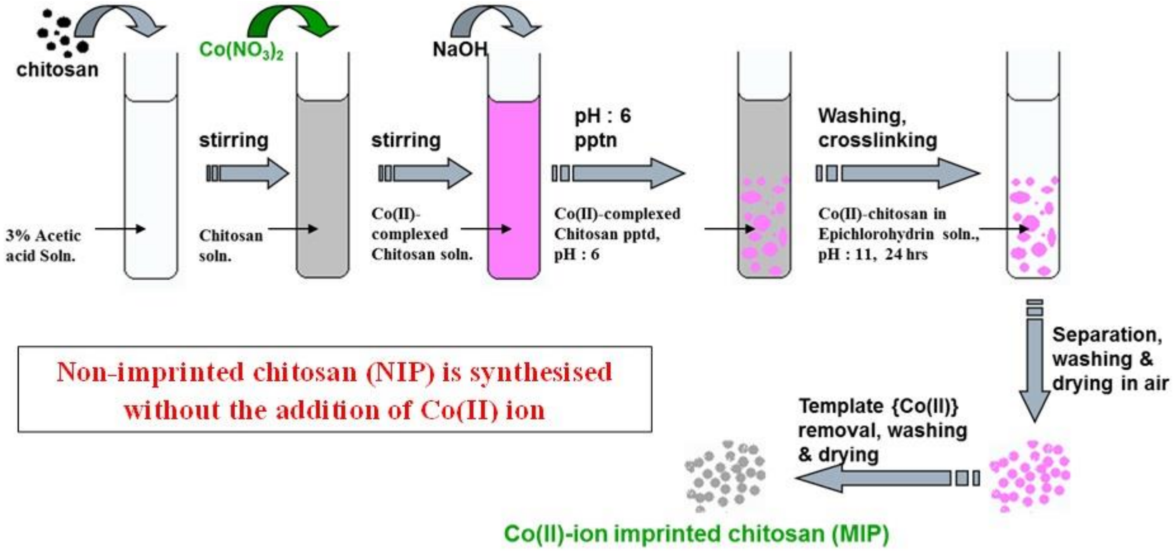

Figure 4.1. Schematic of the procedure for Co(II) ion imprinted (MIP) and non-imprinted (NIP) chitosan synthesis

4.3 Results and Discussions

4.3.1 Synthesis of the Metal-ion Imprinted Polymer

There are many reports on synthesis of metal ion imprinted chitosans for different metal ions using various crosslinking agents namely, glutaraldehyde [51], epichlorohydrin [50] and ethylene glycol diglycidyl ether [127]. We have adopted a two-step process in preparing the MIP, which involved synthesis of cobalt (II) complexed chitosan followed by freezing the complex configuration through crosslinking polymerization with epichlorohydrin. Epichlorohydrin is known to be crosslinking through the hydroxyl groups of chitosan [128]. Thus, the amino groups, the most important complexing groups of the chitosan, remain available for the metal ion binding at the imprinted sites. Acid extraction of the cobalt ions (template) from the crosslinked chitosan gave the metal ion imprinted chitosan (MIP). The amount of template removed was estimated by measuring the amount of cobalt in the acid extracts by ICP-AES. The maximum theoretical capacity that can be attained by the MIP could thus be calculated, and was found to be 500 µmol of Co(II) per g of MIP.

4.3.2 Evaluation of Sorbents under Complexing and Non Complexing Conditions

Uptake of metal ions by chitosan is known to be dependent on the solution nature and pH [115]. The sorption characteristics of the sorbents (MIP, NIP and chitosan) were thus investigated under various solution conditions by batch sorption studies with solutions of Co(II) in ultrapure water, acetate buffer, citrate buffer and in citrate buffer containing NTA. The uptake capacities obtained are tabulated in Table 4.1. The capacity values indicate reduction in sorption capacity in the MIP and NIP as compared to the chitosan. The reduction in capacity is attributable to crosslinking, which reduces the available free binding sites for metal sorption. The presence of the metal ion template ensures an effective availability of the binding sites in MIP unlike in the case of NIP, which was synthesized in the absence of the template ion. Therefore, among the MIP and NIP, the former exhibits a higher capacity for metal ion uptake.

Table 4.1.Co(II)-ion uptake by the sorbents from complexing (citrate and NTA) and non complexing aqueous solutions

Solution	**$pH_{Eq.}$**	**Capacity** (µmol.g^{-1})		
		MIP	**NIP**	**Chitosan**
4.2 mM Co^{2+} in water	6.0	46.7	16.6	72.5
3.9 mM Co^{2+} in 50mM Acetate Buffer	4.9	3.6	BDL*	32.1
5.1 mM Co^{2+} in 50mM Acetate Buffer	5.6	51.0	10.1	117.9
4.1 mM Co^{2+} in 50mM Citrate Buffer	4.7	76.6	16.5	199.6
4.2 mM Co^{2+} and 4mM NTA in 50mM Citrate Buffer	4.5	92.2	32.8	210.9

*BDL–Below Detectable Limit

In the previous chapter, it was shown that the metal ion uptake by chitosan from non complexing medium increases with increase in pH and an optimum pH is generally seen for the metal ion uptake from complexing medium. Accordingly, the uptake of Co(II) by the MIP and chitosan was found to be very less at pH 4.9 in the non-complexing acetate medium (Table.4.1) and it can be attributed to the competition from the H^+ ions for the binding sites. The effect of pH is further demonstrated by the increased uptake of Co(II) from the acetate solution at pH >5. Near similar capacity values in acetate and non-acetate medium at similar equilibrium pH values indicate the absence of any significant interference by acetate on cobalt sorption.

The significant increase in uptake capacities of MIP, NIP and chitosan in presence of citrate solution, as compared to the non-complexing solutions, indicates that there is synergistic effect by the citrate during the Co(II) sorption. This is not the case with other metal ions such as Cu (II), wherein the presence of the complexing agents in the solution is known to reduce the metal ion uptake by chitosan [100]. Similar results were obtained in our earlier studies as well, wherein chitosan showed a reduced uptake of Cu(II) and an increased uptake of Co(II) from their respective complexing (NTA) solutions as compared to the uptake from their non complexing solutions (Section 3.3.2).

This indicates that the uptake mechanism in the citrate medium is different from that in the non complexing medium and that the citrate also plays a role in the enhanced uptake shown by all the three sorbents (MIP, NIP and chitosan). However, in the case of the MIP, the favorable geometry created via imprinting leads to higher selectivity in favor of the Co(II) ion (vide infra). Sorption results obtained in presence of NTA (Table 4.1) showed that the Co(II) uptake was not affected significantly by the presence of NTA.

4.3.3 Evaluation of Sorption Capacities for Co(II) and Fe(II) from Their Respective Citrate Solutions

The sorption capacities of the sorbents for the target ion Co(II) and the competitor ion Fe(II) were investigated in complexing citrate medium. It has been reported that the uptake of metal ions on chitosan from the complexing citrate medium is favored in the pH range of 4.8 – 5.2 [103, 105], which is also the pH range generally maintained during the chemical decontamination. Thus the sorption studies were done with pH 4.8 citrate buffer (50 mM) solution containing 4mM Co(II) or Fe(II). 20 mg of the sorbents (MIP, NIP and chitosan) were treated with 2 mL of the respective metal ion solutions. Raw chitosan displayed a higher uptake capacity for Fe(II) than Co(II) and the non-imprinted chitosan (NIP) showed almost equal capacities for both, whereas the imprinted chitosan (MIP) showed a higher sorption capacity for Co(II) than Fe(II) (Fig. 4.2). The Fe(II) selectivity showed by the chitosan is in agreement with the Irving-Williams series of complex stability [129]. In case of the NIP, the capacity values (Co(II):16.5 ± 1.5 μmol.g^{-1} and Fe(II): 13.3 ± 1.4 μmol.g^{-1}) were very less as the crosslinking reduces the available functional groups. In case of the MIP, however, the presence of template ion ensures relatively higher availability of the functional groups, which were complexed to the template ion during the MIP synthesis.

The effect of imprinting with Co(II) as the template ion is exemplified by the selectivity shown by the MIP in favour of Co(II) over Fe(II) as compared to the NIP and the raw chitosan. Thus, a complete reversal in the selectivity of chitosan was realized through metal ion imprinting. This is due to the presence of the template ion during polymerization, which leads to pre-organization of the available functional groups to yield sorption cavities with geometries more stable for the template ion used (Co(II)) than for the competitor ion (Fe(II)). The viability of imprinting in a chitosan derivative to differentiate two different geometries was earlier demonstrated by Baba et al. using Pd(II) as the template ion [130].

The report showed that the palladium(II)-imprinted-N-[pyridylmethyl]chitosan prepared selectively sorbs ions that form a complex with similar geometry as formed by the template, Pd(II), in the imprinted cavity against other ions that form complexes with different coordination geometry. In the present case, however, the competition is between two adjacent transition metal ions, which have similar oxidation state and predominantly form complexes of similar coordination number and geometry. Despite such similarity, clear differentiation has been realized through imprinting [5]. Theoretical studies carried out by Bhaskarapillai et al. on the observed selectivity of an organic cobalt imprinted polymer for cobalt over ferrous showed that such differentiation was feasible due to favourable formation energy for the template ion within the imprinted sites even though they form similar complexes in the imprinted sites [131]. The results obtained in the present study indicate that such factor must be operating in chitosan as well. However, definite quantitative conclusion requires more studies involving detailed theoretical calculations for various possible geometries.

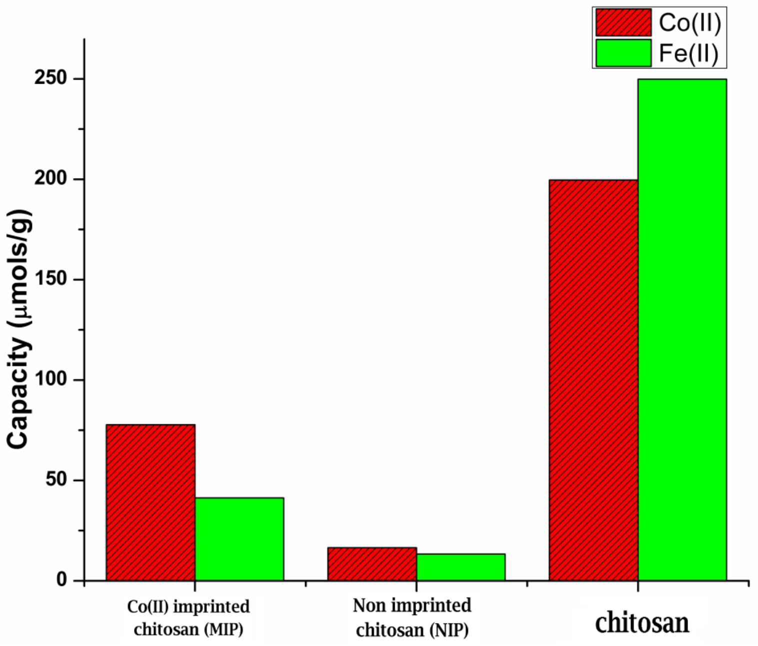

Figure 4.2. Sorption capacities of the sorbents for Co(II) and Fe(II) from their respective citrate solutions

4.3.4 Competitive Sorption of Co(II) and Fe(II) by the Sorbents under Complexing Conditions

For investigating the suitability of the MIP prepared for the intended application in the nuclear industry, the sorbents have been tested for their competitive cobalt sorption ability in presence of ferrous ions under complexing conditions. To study the effect of pH on the uptake capacity and selectivity of the sorbents; batch sorption studies were carried out with MIP, NIP and chitosan (20 mg each) with 2:2:50 mM of Co(II):Fe(II):Citrate solutions (2 mL each) having different pH values.

4.3.4.1 Uptake Capacities

The competitive sorption studies have indicated that both the NIP and chitosan show a higher uptake of Fe(II) than Co(II) in all the pH conditions studied, while the selectivity of the MIP was found to be dependent on the solution pH (Fig. 4.3). Maximum uptake of Co(II), for the MIP and chitosan, was found to be in the region of pH 4. In the case of NIP, both Fe(II) and Co(II) showed an uptake maximum at around pH 4.8. In the case of MIP, while there was a peak maximum for the Co(II) uptake, there was continuous decrease in the Fe(II) uptake capacity. As could be seen in the graphs (Fig. 4.3), the trend in change in capacity with respect to pH was found to be different for MIP, NIP and chitosan cases. There was significant decrease in the uptake of both the metal ions by the MIP at pH > 5.

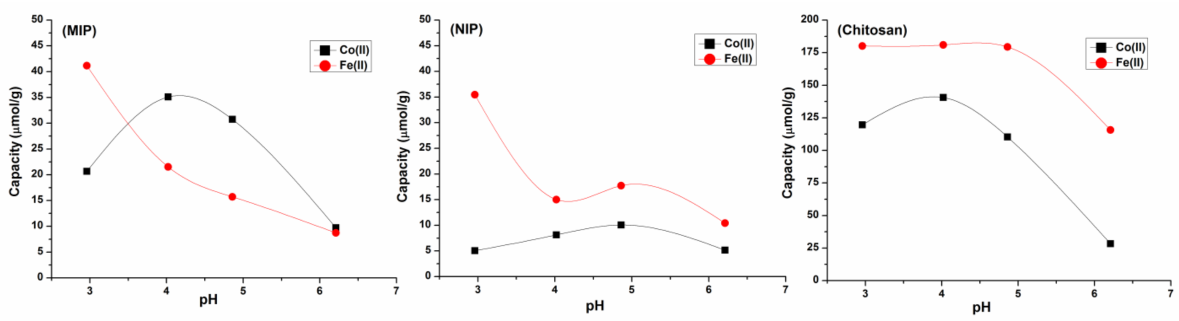

Figure 4.3. Effect of pH on the Co(II) and Fe(II) uptake capacities of MIP, NIP and chitosan: Competitive sorption of Co(II) and Fe(II) by the sorbents

4.3.4.2 Selectivity and Imprinting Factor

The MIP showed maximum selectivity for Co(II) at pH 4.8 (Fig. 4.4(i)). The imprinting factor (i.e., the increase in selectivity due to imprinting) was found to be above 2.0 in all the pH conditions studied (Fig. 4.4(ii)), indicating the effectiveness of imprinting. As the optimum pH range obtained is very near to the pH conditions maintained during the decontamination of the PHWRs, the MIP has the potential to be used for the selective removal of Co(II) from the decontamination formulation.

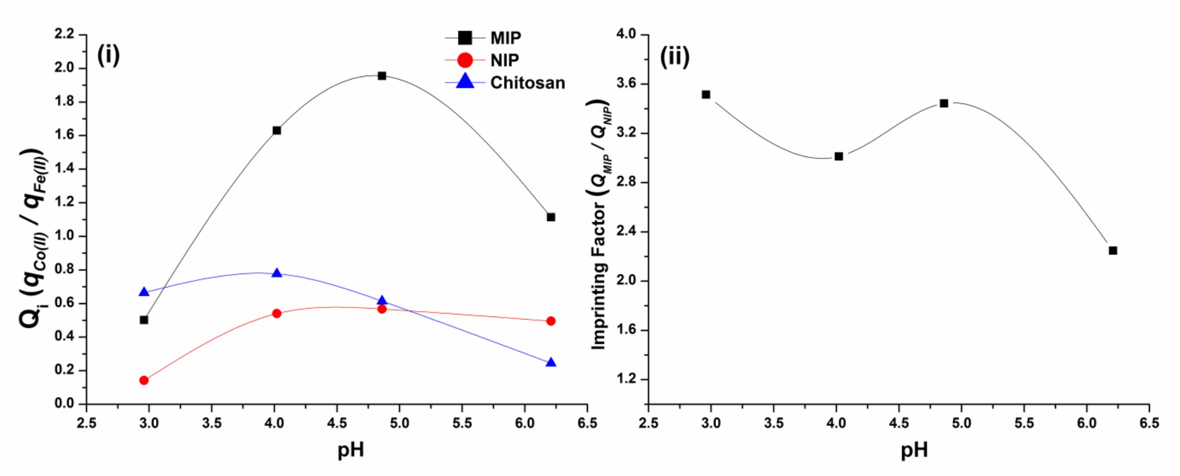

Figure 4.4. Competitive sorption of Co(II) and Fe(II) by the sorbents: Effect of pH on (i) Selectivity (ratio of Co(II) capacity over Fe(II) capacity) of MIP, NIP & chitosan and (ii) Imprinting factor

4.3.5 Evaluation of MIP in a Typical Decontamination Formulation (NAC Medium)

NAC (NTA-Ascorbic acid-Citric acid) based formulations are normally employed for the dilute chemical decontamination of PHWRs [132]. Hence, the ability of the MIP to sorb cobaltous ions present in very low level concentrations, in presence of large excess of ferrous ions, was investigated by conducting batch sorption studies in NAC medium. 20 mg of the MIP (or chitosan) was equilibrated with 2 mL of the test solutions (4.0 mM Fe(II) and 10.0 µM Co(II) in NAC formulation) for this purpose. The typical NAC formulations used contained 1.4 mM NTA, 1.7 mM ascorbic acid and 50 mM citric acid. The results (Table 4.2) show that while chitosan is selective towards Fe(II), the MIP is selective towards Co(II) in the complexing NAC medium. Percentage removal of Fe(II) by chitosan is seen to be almost twice that of cobalt, while for the MIP the Co(II) removal is twice that of Fe(II) removal. Even though 100% exclusion of Fe(II), which would lead to complete separation of Co(II) from Fe(II), was not achieved, significant selectivity for Co(II) could be introduced in chitosan through imprinting. The workability of the MIP with low level cobalt concentrations in the NAC medium indicates its potential for application in nuclear reactor decontamination.

Table 4.2.Evaluation of the sorbents in typical decontamination formulation: Co(II) and Fe(II) removal by MIP and chitosan

Sample	**Percentage removal** (%)	
	Co(II)	**Fe(II)**
MIP	26.3	14.7
Chitosan	45.2	83.1

4.3.6 Sorption Kinetics

Studies were undertaken to monitor the variation in uptake of the metal ions and desorption of the loaded metal ion with time, in order to understand the possibilities of the effective use of the sorbents in column/batch experiments and for reusing the same through regeneration.

4.3.6.1 Variation of Cobalt Uptake with Time

Sorption kinetics was studied in batch mode and periodic samplings were carried out for following the sorption. The variation in cobalt uptake by the MIP with time was monitored and plotted (Fig. 4.5(i)). The uptake increased with time and stabilized over a period of 3 days. The long contact time required for the sorption limits the application of the MIP in online real time applications but it can be made use of in (back end) batch operations.

Co(II) sorption kinetics was found to be following the pseudo second order kinetic rate equation (Eq. 2.12). The fitting parameters obtained were; the adjusted R^2: 0.9926, q_e: 80.45 (μmol. g^{-1}) and K_2: 11.08x10^{-04} (μmol^{-1} $hour^{-1}$).

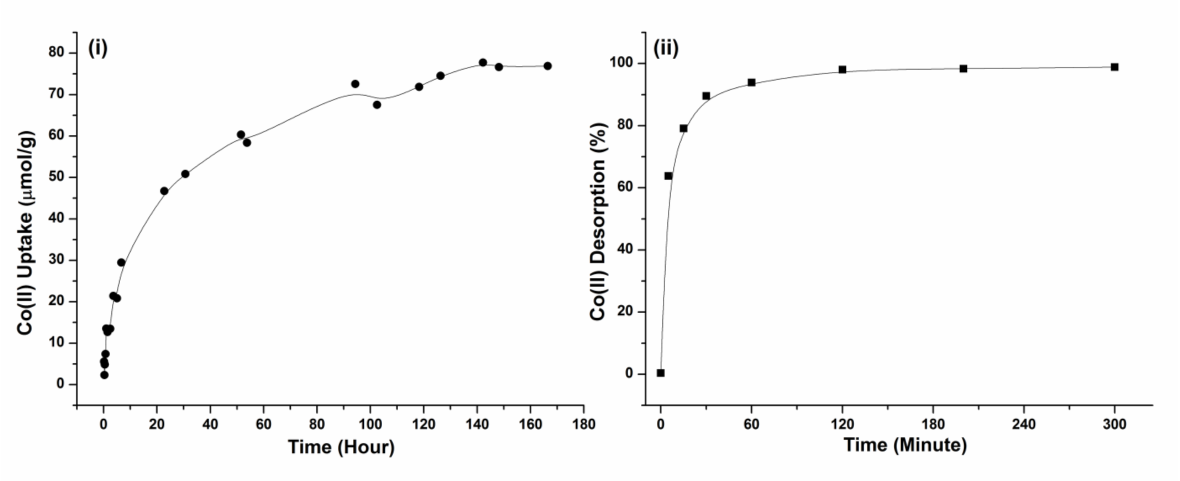

Figure 4.5. Kinetics of Co(II) sorption and desorption: (i) Metal uptake and (ii) Desorption using 0.25 M H_2SO_4 with time

4.3.6.2 *Desorption and Reuse*

Desorption of the Co(II) cations loaded on the MIP was also carried out in batch mode using 0.25 M H_2SO_4 solution as the eluent. Concentration of the cobalt eluted out with time was monitored (Fig. 4.5(ii)). Desorption was found to be fast and complete. Almost 100% of the bound Co(II) was desorbed in less than 1 h of contact with the eluent. The regenerated MIP (even after multiple times of loading and desorption), when equilibrated with the metal ion solutions, was found to have retained the selectivity and capacity. Therefore, repeated use of the sorbent is feasible.

In case of the raw chitosan, it was found that the attainment of sorption saturation was very fast and instantaneous (Section 3.3.3). The long equilibration time required in case of the imprinted chitosan may be because of the very low porosity in the MIP as a result of crosslinking, which makes it relatively difficult to access the binding sites of the MIP as compared to the raw chitosan. Further, the reduction in the concentration of the functional groups in the crosslinked polymer as compared to the raw chitosan also leads to slow kinetics in the former.

4.3.7 Effect of the Crosslinking Agents Used and Irradiation on the Uptake Capacity and Selectivity of the MIPs

In order to study the effect of radiation and the crosslinking agents used on the sorbents performance, metal ion imprinted chitosans were prepared using two different crosslinking agents namely, epichlorohydrin (MIP-Epi) and glutaraldehyde (MIP-Glu). All the conditions were similar to the earlier mentioned synthesis of epichlorhydrin crosslinked MIP (section 2.3), except for the crosslinking conditions. Glutaraldehyde crosslinked MIP (MIP-Glu) was prepared under neutral pH conditions unlike MIP-Epi which was prepared under basic conditions. A different batch of chitosan, compared to the earlier reported Co(II)-MIPs, was used for the syntheses of both the MIPs and the maximum theoretical capacities of the MIPs prepared were obtained as, MIP-Epi: 266 μmol.g^{-1}, and MIP-Glu: 187 μmol.g^{-1} respectively.

4.3.7.1 Comparative Metal ion Uptake by the Sorbents

Comparative metal ion uptake by the sorbents was evaluated by equilibrating 20 mg of the sorbents with 2 mL of the 2:2:50 mM; Co(II):Fe(II):Citrate solutions (pH 4.8) and the uptake capacities obtained are depicted in the Fig. 4.6. The reduction in uptake capacity due to crosslinking was less for the glutaraldehyde crosslinked MIP, while the reversal in selectivity was obtained only with the epichlorohydrin crosslinked MIP. Both chitosan and MIP-Glu were selective for Fe(II) under the conditions provided. This implies that, epichlorohydrin acts as a better crosslinking agent, compared to glutaraldehyde, for the Co(II)-MIPs by preventing all other non-selective interactions.

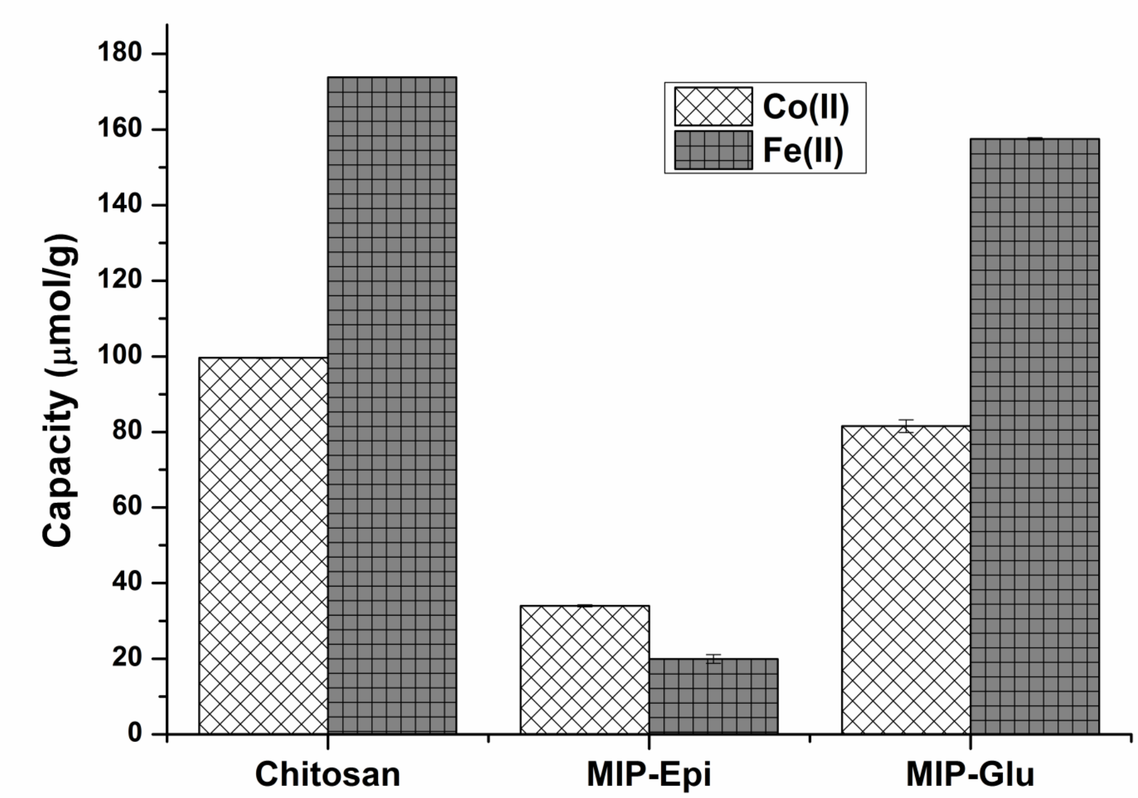

Figure 4.6. Comparative metal ion uptakes by chitosan and MIPs prepared using epichlorohydrin and glutaraldehyde as the crosslinkers

4.3.7.2 Effect of Irradiation on Uptake Capacities and Selectivity of the Sorbents

The imprinted polymers and chitosan were subjected to gamma irradiation using a gamma chamber. A 50 mg of the sorbents, soaked in 10 mL of double distilled water and de-aerated for some time, were subjected to gamma ray irradiation to doses of 2 kGy and 20 kGy. Post irradiation, the supernatants were analysed using TOC analyser for sorbent decomposition. TOC results indicated the radiation resistance of chitosan, which was further improved by crosslinking. The irradiated sorbents were further subjected to comparative sorption studies, as described earlier, and the results obtained are depicted in Fig 4.7. Selectivity of the epichlorohydrin crosslinked MIP was found to increase with increase in the irradiation dose given. Even though the total metal ion capacity of the MIPs ($q_{Co(II)}+q_{Fe(II)}$) were found to decrease with increase in the dose given for both MIP-Epi and MIP-Glu, increase in selectivity was more noticeable with epichlorohydrin crosslinked MIP. Radiation might have introduced fresh crosslinking inside the MIPs leading to reduced non-specific interactions.

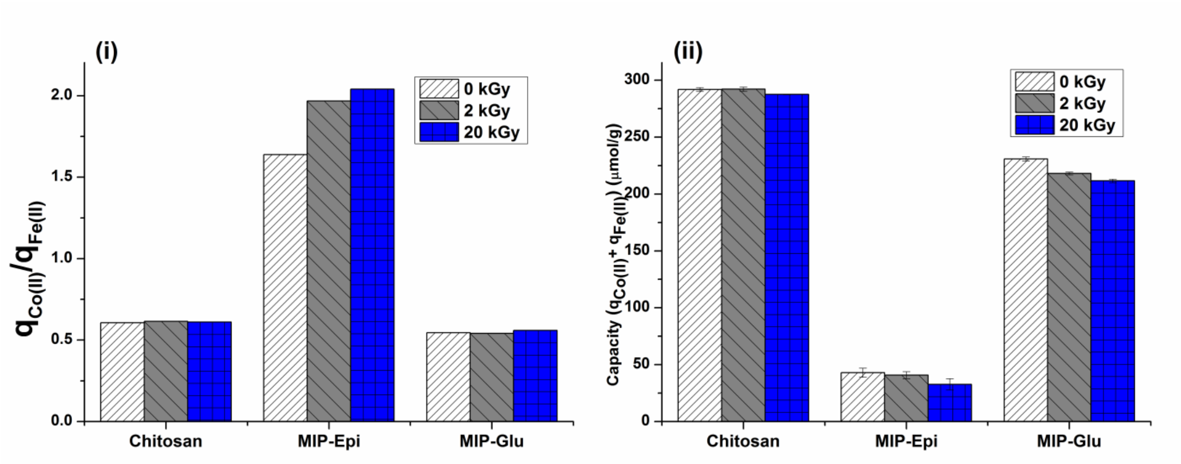

Figure 4.7. Effect of irradiation on the (i) Selectivity for Co(II) and (ii) Total metal ion uptake capacities of the sorbents

4.4 Conclusion

Selectivity of the biosorbent chitosan can be reversed through metal ion imprinting. The cobalt uptake and selectivity of MIP prepared was found to be high in the pH range 4 to 5, in citrate medium, which is the typical pH range encountered during PHWR decontaminations. The sorption of Co(II) by the MIP from strongly complexing media such as NAC formulations indicates its applicability in preferential removal of Co(II) ions from solutions containing mixture of complexing agents. The retention of cobalt selectivity even from solutions having very low concentration of Co(II), and in presence of large excess of Fe(II), make the MIP a potential sorbent for use in nuclear related applications, wherein the Co(II) ions are found in very low concentration levels and Fe(II) in large excess. Further, fast and easy regeneration of the MIP make the imprinted resin suitable for reuse without notable compromise in capacity and selectivity. Though metal ion uptake capacity is significantly reduced on imprinting, since the physical quantity of cobalt that is to be removed during decontamination is very less – typically in the order of sub ppb levels – the reduced capacity is not an impediment when high orders of selectivity is obtained in favor of the targeted radioactive nuclide. As compared to the imprinted organic resins, these have cost advantage and relatively better degradability. The latter is very beneficial as the concentrated active ions are to be removed from the resin for effective immobilisation and the stripped resin is to be decomposed. The fact that the selectivity could be modified to the point of reversing the preference shows that imprinting can be used as an effective tool for making chitosan suitable, as a replacement for organic resins, for various specific applications.

In the case of the imprinted chitosan, the long contact time needed for obtaining the saturation capacity limits its use in (online) column operations, but it can be effectively used in offline batch mode operations. In order to make the imprinted resins suitable for online application in column mode during the chemical decontamination of NPPs, the uptake kinetics has to be improved. Also, complete Fe(II) exclusion, which is not achieved by the cobalt imprinting of chitosan, is to be realized for its effective online use during the decontamination processes. These can possibly be addressed through the imprinting of functionalized chitosan.

Apart from the use of imprinted chitosan in selective concentration of cobaltous ions, the raw chitosan, as shown in this study, exhibits high sorption for the major metal ion removed during decontamination, namely ferrous ions. However, the fact that chitosan sorbs the complexing agent as well would mean that the decontamination cannot be carried out in the regenerative mode and might lead to use of excess complexing agents. Thus, the raw chitosan can potentially replace the mixed bed organic resin which is used towards the end of the decontamination campaign for removing the complexing agents and the excess remaining metal ions. The fast uptake shown by the chitosan makes it a viable approach.

Chapter 5. REMOVAL OF ANTIMONY BY NANO TITANIA IMPREGNATED-EPICHLOROHYDRIN CROSSLINKED CHITOSAN (TA-Cts) BEADS AND OTHER POTENTIAL ANTIMONY SORBENTS

Removal of antimony is a challenging task due to its presence in multi oxidation states under solution conditions and the low concentrations in which it is to be removed. This chapter details, in three sections, the studies carried out in this regard. Batch sorption studies carried out to investigate sorption profiles and the sorption mechanisms associated with the removal of antimony in its two oxidation states (+3 and +5) over potential antimony sorbents are discussed in the first section. The sorbents included three titania sorbents (RADEX® Sb-1000, nano TiO_2– special grade and AEROXIDE® TiO_2 P 25), a strong base anion resin (TULSION® A-33), a chelating resin (Amberlite® IRC-718), and a biosorbent (chitosan). The second section details how the excellent antimony sorption properties of titania based materials, and the ability of crosslinked chitosan to yield a stable composite beads, were made use of to synthesise an antimony sorbent suitable for large scale applications. Third section details the investigations carried out to understand the effect of composition on the physical and sorption properties of the nano titania impregnated-epichlorohydrin crosslinked chitosan (TA-Cts) beads.

5.1 Introduction

Importance of antimony removal and the need for better antimony removing materials/processes in nuclear industry was discussed in detail in chapter 1 (section 1.15). Apart from this specialised application, there is need for better antimony removing materials in view of the concerns in general drinking water treatment processes, and in the treatment of other industrial effluents containing antimony. Antimony is considered as an emerging toxic contaminant in the environment [133, 134]. Major sources of antimony pollution in natural waters are the antimony mining and smelting processes, and coal burning [135]. Leaching of antimony from polyethylene terephthalate (PET) bottles, due to the use of antimony trioxide as catalyst during the PET plastic manufacture, is also a serious concern [136]. Antimony is also a concern as an impurity in the copper electro refining industry as well [137]. A guideline value of 20 µg. L^{-1} has been set by World Health Organisation (WHO) for antimony in drinking water [138]. The maximum contaminant level set for antimony by United States Environmental Protection Agency (USEPA) is 6 ppb [139]. Thus, there is a clear need for better antimony removing materials across various fields.

The complex speciation of antimony in solutions, according to the solution conditions, makes its separation cumbersome [140]. Different materials and methodologies such as ion exchange [137], sorption [141], solvent extraction [142], coagulation [143, 144], membrane separation [145, 146] have been studied for antimony removal. Of these, sorption/ion exchange removal is more suitable for industrial applications, especially in nuclear industry. Anion resins by their very nature can be a viable sorbent for the anionic species of antimony. Titanium dioxide is known to be an effective sorbent capable of sorbing both cations and anions based on the solution pH [147, 148], and is thus a promising sorbent for anionic species of the antimony. High sorption capacity associated with titania materials further makes this an attractive sorbent.

Antimony sorption properties of the three commercially available titania based sorbent materials and a nuclear grade strong base anion resin, Tulsion® A-33 have been studied. Further, in order to understand the speciation during sorption, two different types of sorbent materials namely, Amberlite® IRC-718 (a chelating resin) and chitosan (biosorbent) have also been evaluated. The effect of solution conditions on the sorption efficiency of these sorbents has been probed in detail to understand the sorption behaviour and to evaluate the suitability of the sorbents for antimony removal.

Chitosan and TiO_2 have been reported extensively as sorbent materials for metal ions and organic compounds [99, 149, 150]. The former has been explored widely for developing sorbents for targeted nuclear related applications as well [96, 98], while the later has been reported to be an effective sorbent, in particular for arsenic [151], and a photo catalyst for catalytic removal of anionic species [152]. The sorption mechanism involved in the binding of As by TiO_2 has been dealt in detail in the literature [147, 153]. Mukhopadhyay et al. reported the batch sorption studies that demonstrated fast and irreversible sorption of radioactive antimony (^{125}Sb) by titania [154]. There are reports on the use of Chitosan-nano TiO_2 composite materials, for metal ion removal and dye degradation, from 2006 onwards [155]. S Miller et al have reported the TiO_2 impregnated chitosan beads (TICB) and its arsenic sorption efficiency in 2010 [156, 157]. However, the use of reported TICB in acidic solutions has limitations due to its disintegration in solutions having pH less than 4.0. As the chitosan matrix in the TICB was not crosslinked, the beads lacked stability in acidic media. This could be prevented by cross linking of the chitosan, as it would make the beads insoluble and impart better chemical and mechanical stability. Such attempts have been made to obtain TiO_2 based materials with enhanced photocatalytic activity [49, 155] and high organic decomposition efficiency [158]. Nano titania impregnated-epichlorohydrin crosslinked chitosan (TA-Cts) beads were prepared and studied for its efficiency as a sorbent material for removing antimony. Also its suitability or potential for use in large scale operations has been demonstrated through column studies.

The earlier reports on TiO_2 impregnated chitosan beads for removing arsenic showed that the capacity of the beads prepared was equivalent to the neat TiO_2 fraction present in the beads [156]. Therefore, any associated increase in titania component in the TA-Cts beads should lead to an increase in the uptake capacity of the TA-Cts beads. This aspect - the effect of the composition of the TA-Cts composite beads on the physical and sorption properties - was also studied in detail. For this investigation, TA-Cts beads having varying nano TiO_2 to chitosan ratio had been prepared and their solution and sorption properties were evaluated. Chitosan can be cross-linked using various crosslinking agents such as epichlorohydrin [118], glutaraldehyde [159], sodium tripolyphosphate [160] etc. We have used epichlorohydrin as the crosslinker for synthesising the nano titania-chitosan composite beads. Crosslinking affects not only the solubility but also the physical and chemical properties of the crosslinked chitosan. For example, metal ion uptake capacities generally decrease on crosslinking [161]. Effect of the crosslinking agent amount used on the properties of the final chitosan/chitosan-titania products has not been addressed much in the literature. Effect of crosslinking on properties such as swelling, which are important in view of drug delivery applications, is reported [162]. The extent to which the crosslinker reduces the uptake capacity of chitosan or affects the kinetics of sorption has not been reported widely as in the case of general ion exchange resins [163, 164]. In this regard, TA-Cts and chitosan beads, having different amount of epichlorohydrin content, were synthesised and studied for their physical and sorption properties.

5.2 Experimental Details

5.2.1 Sorbent Materials Studied for Antimony Removal

RADEX® Sb-1000 is a granular titanium dioxide based commercial antimony sorbent. Its specific surface area was estimated (B.E.T) to be 193.3 $m.^2$ $g.^{-1}$. The Raman spectra showed it to be of TiO_2 anatase phase (Fig. 5.1). Nano TiO_2 – special grade (TTPL) used was of anatase phase containing 80-88% of TiO_2 with 10-18% moisture content, and specific surface (BET) area of 146 $m^2.g^{-1}$. AEROXIDE® TiO_2 P 25 is a hydrophilic fumed titanium dioxide with typical average primary particle size of 21 nm, and specific surface area (BET) of 50±15 $m^2.g^{-1}$. The nuclear grade anion resin (TULSION® A-33) used has polystyrene copolymer as the matrix and quaternary ammonium functional groups with $(-\mathrm{OH})$ groups as the counter (exchangeable) ions, and the moisture content was 60%. Amberlite® IRC-718 is a macro porous chelating resin containing iminodiacetic acid functional groups with about 65% moisture content.

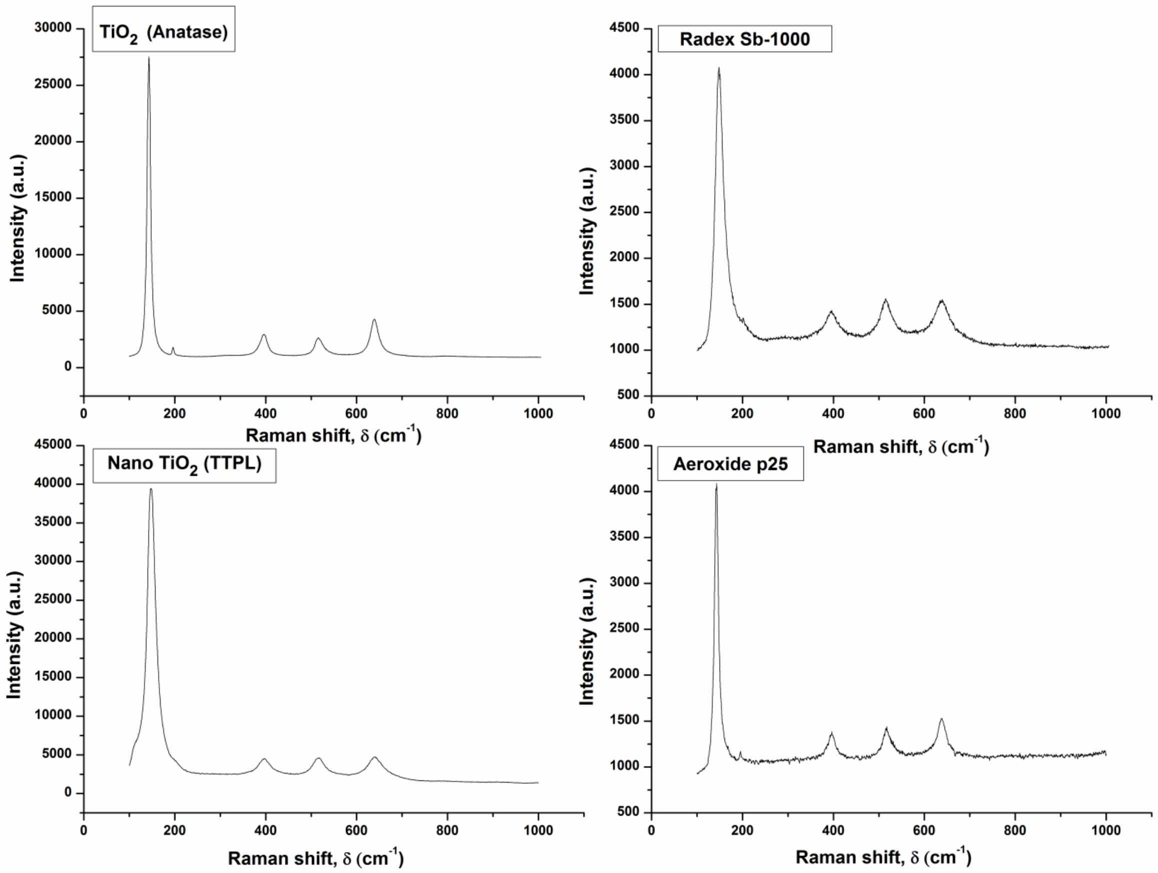

Figure 5.1. Raman spectra of various TiO_2 samples used

5.2.2 Synthesis and Characterisation of the Nano Titania Impregnated-Epichlorohydrin Crosslinked Chitosan (TA-Cts) Beads

Synthesis of the TA-Cts beads has been discussed in detail in section 2.4. The synthesis scheme used for preparation of the TA-Cts beads is shown in Fig. 5.2. The Raman spectra of the starting materials (chitosan, nano-TiO_2–special grade) and the TA-Cts beads synthesised were recorded.

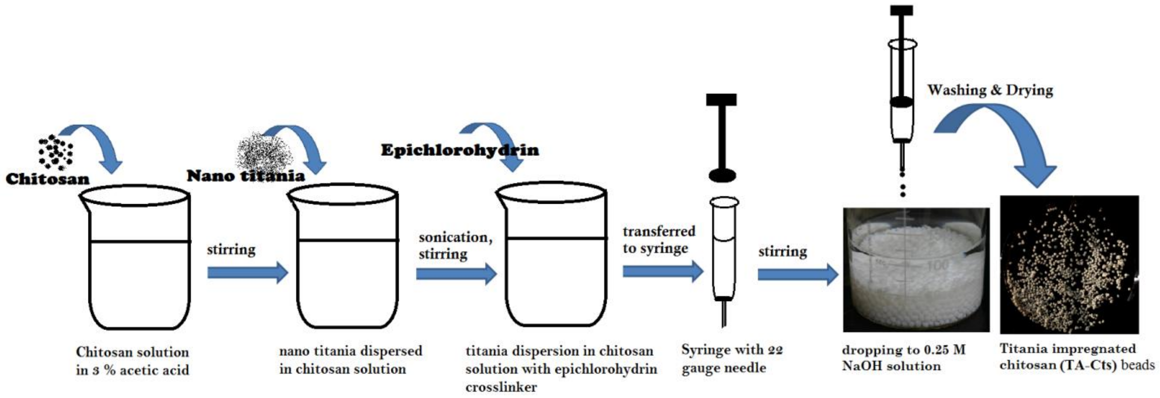

Figure 5.2. Scheme for the synthesis of TA-Cts beads

5.2.3 Synthesis of TA-Cts Composite Beads with Varying TiO_2 to Chitosan Compositions

To synthesise the composite beads having varying TiO_2/chitosan compositions; the dropping solutions were prepared according to the compositions given in Table 5.1. The solutions were dropped using a peristaltic pump into a 1 M NaOH solution (100 to 200 mL) through a 20 gauge needle to obtain the beads. 1 mL more epichlorohydrin was added to all the precipitating media after the bead formation; i.e., while ageing of the beads (24 h). The beads were then separated and dried. Any unreacted materials were removed by washing with 0.5 M HCl solution (40 mL). The beads were further washed with demineralised water, several times, and then dried in a vacuum oven to obtain the TA-Cts composite beads having varying amounts of nano TiO_2 and chitosan.

Table 5.1.Synthesis of the TA-Cts beads of varying compositions: Composition of the dropping solution used for the synthesis

Name	**Composition of the dropping solution**			
	Chitosan (g)	**TiO_2** (g)	**Epichlorohydrin** (mL)	**Dispersion Volume** (mL)
Cts-CL	1.0	0	2.0	40
1TA-5Cts	1.0	0.2	2.0	40
2TA-4Cts	0.4	0.2	1.0	16
3TA-3Cts	0.3	0.3	0.6	12
4TA-2Cts	0.4	0.8	0.8	16
1p25-5Cts[#]	1.0	0.2	2.0	40

[#] TA-Cts composite beads prepared using AEROXIDE® TiO_2 P 25

5.2.4 Synthesis of the Nano TiO_2-Chitosan (TA-Cts) and Chitosan (Cts) Beads with Varying Epiochlorohydrin (Crosslinker) Content

5.2.4.1 Nano TiO_2 impregnated-chitosan beads with varying epiochlorohydrin content (TA-Cts-Epi Beads)

Non-crosslinked nano titania impregnated-chitosan (TA-Cts) beads were prepared as discussed earlier without the addition of the crosslinking agent epichlorohydrin. For this, a neat nano titania dispersion in chitosan solution (0.1 g nano TiO_2 to 0.5 g chitosan in 20 mL 3% acetic acid solution) was precipitated in bead format by dropping it into an alkaline solution. The beads thus obtained were subjected to work-ups and dried to obtain the non-crosslinked TA-Cts beads. About 300 mg of the non-crosslinked beads thus prepared were swollen overnight in ultrapure water and then crosslinked by treating with different amounts of epichlorohydrin under alkaline conditions. The various amounts of epichlorohydrin used and the yield of the TA-Cts beads obtained are tabulated in Table 5.2.

5.2.4.2 Chitosan beads with varying epiochlorohydrin content (Cts-Epi Beads)

Chitosan beads were prepared by dropping of chitosan solution (in acetic acid) into alkaline solution. The non-crosslinked chitosan beads thus obtained, after the work up procedure, were subjected to crosslinking using epichlorohydrin. The amount of epichlorhydrin added to each of the samples for preparing the crosslinked chitosan beads with different amounts of epichlorohydrin content, and the yield obtained are given in Table 5.3.

Table 5.2. Synthesis of the crosslinked TA-Cts beads: Amount of cross linker added and yield

Name	**TA-Cts beads (Non-crosslinked)** (mg)	**Epichlorohydrin** (µL)	**TA-Cts beads (crosslinked) Yield** (mg)
TA-Cts-NCL	306	0	299
TA-Cts-Epi050	302	50	334
TA-Cts-Epi100	302	100	354
TA-Cts-Epi200	302	200	374
TA-Cts-Epi350	301	350	384
TA-Cts-Epi500	311	500	417

Table 5.3. Synthesis of crosslinked chitosan beads: Amount of crosslinker added and yield

Name	**Chitosan beads (Non-crosslinked)** (mg)	**Epichlorohydrin**		**Crosslinked chitosan beads Yield** (mg)
		(µL)	mmol	
Cts:Epi-1:1	189	78.5	1	223
Cts:Epi-1:2	190	157	2	248
Cts:Epi-1:5	189	393	5	270
Cts:Epi-1:10	190	785	10	283

5.3 Results and Discussion

5.3.1 Antimony Removal by the Sorption Materials

Antimony uptake studies using the potential antimony sorbents were carried out both in batch mode and column mode. Sb(V) and Sb(III) solutions were prepared from $KSb(OH)_6$ and potassium antimony(III) tartrate respectively. Solution pH was adjusted with dil.NaOH/HCl solutions for batch studies. All the sorption experiments were carried out in duplicate and the mean values are reported.

5.3.1.1 Antimony Removal by the Sorbents: Batch Studies

Results obtained for the batch sorption studies using 10 mg of the sorbents to 2 mL of the respective 1 mM antimony solutions are plotted in Fig. 5.3. Titania based sorbents (i.e., RADEX® Sb-1000, nano TiO_2 and AEROXIDE® TiO_2 P 25) showed good pickup of antimony, for both Sb(III) and Sb(V); while the strong base anion resin, TULSION® A-33, showed good pickup of the anionic species of Sb(V). Most of the sorbents, including Amberlite® IRC-718 and chitosan, exhibited significant sorption capacity for Sb(III). In the case of anion resin, though it showed reduced Sb(III) concentration in the equilibrated solution, it was observed that, Sb(III) gets precipitated over the resin beads (as white powder) at higher concentrations studied.

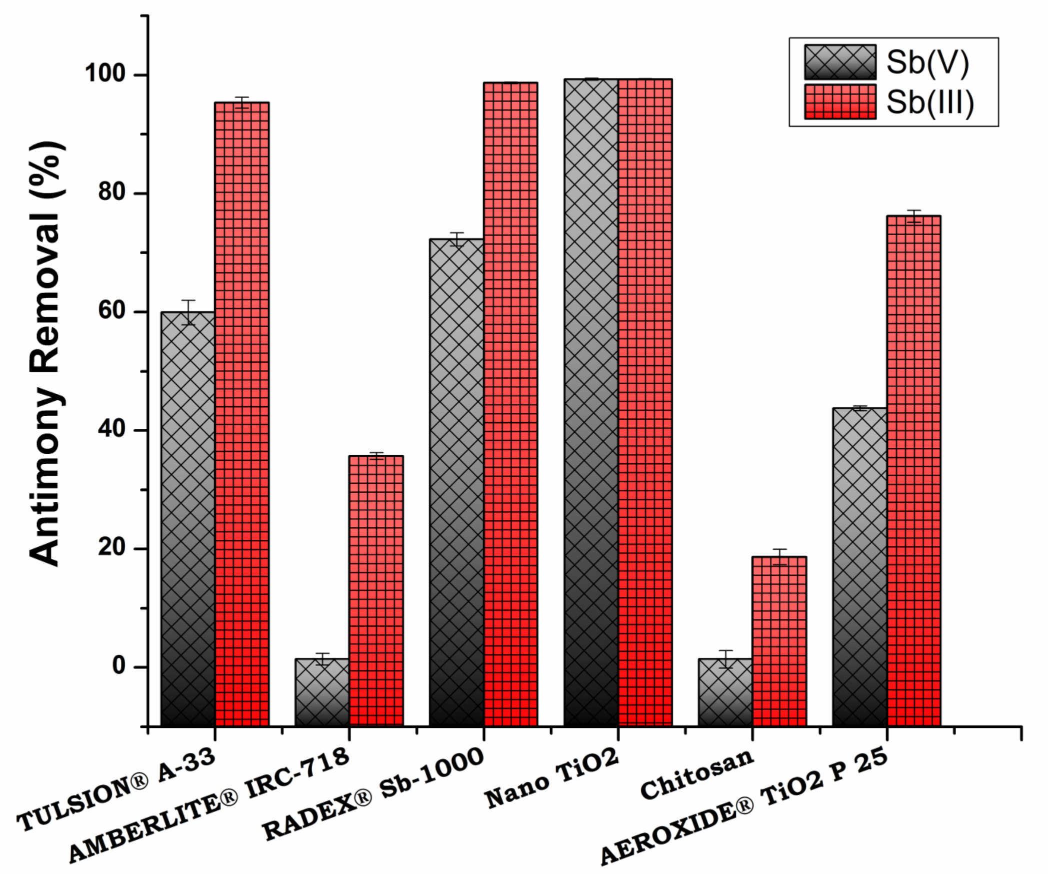

Figure 5.3. Antimony removal by the potential antimony sorbents

5.3.1.2 Effect of Solution pH (Initial) on Antimony Removal: Batch Studies

Most sorbents exhibit a pH dependent sorption as the solution pH influences the nature of surface charge over the sorbent and the speciation of the sorbate in solution [165]. The effect of pH on the sorption of antimony (as Sb(V) or Sb(III)) over various sorbents was studied in this regard. Sorption results obtained for the batch sorption studies carried out by equilibrating 5 ml of the 1 mM solutions of Sb (V) or Sb (III) with 25 mg of the sorbents for 24 h are tabulated in Table 5.4 (for Sb(V)) and in Table 5.5 (for Sb(III)). The respective equilibrium pH values attained on sorption are also shown in the tables. The results demonstrate the influence of initial and equilibrium pH on antimony removal by the sorbents. The change in solution pH during sorption and the uptake capacity of the sorbent gives an insight into the possible sorption mechanisms.

Table 5.4. Effect of solution pH on antimony removal: Batch sorption studies using Sb(V) solutions

Sorbent Used	**Initial pH: 3.0**			**Initial pH: 6.5**			**Initial pH: 11.1**		
	Sb Uptake		**pH** (Eq.)	**Sb Uptake**		**pH** (Eq.)	**Sb Uptake**		**pH** (Eq.)
	(μmol.g^{-1})	(%)		(μmol.g^{-1})	(%)		(μmol.g^{-1})	(%)	
TULSION® A-33	133	71	7.7	109	57	8.2	35	19	9.2
RADEX® Sb-1000	188	98	6.8	145	75	8.8	77	42	10.4
Nano TiO$_2$-Special grade	202	100	2.3	185	100	2.6	179	100	2.6
AEROXIDE® TiO$_2$ P 25	182	94	3.1	85	44	7.7	37	19	10.8
Chitosan	118	59	5.9	BDL	0	7.4	BDL	0	10.8
Amberlite® IRC-718	BDL	0	4.0	BDL	0	5.9	BDL	0	6.3

5.3.1.2.1 Sorption by strong base anion resin, TULSION® A-33

In the case of strong base anion resin TULSION® A-33, Sb(V) uptake capacity decreased with increase in solution pH (Table 5.4). TULSION® A-33 contains quaternary ammonium functional groups ($^{+}NR_4$) with (^{-}OH) as the counter (exchangeable) ions. The results show that there was concomitant increase in the pH ($pH_{Eq.} > pH_{Ini.}$) except when $pH_{Ini.}$=11.1, with sorption. This shows that the ion exchange equilibrium involves exchange of surface hydroxyl ions with the anionic species of antimony present in the solution. When the initial pH was 11.1, there was reduction in pH on sorption indicating higher pick up of excess hydroxyl ions present in the solution than the amount of hydroxyl ions released in exchange of pickup of antimony species. High solution pH, due to excess hydroxyl ion concentration in the solution, shifts the equilibrium towards retention of antimony species in the solution leading to reduced pick up from more alkaline solutions.

Table 5.5. Effect of solution pH on antimony removal: Batch sorption studies using Sb(III) solutions

Sorbent	**Initial pH: 3.1**			**Initial pH: 6.9**		
	Sb Uptake		**pH** (Eq.)	**Sb Uptake**		**pH** (Eq.)
	(µmol.g^{-1})	(%)		(µmol.g^{-1})	(%)	
TULSION® A-33[a]	180	97	7.8	165	97	9.0
RADEX® Sb-1000	193	100	6.5	175	99	7.8
Nano TiO_2-Special grade	188	100	2.4	173	99	2.7
AEROXIDE® TiO_2 P 25	153	86	3.2	117	96	6.1
Chitosan	94	52	6.3	BDL	0	7.5
Amberlite® IRC-718	35	18	4.3	60	34	5.7

[a] Sb(III) precipitated as white powder over the resin surface

In case of Sb(III), it was seen to have precipitated (as white powder) over the resin beads. The almost complete precipitation of the Sb(III) on the resin (Table 5.5) is due to the excess exchangeable hydroxyl ions present in the anion resin, which leads to enhanced precipitation of the Sb(III) species on the resin beads. Hydrolysis of Sb(III)-chelates above pH 6 is reported [166]. Hydroxyl species of Sb(III) are known to be $Sb(OH)_2^+$ at pH < 2 and $Sb(OH)_4^-$ at pH > 11. The uncharged $Sb(OH)_3^0$ species is known to be the predominant one in between this wide pH range (2 to 11) [167], and it has limited solubility [168]. The solution pH was seen to go up on equilibration. This could be due to the exchange of hydroxyl ions from the resin surface with the tartarate anions in the solution. The results indicate that strong base anion resins, such as TULSION® A-33, may not be viable for sorptive removal of Sb(III).

5.3.1.2.2 Sorption by the titania sorbents

Titania is a well-known photo catalyst and had been studied, in neat and modified formats, as a cation or anion exchange material, in particular for arsenic ions [169]. Sorption by titania materials are mostly facilitated by the surface hydroxyl groups. There are two types of surface hydroxyl groups present over the titania surfaces, which make it acidic or basic (Fig. 5.4). Terminal hydroxyl groups that are coordinated with single Ti atoms possess basic (or electron donor; Lewis base) properties and can act as cation exchanger sites. Bridging hydroxyl groups that are coordinated with two Ti atoms possess acidic (or electron acceptor; Lewis acid) properties and can act as anion exchanger sites [170]. But in solutions, these hydroxyl groups may get protonated or deprotonated according to the solution pH. i.e., the surface charge varies with change in solution pH and the zero point charge (pZc) of the TiO_2 will decide the sorption mechanism.

Any conclusion on the sorption mechanism should take care of, not only the surface charge on the sorbent, but also the speciation of the sorbate in solution. Majority of the values reported for the pZc of titania range from 5 to 7, and a ‘recommended’ value, irrespective of the phase present, is 5.9 [171, 172]. Generally, when the solution pH ≥ pZc; it will act as a cation exchanger. However, due to the possibilities of hydrolysis of metal ions (e.g., many transition metal ions) at higher pH conditions, net charge and solubility of the corresponding metal hydroxides formed also should be considered. At pH < pZc; it will act as an anion exchanger. Here, in both the cases, sorbent-sorbate interaction is of electrostatic in nature. In addition, inner sphere complex formation for anions e.g., arsenate has been reported [147]. Similar reaction was proposed for sorption of antimony over SiO_2/TiO_2 binary oxide surface as well [173]. Sb(V) and As(V) were shown to be picked up as their respective oxy anions and binding was preferred at pH below the pZc [174]. Even when the uptake is through irreversible binding (chemisorption), there should be a favourable pH and surface charge requirement for the initial sorption to occur.

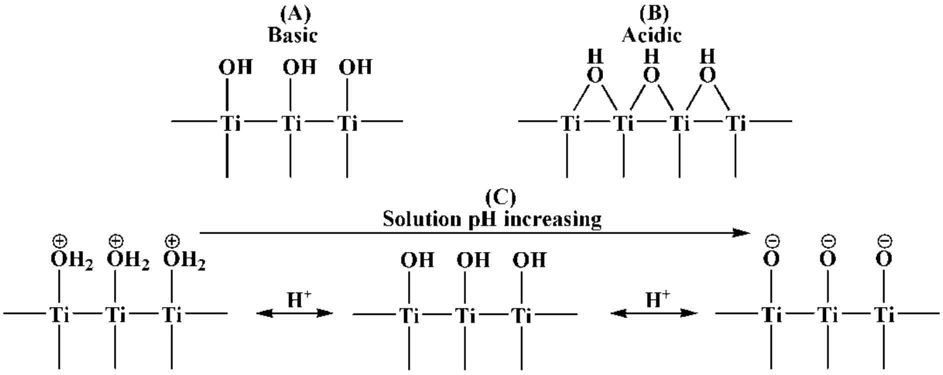

Figure 5.4. Surface hydroxylation of TiO_2 surface: (a) basic, (b) acidic and (c) change in surface charge with suspension pH

The titania based sorbents, RADEX® Sb-1000, AEROXIDE® TiO_2 P 25 and nano titania (special grade) showed good pick up of antimony. Both RADEX® Sb-1000 and AEROXIDE® TiO_2 P25 exhibited similar decreasing trend in sorption of Sb(V) with increasing equilibrium pH. This is explainable by the fact that the surface charge of TiO_2 becomes more negative at higher pH and thus making it less preferred by the anionic species of the antimony present in the solution. Nano titania (special grade), however, showed almost complete removal of Sb(V) at all the (initial) pH conditions studied (Table 5.4), which is explained by the almost identical (acidic) equilibrium pH achieved irrespective of the initial pH. The acidic equilibrium pH ensures positive surface charge enabling sorption of the anionic species of antimony from the solution. The results show that there is an optimum pH for the anionic species,$\mathrm{Sb(OH)_6^-}$, to get sorbed over the titania surfaces through electrostatic interactions. Moderately acidic or neutral pH is needed for Sb(V) sorption. Almost similar (as with Sb(V)) sorption capacity and sorption associated change in pH were observed for Sb(III) as well (Table 5.5) indicating their sorption as anionic species (Sb(III)-Tartrate anion). The effect of pH on the Sb(III) sorption over titania could not be investigated at alkaline conditions due to the hydrolysis of Sb(III)-Tartrate at higher pH conditions.

The batch sorption results (vide supra) obtained indicate that antimony was sorbed as anionic species. This was investigated further through sorption studies with two distinct types of sorbents namely, chitosan, which is capable of sorption through electrostatic interations, and Amberlite® IRC-718 which sorbs through chelation of cations.

5.3.1.2.3 Sorption by chitosan and Amberlite® IRC-718

The biosorbent chitosan has amino and hydroxyl groups as the binding functionalities. The sorption occurs through electrostatic attraction as well as complexation. The extent to which each mode operates depends on speciation in the solution state and that of the chitosan functional groups [112]. Both these are in turn affected predominantly by the solution pH (Section 3.3.1).

Chitosan showed 60% sorption of Sb(V) (used as $\mathrm{Sb(OH)_6^-}$) at initial pH of 3.0 (Table 5.4). The solution pH increased during equilibration as a result of the protonation of the amine groups (Eq. 3.2). The equilibrium pH obtained (5.9, Table 5.4), which is less than the amine pKa (~6.5) of chitosan shows that the majority of the amine groups were protonated. Hence, the sorption was predominantly through electrostatic interaction involving anionic species of Sb(V) and the protonated amine groups. At higher pH conditions, as the amine groups would be present in deprotonated (neutral) form, there was no sorption of Sb(V) as it would be predominantly present as anionic species in the alkaline solution. The uptake of Sb(III) (Table 5.5) at (equilibrium) pH 6.3 was found to be close to 52% while there was no sorption at the higher pH conditions, confirming the uptake to be as anionic species of antimony (i.e., antimony tartarate complex).

Amberlite® IRC-718, which is a chelating resin with iminodiacetic acid as the chelating functional group (Fig. 5.5), did not pick up Sb(V) at any of the pH conditions studied (Table 5.4), while it showed noticeable uptake of antimony from Sb(III) tartrate solution. The Sb(III) uptake increased with increase in pH (Table 5.5), which is typical of binding through carboxylic acid groups. The results indicate that the iminodiacetic acid groups in the Amberlite had bound the antimony as cations through the deprotonated carboxylic groups, Fig. 5.5 [5], and that the groups were able to force the equilibrium towards the cationic species in case of Sb(III). This is in line with the marked tendency of Sb(III) to form complexes with multi-dentate carboxylic ligands [175]. However, such complexation was not seen to be feasible in case of Sb(V) as indicated by the absence of its sorption by Amberlite® IRC-718. This is perhaps due to the high stability of the $\mathrm{Sb(OH)_6^-}$ anions. The results indicate that Sb(V) was removed as anionic species, while Sb(III) was removed either as an anionic species or as cationic species according to the functional groups present in the sorbent and the solution conditions.

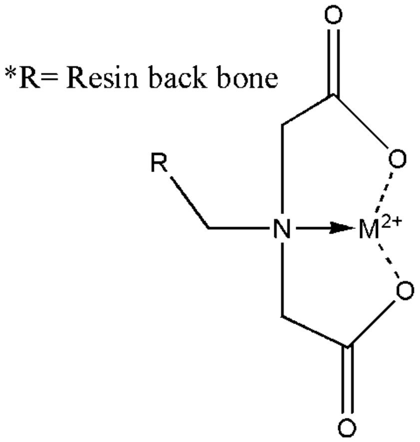

Figure 5.5. Metal chelation by iminodiacetate groups

5.3.1.3 Suitability of the Sorbents for Column Mode of Operation

The utility of any sorbent for large scale applications requires the sorbent to be suitable for column mode of operation. Amberlite® IRC-718, though the best suited for column operations, has shown poor sorption capacities. Chitosan also showed some sorption, but its physical format is not suitable for column operation. Out of the three titania materials studied, Nano TiO_2-special grade showed the best sorption characteristics across all the pH conditions studied. However, its current available physical format was found to be not suitable for column application. Further modifications are required to be able to use it in column mode. AEROXIDE® TiO_2 P 25 format is also not suitable for column application moreover it performed poorly once the initial pH was basic or closer to neutral, during Sb(V) sorption. RADEX® Sb-1000, whose sorption characteristics were slightly inferior to that of Nano TiO_2-special grade, but much superior to AEROXIDE® TiO_2 P 25, was found to be having flow characteristics suitable for column mode of operation. Thus RADEX® Sb-1000 was chosen among the TiO_2 materials for column studies. Its performance under column operation was compared to that of the strong base anion resin, as the latter is a predominant choice for large scale applications. The column studies were restricted to Sb(V) as Sb(III) was seen to be prone to hydrolysis under alkaline conditions (vide supra). Validation of the H_2O_2 process under PHWR conditions also requires the studies to be carried out with Sb(V) under alkaline pH conditions. The effect of pH and antimony concentration in the inlet solution on the breakthrough of the sorbent column was studied. For this, about 5 L of the Sb(V) solution, de-aerated and pH adjusted with LiOH was passed through a glass column filled with the resin - 10 mL (wet volume) in case of anion resin and 10 g (dry weight) in case of RADEX® Sb-1000 - with a flow rate of 10 $mL.min.^{-1}$ in once through mode (Fig. 2.1). The solution was passed through the column using a peristaltic pump. Sb(V) concentration and pH of the effluent collected at the outlet of the column were monitored with time.

5.3.1.3.1 Effect of solution pH and Sb concentration on the Sb(V) removal/column breakthrough volume

To know the effect of pH on the Sb(V) pickup and on the breakthrough volume, Sb(V) solutions of varying pH conditions were passed through the column. The influent antimony concentration was 1.1 ppm. Sb(V) concentration and pH of the effluent solutions collected at the outlet of the column were monitored with time. Ratio of the effluent antimony concentration to the influent antimony concentration was calculated and plotted (Fig. 5.6).

TULSION® A-33 showed a strong dependence of influent solution pH on the Sb(V) removal over the resin (Fig. 5.6A). At pH below 10.0, anion resin showed excellent sorption profile. Breakthrough occurred earlier in case of solutions with pH higher than 10.0, which indicates competition for the anion exchange sites by the excess hydroxyl ions. RADEX® Sb-1000 also showed strong dependence of Sb(V) sorption on pH (Fig. 5.6B). There was gradual increase in the effluent antimony concentration with time at pH 7.4, while the increase was sharper in the higher pH conditions, indicating reduced sorption at alkaline conditions. Under alkaline conditions; the sorption was not efficient in both the resins, though the anion resin could perform better till pH 10. In the case of RADEX, the sorption was reduced even under slightly alkaline conditions and sorption saturation was not attained within the studied eluent volume indicating a relatively slower kinetics.

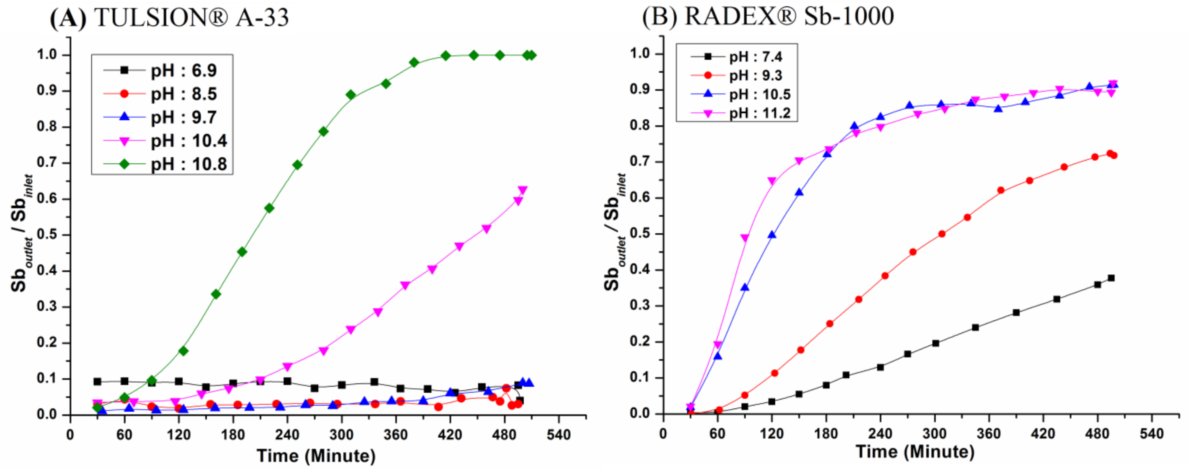

Figure 5.6. Suitability of the potential antimony sorbents for column mode of operation: Effect of influent solution pH on breakthrough

In order to understand the effect of influent Sb(V) concentration on the breakthrough, Sb(V) solutions of different concentrations were passed through the sorbent columns. The influent solution pH was adjusted to 10.4 in case of the strong base anion resin and close to 9.4 in case of RADEX$^{®}$ Sb-1000. Ratio of the effluent antimony concentration to the influent antimony concentration was calculated and plotted in Fig. 5.7. In the case of strong base anion resin, same breakthrough curve was obtained for all the three concentrations studied (for pH 10.4, Fig. 5.7A). Thus, in the case of TULSION® A-33, the breakthrough was determined by the pH rather than the influent concentration, while in the case of RADEX® Sb-1000, breakthrough was seen to occur earlier at higher antimony concentration (Fig. 5.7B). The plots clearly show that in both the cases sorption profile is predominantly affected by pH rather than the concentration.

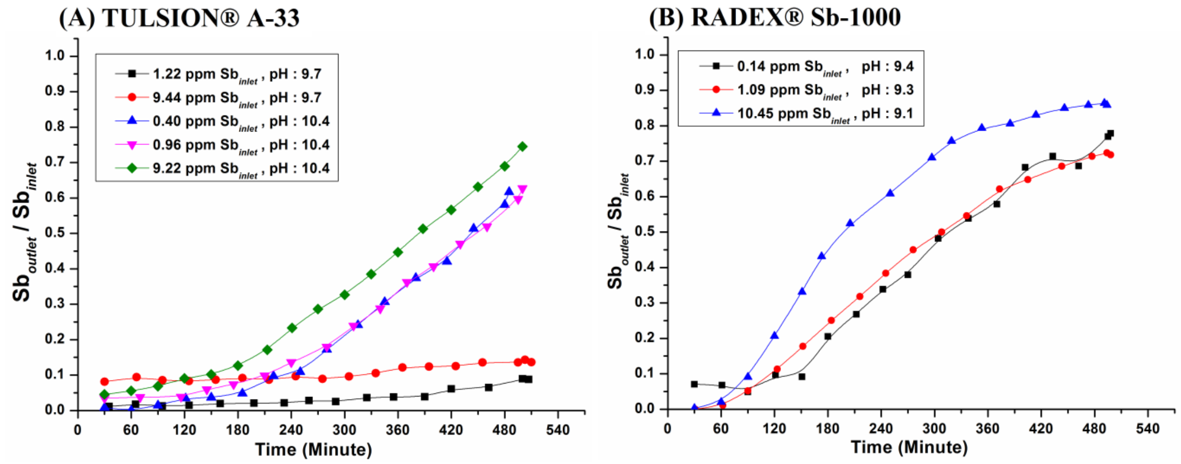

Figure 5.7. Suitability of the potential antimony sorbents for column mode of operation: Effect of influent Sb(V) concentration on column breakthrough

5.3.1.4 Evaluation of the Sorbents' Ability to Remove Antimony from a Typical Tap Water Sample: Batch Studies

The ability of the chosen sorbents to remove antimony from real life drinking water sample was examined using tap water sample spiked with antimony (to ppb levels) as test sample. Results obtained on equilibrating the test sample (10 ml) with various sorbents (10 mg) are shown in Table 5.6, which demonstrate that the titania based sorbents are the most suited to remove antimony present at low levels from complex matrices. Amberlite$^{®}$ IRC-718 was able to sorb Sb(III), but not Sb(V). Antimony is generally present in higher oxidation state

(+5, mostly as $[\mathrm{Sb(OH)_6}]^-$ in environmental samples, while Sb (III) is present only in trace levels [176]. Hence, Amberlite® IRC-718 may not be suitable for antimony removal from most environmental samples. Chitosan did not show any binding. These results are in tune with their sorption behaviour at high concentrations of antimony (vide supra). Surprisingly, anion resin was found to be incapable of removing antimony at low levels from tap water samples. This can be attributed to the interference from other anionic impurities (such as carbonates) present in the water sample.

Table 5.6.Evaluation of the sorbents' ability to remove antimony from a typical tap water sample: Batch sorption studies

Sorbents	**205 ppb Sb(V), pH: 8.1**			**224 ppb Sb(III), pH: 7.6**		
	Antimony Removal		**$pH_{Eq.}$**	**Antimony Removal**		**$pH_{Eq.}$**
	(µg.g^{-1})	(%)		(µg.g^{-1})	(%)	
RADEX® Sb-1000	176	91.7	7.9	195	90.5	7.6
Nano TiO_2	186	97.1	3.9	203	97.4	3.8
AEROXIDE® TiO_2 P 25	188	96.7	7.7	212	98.9	7.4
TULSION® A-33	3	1.7	8.8	BDL	0	7.9
Amberlite® IRC-718	BDL	0	4.4	94	42.8	4.7
Chitosan	BDL	0	8.0	BDL	0	7.6

5.3.2 Nano Titania Impregnated-Epichlorohydrin Crosslinked Chitosan (TA-Cts) Beads for Antimony Removal

Antimony removal studies using chitosan and nano TiO_2 showed promising results. TiO_2 in nano form showed excellent sorption properties for antimony due to the enhanced surface area available for the sorbate. However, it has post treatment issues, in removal of the sorbent from solution, which make it unviable for large scale applications. Thus, in order to make use of the sorption efficiency of the nano-TiO_2, it is important to be able to prepare them in usable format, such as beads of regular size and shape. As it is difficult to prepare the oxide in bead formats, a logical approach would be to incorporate the TiO_2 into a matrix, such as chitosan, that can be prepared in such a format. Such kind of TiO_2-chitosan combinations were reported and the mechanical properties of the chitosan was reported to be improved by the addition of TiO_2 [177, 178]. This was attributed to the homogeneous distribution of the titania particles in the chitosan matrix by the interfacial interaction between the basic amine sites ($–NH_2$) in the biopolymer with the Lewis acid sites present on the titania surfaces [178].

5.3.2.1 Synthesis and Characterisation of the TA-Cts Beads

The dispersion containing chitosan solution, nano TiO_2 and epichlorohydrin (crosslinker) was precipitated in the form of beads by dropping into alkaline solution. The bead sizes could be controlled based on the gauge of the needle used for dropping the mixture. As the process involved is simple and easy to scale up, proper control over the bead size and properties can be achieved with minimal efforts. The bead size (diameter) of the synthesised beads was found to be 0.79 mm (± 0.09 mm). The bead size was obtained as mean of the diameters of 16 randomly chosen beads.

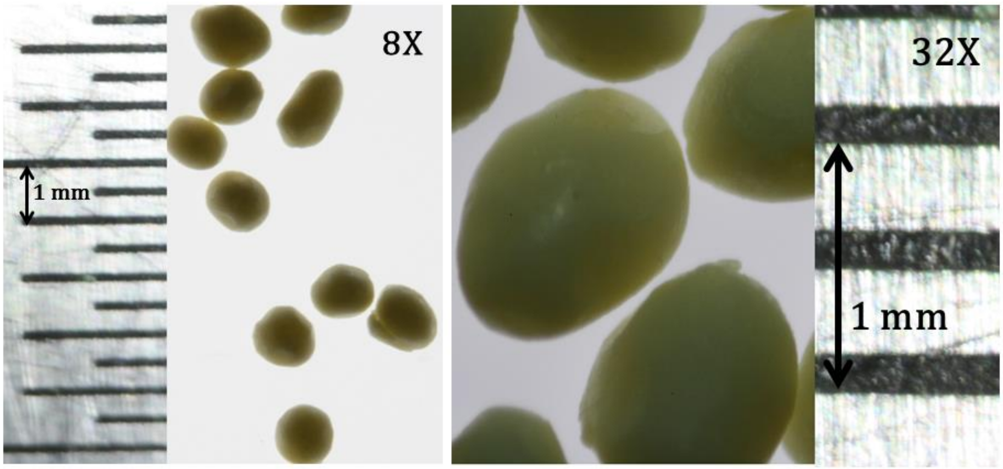

Figure 5.8. Microscopic pictures of the TA-Cts beads with (a) 8X and (b) 32X optical zooming

Raman spectrum of the nano-TiO_2 (Special Grade) (Fig. 5.1) containing 17-18% moisture, used for the synthesis of the beads, showed it to be of anatase phase. On oven drying at 150 ^{O}C for 1 h, the Raman peaks corresponding to water disappeared indicating the presence of water in the nanao-TiO_2 as moisture content (Fig. 5.9a). Specific surface area of the nano-TiO_2 was found to be 146.1 $m^2.g^{-1}$. The lattice parameter calculated from the XRD spectrum of the nano TiO_2 (Fig. 5.9b) used for the synthesis matched with the reported values for anatase [179] indicating the presence of single phase (anatase) in the nano-TiO_2 used for preparation of the beads.

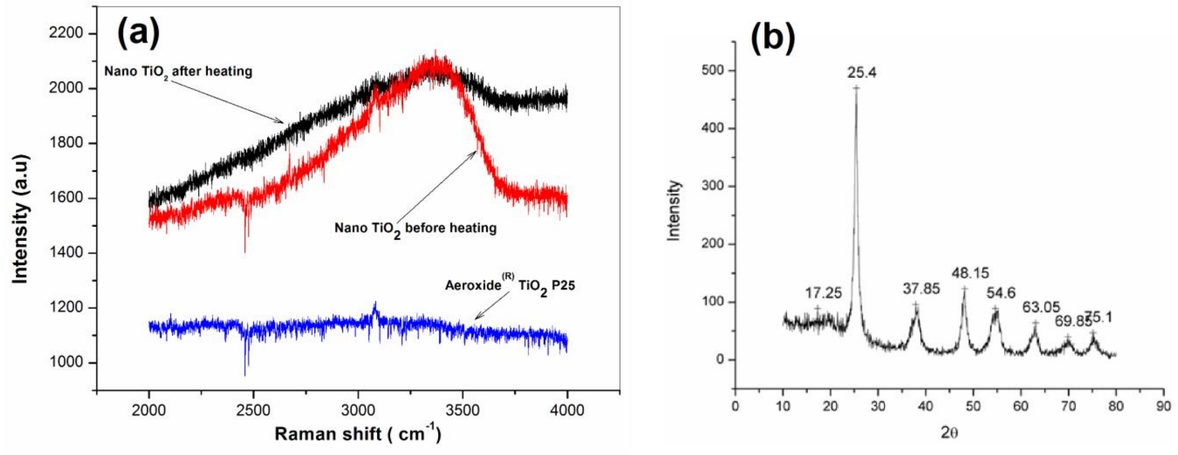

Figure 5.9.(a) Raman spectra (before and after heating at 150 ^{O}C for 1 h), and (b) XRD spectrum of the nano-TiO_2 (special grade; TTPL, Trivandrum)

The Raman spectra of the starting materials namely, chitosan, nano-TiO_2 and the TA-Cts beads synthesised are shown in Fig. 5.10. The Raman spectra of the TA-Cts beads showed TiO_2 peaks (148 (not shown in the spectrum of the TA-Cts beads due to the high intensity), 394, 515 and 638 cm^{-1}) and the peaks due to chitosan (899, 1110 and 1378 cm^{-1}), indicating their respective presence. The surface area measurements (BET) have shown the specific surface area of the TA-Cts beads to be 3.9 $m^2.g^{-1}$. The low surface area of the beads can be explained by the fact that the major component of the beads was chitosan, whose surface area was found to be 5.8 $m^2.g^{-1}$. Porosity measurements (mercury porosimetry) have shown that the TA-Cts beads were mesoporous (median pore diameter: 6.95 nm at 14.6 $mm^3.g^{-1}$) with narrow pore size distribution. The accessible porosity of the beads was found to be 4.3%.

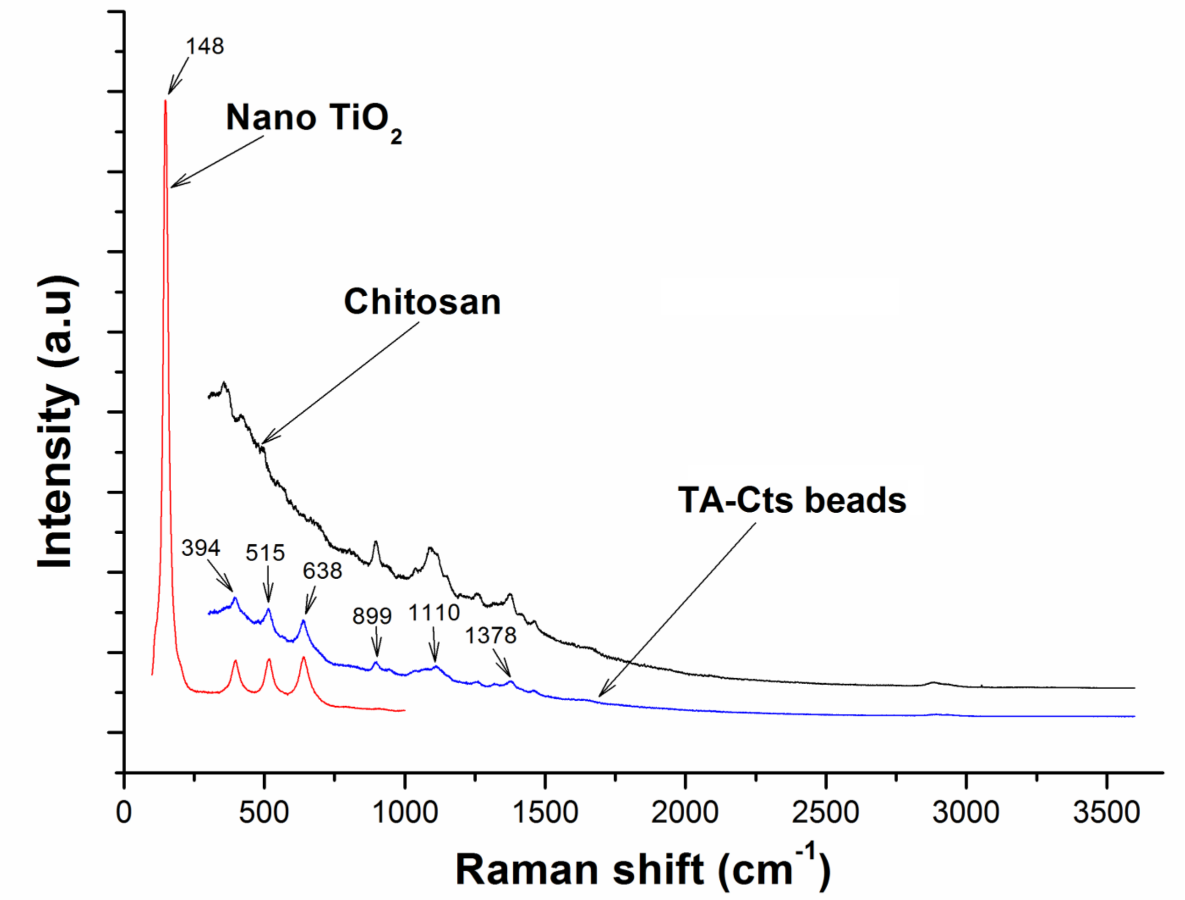

Figure 5.10. Raman spectra of nanoTiO_2, Chitosan, and TA-Cts beads

Swelling behaviour of the TA-Cts beads were measured by overnight swelling of the dry beads in ultra-pure water (swelling agent). About 400 mg of the TA-Cts beads were swollen by adding it to a measuring cylinder containing 3 mL ultra-pure water. TA-Cts beads showed an almost instantaneous swelling; nearly 90% of the volume expansion was achieved within 5 min. The wet volume of the swollen TA-Cts beads was about 2.0 mL. Equilibrium swelling ratio and equilibrium water content were calculated to be 200.1% and 66.6% respectively. Similar swelling parameters have been reported for glutaraldehyde and glyoxal crosslinked chitosan microspheres [180].

5.3.2.2 Evaluation of Sb(V) Sorption Properties of the TA-Cts Beads

5.3.2.2.1 Sorption of Sb(V) by the TA-Cts beads, chitosan and nano TiO_2: Effect of solution pH (initial)

Antimony (V) (as $[Sb(OH)_6]^-$) sorption efficiency of the composite TA-Cts beads and the constituents of the beads namely, chitosan and nano TiO_2 were studied in batch mode. 10 mg of the respective sorbent was equilibrated (for 48 h) with 1 mL of the 1mM solutions of Sb(V). The initial solution pH was adjusted to the desired value using dilute HCl or NaOH solutions. The effect of initial pH on Sb(V) sorption was analysed and plotted in Fig. 5.11. Chitosan sorbed Sb(V) only at acidic conditions. This is expected, as the amino groups of the chitosan are protonated under acidic conditions [115] and the resultant quaternary amine groups bind the anionic $[Sb(OH)_6]^-$ species. Unlike chitosan, nano-TiO_2 and TA-Cts beads showed high pick up of Sb(V) over wide range of pH conditions (Fig. 5.11).

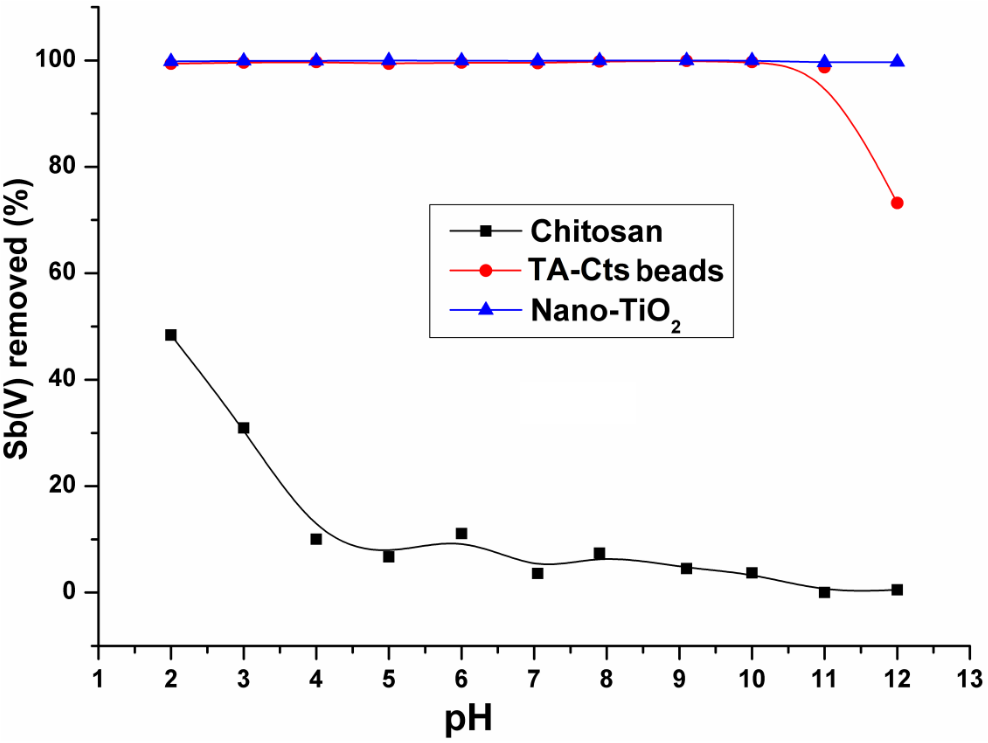

Figure 5.11.Sb(V) sorption properties of the TA-Cts beads: Effect of solution pH (initial) on Sb(V) sorption

It can be seen that the sorption properties of the TA-Cts beads are almost identical with that of nanoTiO_2. Thus, the removal of Sb(V) by the TA-Cts beads can be attributed to the nano titania rather than the chitosan. Chitosan serves as a stable matrix that holds the nano TiO_2 responsible for the antimony sorption. Crosslinking of the chitosan has made the composite beads insoluble in acidic solutions, thus giving the beads stability under wide pH conditions.

The pH values shown in Fig. 5.11 correspond to the initial solution pH. The equilibrium pH values attained during the sorption studies with low (ppb level) solution concentrations of Sb(V) (sorbent to solution ratio: 10 mg to 50 ml) are shown in Table 5.7. During sorption, it was observed that the pH of the solution changed significantly on equilibration. The solution pH was seen to change drastically from the initial value of 10.0 to 4.9 on equilibration (48 h), accompanied with complete removal of antimony. The results in the table clearly indicate the strong dependence of the sorption on equilibrium pH.

Table 5.7. Effect of solution pH on Sb(V) sorption: Sb uptake and the equilibrium pH obtained

Sorbent	**Sb(V) initial concentration (ppb)**	**Solution pH**		**Sb(V) sorbed (%)**
		Initial	**Eq.**	
Nano-TiO_2	154	10.0	4.9	100
TA-Cts beads	154	10.0	4.8	95.8
TA-Cts beads	155	10.8	10.7	Nil

5.3.2.2.2 Sb(V) sorption by the TA-Cts beads when solution pH is (forcefully) kept constant

The dependence of sorption on the equilibrium pH was further evaluated in detail by maintaining constant solution pH (using dilute HCl/ NaOH) till the sorption was complete. For this, 30 mg of the TA-Cts beads were equilibrated with 6 mL of 1 mM Sb(V) solutions, and for each experiment the addition of dilute HCl/NaOH was continued till there was no more sorption and any associated measurable change in the solution pH. The results are plotted in Fig. 5.12.

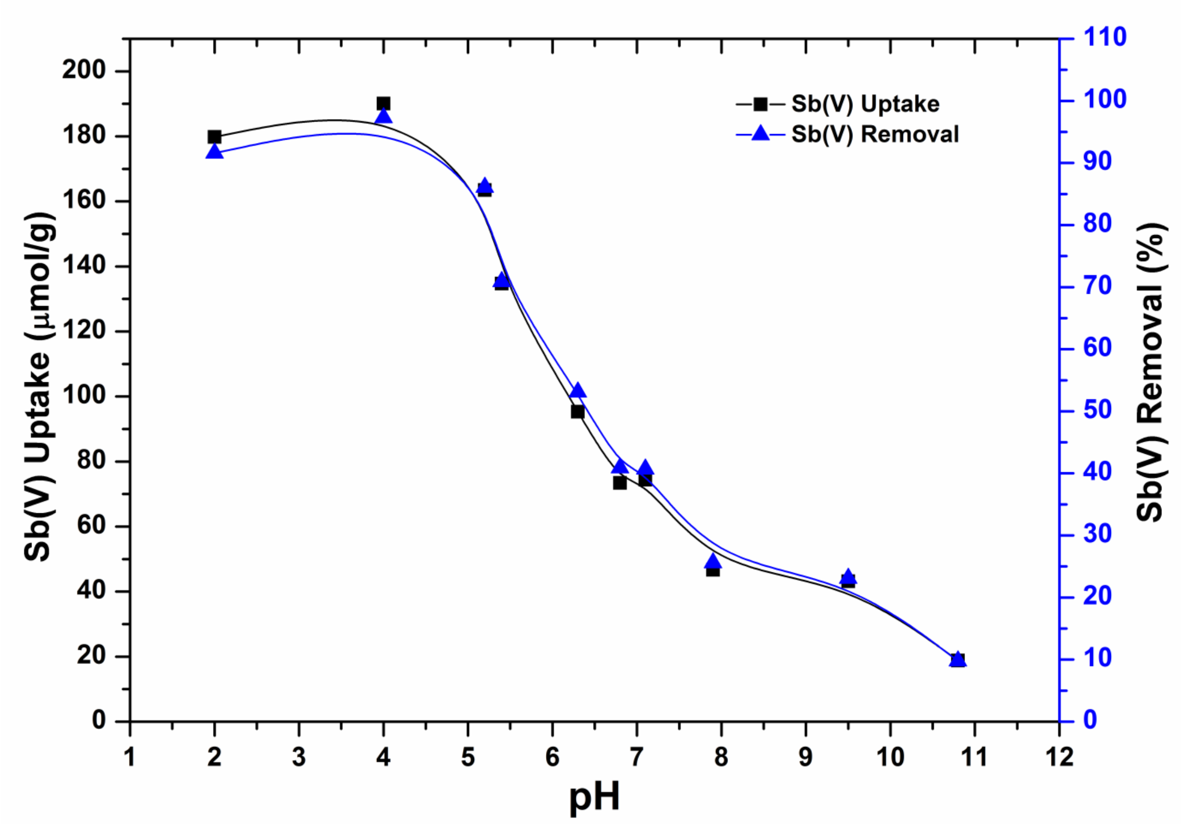

Figure 5.12. Sb(V) sorption properties of the TA-Cts beads: Sb(V) sorption by TA-Cts beads when the solution pH was (forcefully) kept constant

The solution pH increased slowly on addition of the sorbent to the solution having initial pH of 2.0, while in all other cases there was a decrease in solution pH during sorption. These observations can be explained based on the pH dependant nature of charge density present on the TiO_2 surface exposed to water. As shown in Fig. 5.4, which depicts the pH dependent surface charge on TiO_2, at low pH, the surface is predominantly positively charged, leading to sorption of hydroxyl and other anionic species. The hydroxyl ion sorption leads to reduction in the solution pH when the sorbent is equilibrated with the alkaline solution.

As the work up procedure during the synthesis of the beads involved treatment with dilute acid, majority of the surface is expected to be positively charged (protonated). When exposed to antimony solution of very low pH (2.0), there will be increased protonation of sites that were not protonated (or sites that got de-protonated during the final aqueous wash) during the synthesis, leading to increase in the solution pH. The decrease in solution pH on exposure of the beads to pH beyond 2 is attributable to the sorption of hydroxyl ions by the positive sites on the beads. As the pH increases, the surface tends more towards negative charge, thereby leading to reduced pick up of $[\mathrm{Sb(OH)_6}]^-$, as reflected by the drastic reduction in Sb(V) sorption at equilibrium pH beyond 5.0 (Fig. 5.12). It is to be noted that when antimony solution of initial pH of 10.0 was equilibrated with the beads, there was complete sorption and the equilibrium pH was close to 5.0. This observation indicates that the very high capacity of the beads makes it possible for the sorbent to sorb the anionic species of Sb(V) even from such highly alkaline solution. Such a high capacity is attributable to the nano form of the TiO_2 and the hydrophilic nature of the composite beads that gives easy access to the anionic species.

5.3.2.2.3 Contribution towards change in pH during sorption by the individual components of the composite (TA-Cts) beads

In order to investigate the contribution towards change in pH during sorption by the individual components of the composite beads, 8 mL of the 1 mM Sb(V) solutions were equilibrated with 40, 7 and 34 mg of the TA-Cts beads, nano-TiO_2 and chitosan respectively. The amount of titania and chitosan to be used in the sorption was calculated to correlate with their respective amounts present in the TA-Cts beads. The change in pH and the sorption capacities of the sorbents (Table 5.8) indicate that the sorption was essentially by the TiO_2 component rather than the chitosan matrix. The pH increase associated with equilibration of chitosan was due to proton abstraction by the amino groups present, as the initial pH was less than the pKa (~6.5) of the NH_2 groups of the chitosan [115]. Its contribution is reflected in the reduced change in pH with the beads as compared to that of the nano-TiO_2. The third column in Table 5.8 shows the capacity values calculated for the amount of TiO_2 present per unit mass of the TA-Cts beads. The capacity values thus obtained shows that the sorption by the TA-Cts beads was nearly 1.7 times more than the sorption capacity of its nano-TiO_2 part present in the TA-Cts beads. Thus it is evident that nano-titania in combination with chitosan in the form of composite beads is a much better sorbent for Sb(V) as compared to neat nano-titania.

Table 5.8.Contribution towards change in pH during Sb sorption by the individual components of the TA-Cts beads: Change in pH associated with Sb(V) sorption by the sorbents

Sorbent	**Amount of Sb(V) sorbed**			$\mathbf{pH_{eq}}$	**ΔpH** (pH_{eq}-pH_{in})*
	($\mu mol.g^{-1}$ of TA-Cts beads)	($\mu mol.g^{-1}$ of nano-TiO_2 present in the sorbent)	(%)		
Nano TiO_2	799	799	69.7	3.3	-2.0
TA-Cts beads	202	1357	98.6	3.7	-1.6
Chitosan	4	--	2.9	7.0	+1.7

* $pH_{eq.}$ – equilibrium pH, $pH_{in.}$ – initial pH

5.3.2.2.4 Kinetics of Sb(V) sorption/desorption by TA-Cts beads

Kinetics of Sb(V) sorption over TA-Cts beads was studied by equilibrating 40 mg of the TA-Cts beads with 8 mL of 1 mM Sb(V) solution having an initial pH of 5.2. Samples were taken at regular intervals and analysed for antimony concentrations. TA-Cts beads showed fast uptake of antimony with almost complete removal of antimony from the solution within 30 min (Fig. 5.13a). Desorption of the sorbed antimony from the recovered, washed and dried Sb-loaded TA-Cts beads was attempted using 0.25 M NaOH. Complete desorption of the sorbed Sb(V) from the sorbent could not be achieved, by changing the solution pH, indicating a strong binding of Sb(V) by the sorbent. Maximum desorption attained by prolonged equilibration (about 70 h) using 0.25 M NaOH was about 30-40% (Fig. 5.13b). Apart from electrostatic attraction of the anionic species by the surface charges on the TiO_2, there is a possibility of strongly bound complex formation with the surface titanium dioxide sites [173]. The low rate of desorption indicates the possibility of such a strong binding of antimony by the sorbent.

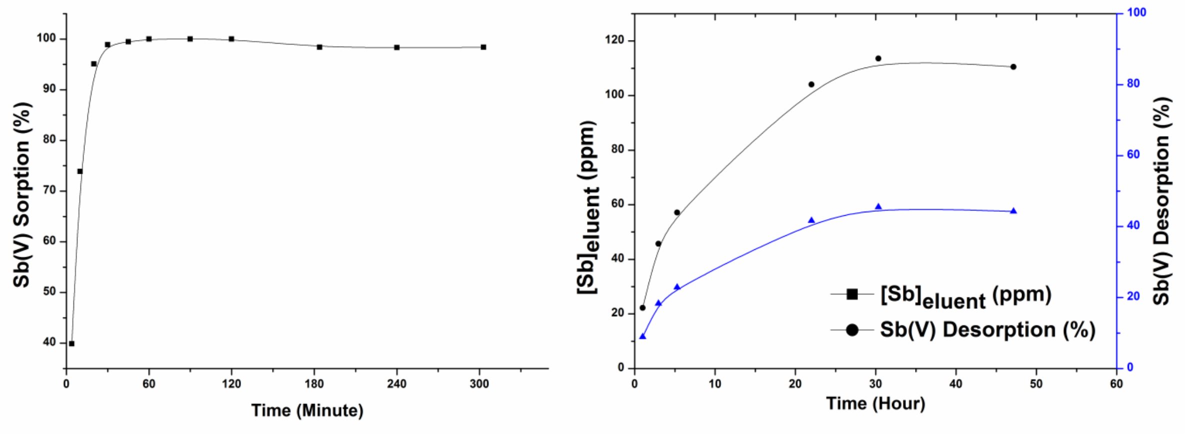

Figure 5.13. Kinetics of Sb(V) (a) Sorption and (b) Desorption by TA-Cts beads

5.3.2.3 Evaluation of Sb(III) Sorption Properties of the TA-Cts Beads

5.3.2.3.1 Sb(III) uptake over TA-Cts beads from Sb(III)-Tartrate solutions of different concentrations

To find the saturation capacity of the TA-Cts beads prepared, about 7.5 mg of the TA-Cts beads were equilibrated (for 24 h) with 1.5 mL of the Sb(III) solutions of varying concentrations. The concentrations of Sb(III) solutions used for the studies ranged from 0.01 mM to 20.0 mM (C_0). Complete sorption of Sb(III) was seen even at low solution concentrations (Fig 5.14a). Figure 5.14b shows that the saturation capacity of 259 $mg.g^{-1}$ (2.13 $mmol.g^{-1}$) was obtained with an initial concentration (C_0) of above 2450 ppm (Equilibrium concentration, C_e: 1132 ppm).

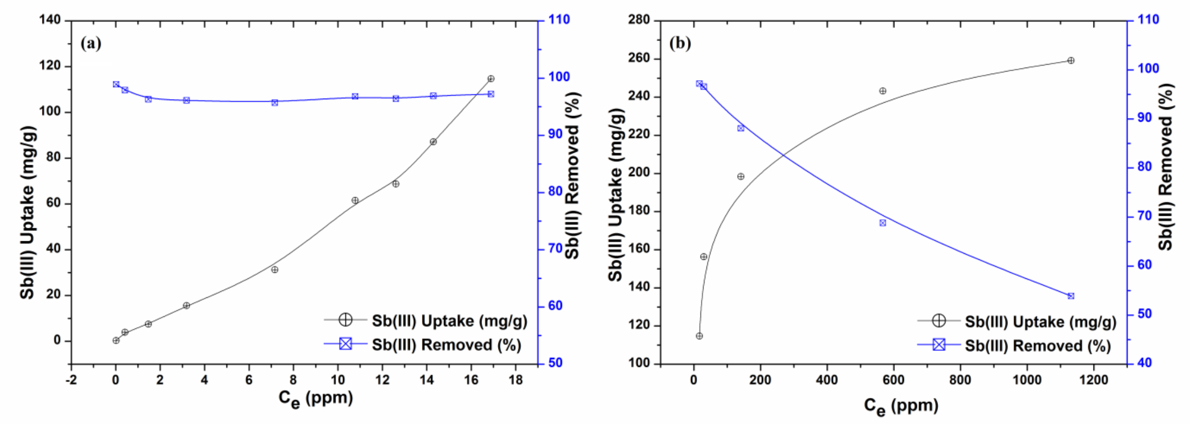

Figure 5.14.Sb(III) sorption over TA-Cts beads: Sb(III) uptake from solutions having different concentrations of antimony

Sb(III) sorption data over the TA-Cts beads were fitted with Langmuir and Freundlich sorption isotherm models (Eq. 2.6 & 2.8 respectively). The Langmuir parameters Q^0 and b; and the Freundlich parameters K_F and n were calculated by least squares method respectively from the plot of C_e/q_e against Ce, and log q_e against log C_e. Sb(III) sorption was found to be fitting in both Langmuir and Freundlich models in the equilibrium concentration range of 0.245 to 9.295 mM. While Sb(III) sorption in the equilibrium concentration range of 1.56 x 10^{-04} to 1.39 x 10^{-01} was found to fit only in Freundlich model. The corresponding plots are given in Fig. 5.15. Table 5.9 gives the Langmuir and Freundlich parameters obtained from the plots.

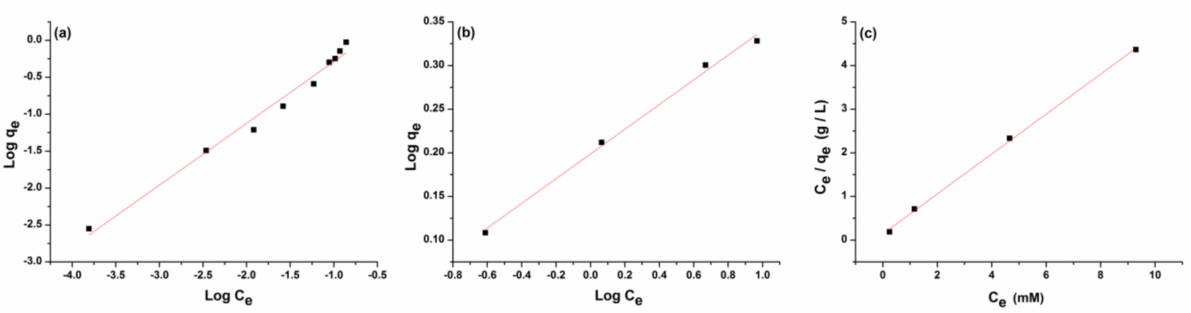

Figure 5.15.Sb(III) Sorption by TA-Cts beads: Isotherm plots - Freundlich plots for C_e: (a) 1.56 x 10^{-04} to 1.39 x 10^{-01} mM Sb(III), (b) 0.245 to 9.295 mM Sb(III), and Langmuir plot for C_e: (c) 0.245 to 9.295 mM Sb(III)

Table 5.9. Langmuir and Freundlich isotherm parameters for Sb(III) sorption over TA-Cts beads

Concentration range, C_e (mM)	**Langmuir Parameters**			**Freundlich Parameters**		
	Q^0 (mmol.g^{-1})	**b**	**R^2**	**K_F** (L.g^{-1})	**n**	**R^2**
1.56 x 10^{-04} to 1.39 x 10^{-01}	--	--	--	3.551	1.195	0.9813
0.245 to 9.295	2.184	3.216	0.9986	1.580	7.068	0.9928

5.3.2.3.2 Sb(III) uptake over TA-Cts beads from Sb(III)-Tartrate solutions having different solution pH

To study the effect of solution pH on Sb(III) sorption over TA-Cts beads, about 25 mg of the TA-Cts beads were equilibrated with 5 ml of the 1 mM Sb(III) solutions, having different initial pH values, for 24 h. The results obtained (Table 5.10) were compared with the values obtained for Nano TiO_2 and Chitosan (section 5.3.1.2, Table 5.5). TA-Cts beads showed good pickup of Sb(III) in a similar fashion to nano TiO_2. Table 5.10 shows the effect of solution pH on the Sb(III) sorption and the extent of sorption induced change in the solution pH by the TA-Cts beads. There was Sb(III) hydrolysis leading to its precipitation at pH conditions above neutral pH. As with Sb(V) sorption, there was significant change in the pH during sorption, as evidenced by the equilibrium pH values. Thus, the synthesised beads are effective sorbents for both the forms of antimony from aqueous solutions

Table 5.10. Sb(III) uptake over TA-Cts beads: Effect of solution pH

Sorbent	**pH (initial): 3.1**			**pH (initial): 6.9**		
	Sb(III) Uptake		**pH_{eq}**	**Sb(III) Uptake**		**pH_{eq}**
	(µmol.g^{-1})	(%)		(µmol.g^{-1})	(%)	
TA-Cts beads	182	97.1	3.5	170	95.5	4.2

5.3.2.4 Evaluation of the TA-Cts Beads Suitability for Column Mode of Operation

The utility of a resin is enhanced if it has flow properties and sorption kinetics suitable for column mode of operation. Therefore, suitability of the TA-Cts beads for using as a column material was evaluated. The sorbent was filled by pouring the TA-Cts beads suspended in water into a glass column (fitted with a Teflon stopper) of 15 cm length and diameter of 0.45 cm. A small amount of glass wool was packed at the end of the column, over which the sorbent was filled to a length of 10 cm. About 250 mg (dry weight) of the TA-Cts was fully wet in ultra-pure water and then used for column filling. Compact channel free filling was ensured by slow filling under constant flow and continuous tapping of the column while filling. The bed volume was 2 mL. About 2.5 L of Sb(V) solutions of concentrations 1.2 ppm and 11.1 ppm were passed through the TA-Cts column in once through mode at a constant flow rate of 2 mL/min. Schematic of the sorption studies done in column mode is shown in Fig. 2.4. A flow rate of one bed volume per minute was maintained during the course of experiment.

The column was found to be very stable and the flow rate could be maintained constant throughout during the operation without any sign of back pressure. Thus, the beads were found to have flow properties suitable for column mode of operation. The Sb(V) concentrations in the outlet of the column were measured with time, and the amount of antimony removed by the TA-Cts beads column was computed. A plot of the ratio of Sb(V) concentrations at the outlet to inlet of the column with the volume of the Sb(V) solution passed through the column is shown in Fig. 5.16.

There was a gradual increase in antimony concentration at the outlet of the column with time. The small dips around 840 and 1800 mL (420 and 900 min.) were because of the stagnant solution inside the column during its stoppage and restarting on the consecutive days. The maximum sorption capacity obtained was 508 µmol of antimony per gram of the TA-Cts sorbent on passing 2.5 L of 11.1 ppm Sb(V) solution.

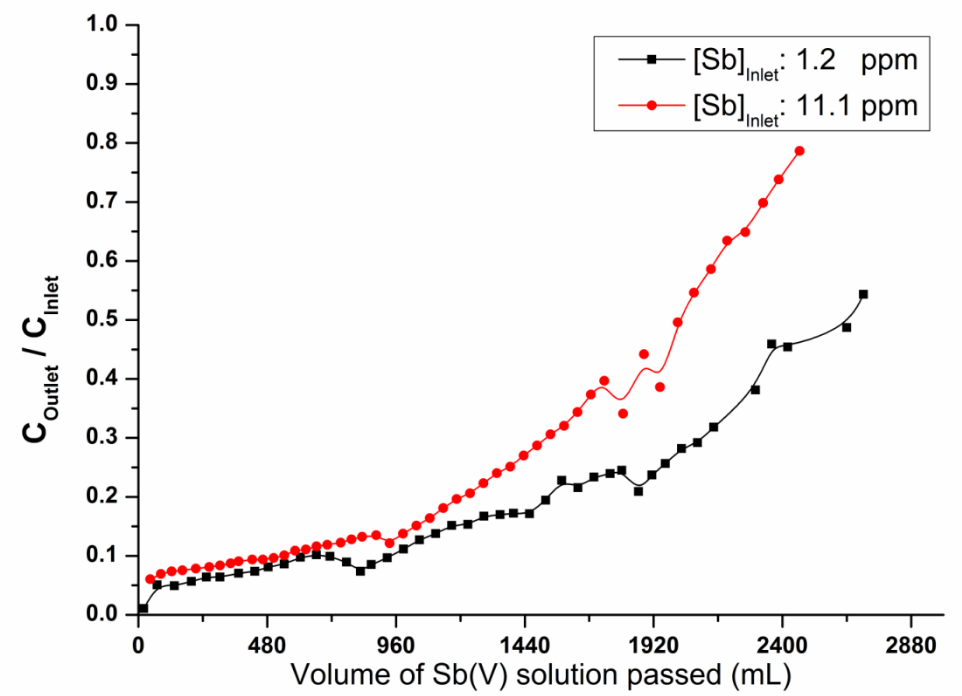

Figure 5.16.Evaluation of the TA-Cts beads suitability for column mode of operation: Removal of Sb(V) over TA-Cts beads column with the volume of the solution passed, in once through mode

5.3.3 Nano Titania Impregnated - Epichlorohydrin Crosslinked Chitosan (TA-Cts) Beads of Varying TiO_2 and Chitosan Compositions

5.3.3.1 Synthesis

The optimisation of the synthesis parameters that affect the formation of stable beads have been carried out in detail. The important step in the synthesis is the formation of stable beads. The major factors that affect the formation of the stable beads are the solute to solvent ratio (of chitosan to acetic acid solution) and the strength of the precipitating (NaOH solution) media. The solute to solvent ratios, 0.4 g chitosan to 20 mL and 0.4 g chitosan to 30 mL of 3% acetic acid solutions, made the bead formation easy; but the formed beads were deformed easily. Increase in the solute to solvent ratio (i.e., decreasing the acetic acid solution from 20 mL to 16 mL for 0.4 g of chitosan) made the dispersion very thick and the dropping syringe needle was blocked easily while passing the solution. To circumvent this, needle gauge has been decreased from 22 (used for making the earlier reported TA-Cts beads, section 2.4) to 20. Further, nano TiO_2 particles were dispersed thouroughly in the chitosan solution by repeated stirring and sonication. Strength of the precipitating media (NaOH solution) was increased from 0.25 M to 1 M in order promote fast precipitation and to avoid the bead breakage. Uniform spherical beads were obtained for all the ratios studied (section 5.2.3). The 4TA-2Cts beads alone got flattened and disc like structures were obtained on drying.

Percentage yield of the TA-Cts beads obtained (Table 5.11) were calculated based on the weights of the chitosan and the TiO_2 used. Any yield of more than 100% is contributed by the crosslinking agent, epichlorohydrin. The decrease in yield may be due to the increase in relative loss of dropping solution over the dropping system during the synthesis. That is, the effect of 1 mL loss in the total dispersion volume for the 4TA-2Cts beads (total dropping solution was 16 mL) will be significantly higher compared to 1TA-5Cts beads (total dropping solution was 40 mL) on the final yield of the beads obtained. Nano titania addition was found to decrease the density of the beads, for lower ratio, compared to chitosan. But addition of more titania was found to increase the density of the beads due to the increased titania content.

Table 5.11. Synthesis of the TA-Cts beads of varying compositions: Yield and Physical properties of the composite beads obtained

Sorbent Name	**Yield**		**Diameter**	**Dry Density**
	(g)	(%)	(mm)	(g.cc^{-1})
Cts-CL	1.11	110.8	0.82±0.07	1.74
1TA-5Cts	1.27	105.8	0.92±0.05	1.52
2TA-4Cts	0.57	95.7	0.87±0.05	1.57
3TA-3Cts	0.54	90.0	0.99±0.04	1.77
4TA-2Cts	1.01	84.1	--	--
1p25-5Cts	1.29	107.1	--	--

5.3.3.2 Swelling Properties of the Composite Beads

Swelling parameters (ESR and EWC) of the composite beads were obtained by treating 100 mg of the TA-Cts beads with 25 mL of the ultra-pure water (swelling agent) for 48 h. The TA-Cts beads were found to take up and retain good amount of water as indicated by the swelling parameters. The pH of the ultrapure water (pH_{in}: 6.0) decreased on equilibration with the TA-Cts beads. Both ESR and EWC were found to decrease with increase in titania content (Table 5.12). Since the biopolymer chitosan is responsible for the water uptake, decrease in swelling with decrease in chitosan content is explainable. The increase in titania content in the beads decreases the polymeric content of the beads. The higher values of EWC and ESR for the 1TA-5Cts beads compared to the TA-Cts beads (discussed in the section 5.3.2.1), even though they had similar compositions, indicates the effect of crosslinker added. During the synthesis, addition of an additional (over and above the amount taken in the pre-polymerisation mixture) 1 mL epichlorohydrin during the ageing of the beads may be responsible for the high swelling. Addition of more amount of the crosslinker was found to increase the swelling. Wet densities of the beads were found to increase with increase in titania content. TA-Cts composite beads prepared using AEROXIDE® TiO_2 P 25 (i.e., 1p25-5Cts) showed similar swelling parameters compared to the 1TA-5Cts, which contain the same ratio of TiO_2 and chitosan.

Table 5.12. Swelling properties of the TA-Cts beads of varying compositions

Sorbent Name	**$pH_{Eq.}$**	**EWC** (%)	**ESR** (%)	**True Swollen density** ($g.mL^{-1}$)
Cts-CL	3.3	94.9	1882	1.029 ± 0.006
1TA-5Cts	3.2	91.8	1122	1.031 ± 0.002
2TA-4Cts	3.4	86.0	615	1.067 ± 0.004
3TA-3Cts	3.5	82.4	468	1.089 ± 0.003
4TA-2Cts	5.4	55.0	122	1.269 ± 0.024
1p25-5Cts	3.3	93.5	1440	1.028 ± 0.004

5.3.3.3 Antimony Uptake Properties of the Composite Beads: Batch Studies

Antimony uptake by the sorbents were studied in batch mode by equilibrating 20 mg of the sorbents with 10 mL of the 5 mM solution of Sb(V), having pH 5.1, for 48 h on a test tube rotator. Sb(V) sorption by the parent nano TiO_2 was also studied for comparison. The respective capacities and equilibrium pH obtained for each sorbent are given in Table 5.13. Antimony uptake was in tune with the swelling parameters and was found to decrease with increase in titania content. Crosslinked chitosan showed the maximum uptake capacity, 2.15 $mmol.g^{-1}$. Most of the TA-Cts beads showed a better uptake compared to the parent nano TiO_2 powder, even at higher equilibrium pH values. The decrease in uptake capacity with increase in TiO_2 content (or decrease in chitosan content) indicates the involvement of crosslinked chitosan in the antimony uptake. Unlike the non-cross linked chitosan (section 5.3.1.2.3), crosslinked chitosan showed higher antimony uptake capacity.

Table 5.13. Sb(V) uptake by the TA-Cts composite beads of varying compositions: Batch studies

Sorbent	**$pH_{Eq.}$**	**Antimony Uptake**	
		($\mu mol.g^{-1}$)	(%)
Cts-CL	5.1	2153 ± 33	85.9
1TA-5Cts	5.2	1959 ± 33	81.8
2TA-4Cts	5.7	1628 ± 31	63.7
3TA-3Cts	5.9	1273 ± 25	50.6
4TA-2Cts	7.5	336 ± 48	13.4
1p25-5Cts	5.2	2040 ± 28	81.8
Nano-TiO_2	3.6	1345 ± 60	52.3

The increased uptake by the crosslinked chitosan may be due to the presence of protonated amine functional groups present over the chitosan back bone which pave the way for Sb(V) anion uptake through electrostatic interactions (section 3.3.1). Decrease in uptake capacity with increase in titania content may be attributed to the corresponding decrease in the protonated amine functional groups (due to the reduced chitosan content in the composite beads) and the increase in equilibrium pH. The largely reduced uptake of Sb(V) by 4TA-2Cts beads, less than what is expected from the corresponding TiO_2 component, is an indication of the role of pH on sorption. The high equilibrium pH obtained for the 4TA-2Cts beads indicate the deprotonation of chitosan amine groups and titania hydroxyl groups (section 5.3.1.2.2) which results in less pickup of antimony. TA-Cts composite beads prepared using AEROXIDE® TiO_2 P 25 was also found to have good antimony uptake capacity, 2.04 $mmol.g^{-1}$, and was comparable to the uptake by 1TA-5Cts beads (1.96 $mmol.g^{-1}$), which has similar chitosan/TiO_2 composition.

5.3.4 Nano TiO_2-Chitosan (TA-Cts) and Chitosan (Cts) Beads with Varying Epiochlorohydrin Content

5.3.4.1 Synthesis

Non-crosslinked nano titania impregnated-chitosan (TA-Cts) beads (and the non-crosslinked chitosan beads (Cts)) were obtained as homogenous, uniform sized beads using the simple procedure followed (sections 5.2.4.1 & 5.2.4.2). In order to study the effect of the crosslinker amount added on the properties of TA-Cts and Cts beads, non crosslinked beads thus prepared were treated with different amounts of epichlorohydrin (Fig. 5.17b). Epichlorohyrin is known to crosslink through the hydroxyl functional groups under basic conditions [123]. About 50 to 500 µL of epichlorohydrin was added to each 0.3 g lot of the non-crosslinked TA-Cts beads for crosslinking. The increase in yield of TA-Cts-Epi beads with increase in epichlorohydrin added indicates associated increase in the epichlorohydrin moieties in the resultant beads (Table 5.2).

To obtain chitosan beads with different amounts of epichlorohydrin, fixed amount (189 mg) of non-crosslinked chitosan beads were crosslinked with varying amounts (1, 2, 5 and 10 mmol) of epiclorohydrin. The increase in the yield of Cts-Epi beads with increase in epichlorohydrin added indicates the increased incorporation of epichlorohydrin in the resultant beads (Table 5.3).

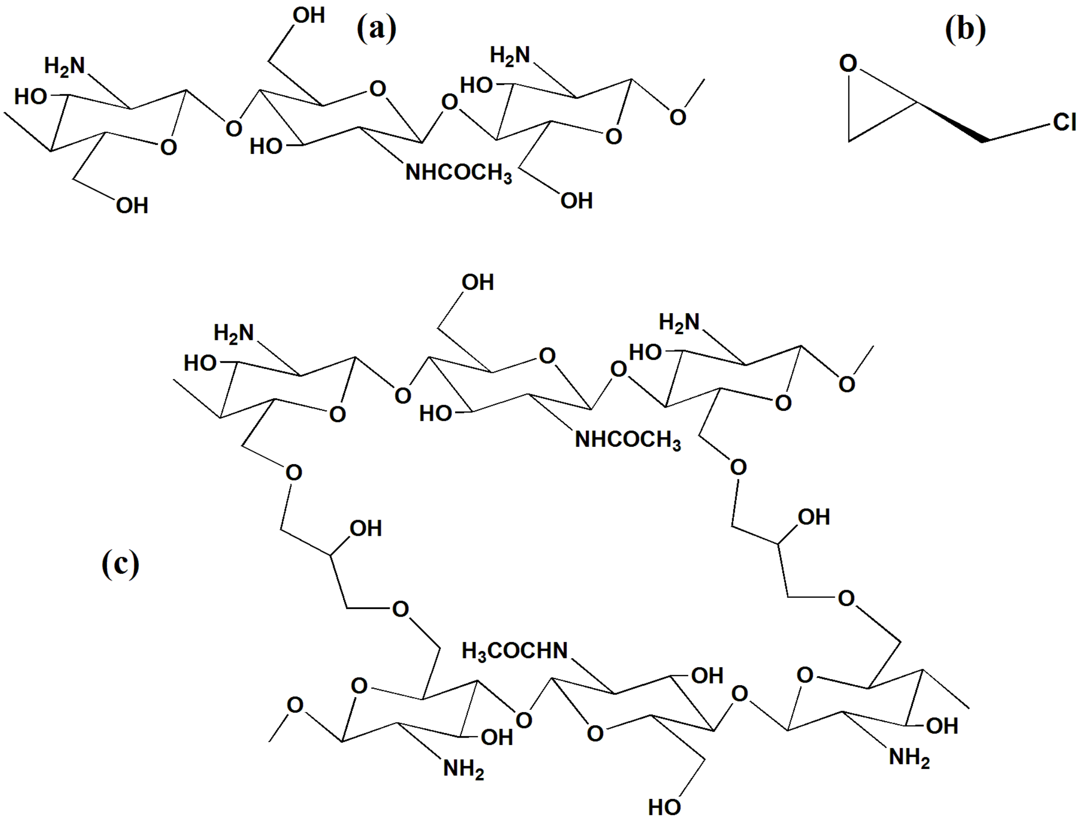

Figure 5.17.Structures of (a) Chitosan (b) Epichlorohydrin and (c) Epichlorohydrin crosslinked chitosan

5.3.4.2 C-13 NMR characterization of chitosan and epichlorohydrin crosslinked chitosan beads

Fig. 5.18(a) shows the C-13 NMR spectrum of chitosan. The peak assignments have been made based on literature reports [181]. Figs. 5.18(b) and 5.18(c) show the NMR spectra of the epichlorohydrin crosslinked chitosan beads prepared with chitosan:epichlorohydrin ratio of 1:2 & 1:10 respectively. It is known that the C-13 NMR of homo/copolymers of epichlorohydrin show 3 major peaks at $\delta \sim 78$ (CH backbone), $\delta \sim 68$ (CH_2 backbone) and $\delta \sim 44$ (CH_2Cl) [182, 183]. The broadening observed in the spectra of the crosslinked chitosan clearly indicates the incorporation of epichlorohydrin. Moreover the peak in crosslinked chitosan at δ ~ 46 is a clear indication of the incorporation of the methyl groups ($-CH_2Cl$) of epichlorohydrin. The increase in intensity of this peak with increase in epichlorohydrin adds support to this argument.

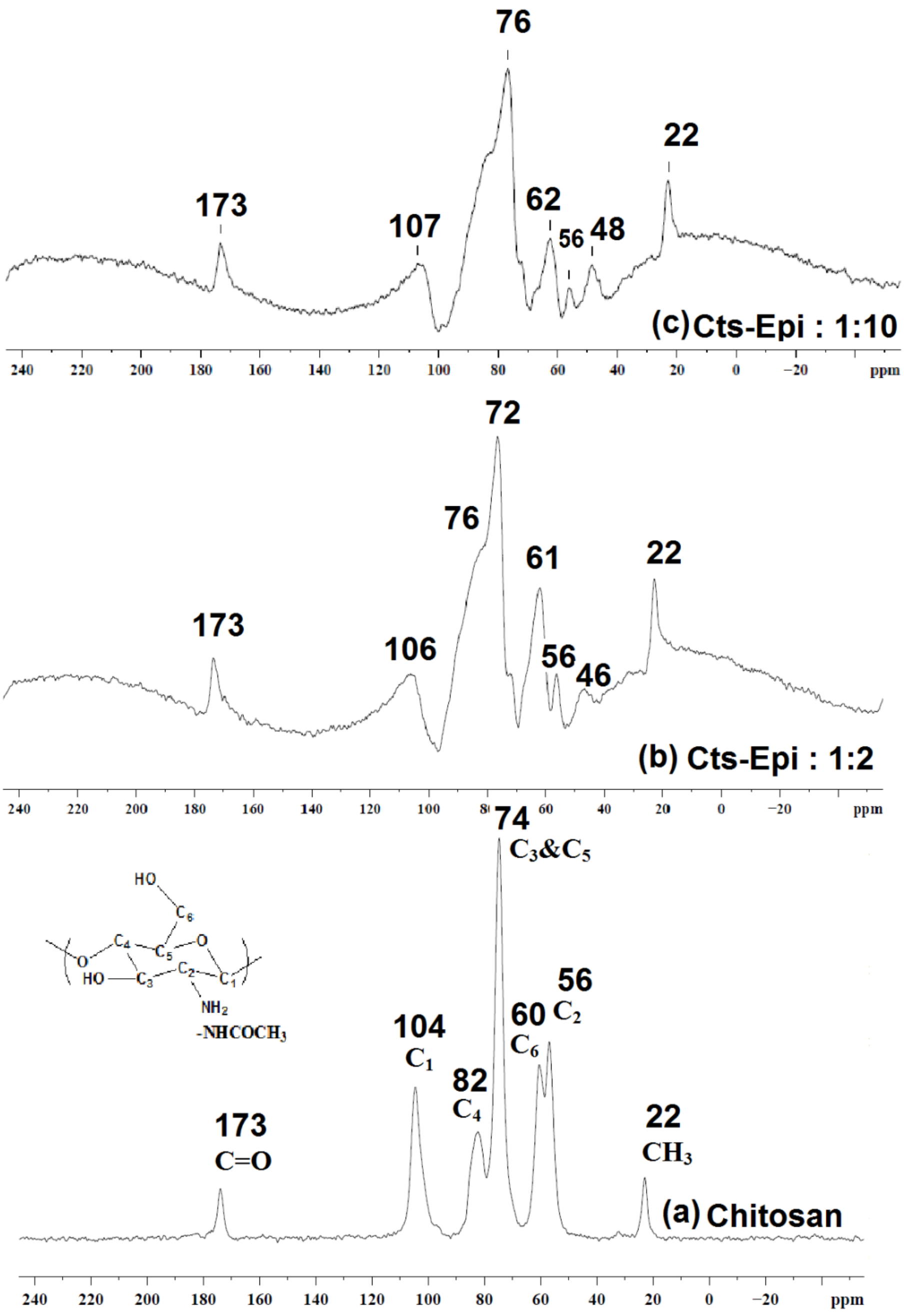

Figure 5.18. C-13 NMR spectra of (a) chitosan, (b) Cts-Epi; 1:2, and (c) Cts-Epi; 1:10

5.3.4.3 Physical Properties of the TA-Cts-Epi and Cts-Epi Beads

5.3.4.3.1 TA-Cts-Epi Beads

Effect of the amount of crosslinker added on the physical and solution properties of the TA-Cts-Epi beads prepared was analysed in detail. Size of the TA-Cts-Epi beads was found to increase with increase in crosslinker amount added (Table 5.14). Density values showed an initial increase with increase in the amount of crosslinker used (up to 100 µL), which then decreased with further increase in the amount of crosslinker added. Crosslinker may be acting like a spacer between two adjacent chitosan chains and hence the introduction of the crosslinker may make the bead bulkier as compared to the raw beads. There are chances for self-polymerisation of epichlorohydrin as well. Homo and co-polymerisation of epichlorohydrin through ring opening has been reported [184]. Reduction in the density of the TA-Cts beads with increase in epichlorohydrin (in excess) indicates the possibility of homopolymerisation of the epichlorohydrin through glycidol moieties and their incorporation in between the chitosan chains.

Swelling parameters such as equilibrium swelling ratio (ESR) and equilibrium water content (EWC) did not show any regular trend with the amount of epichlorohydrin added. About 0.1 g of the TA-Cts beads were used for the swelling studies with ultra-pure water as the swelling agent. Both ESR and EWC values were found to reduce, while the true swollen density increased, with introduction of crosslinking. The reduction in swelling with crosslinking is expected, as the crosslinking will hinder the movement of the chitosan chains. The hydroxyl ether functional groups generated via crosslinking through the hydroxyl groups of the chitosan (Fig. 5.17c), under basic conditions, is more hydrophilic and its concentration inside bead increases with increase in addition of epichlorohydrin.

Hence, the uptake of water by the TA-Cts beads may also increase with increase in epichlorohydrin added.

Table 5.14. Physical properties of the TA-Cts-Epi beads

Sorbent Name	**Diameter** (mm)	**Dry Density** ($g.cc^{-1}$)	**Swollen density** ($g.mL^{-1}$)	**EWC** (%)	**ESR** (%)	$pH_{Eq.}$
TA-Cts-NCL	0.88 ± 0.06	1.51	1.22	54.2	118.4	6.2
TA-Cts-Epi050	0.93 ± 0.06	1.51	1.36	27.4	37.7	3.1
TA-Cts-Epi100	0.95 ± 0.09	1.52	1.40	26.4	35.9	3.1
TA-Cts-Epi200	0.98 ± 0.05	1.47	1.31	31.8	46.8	3.2
TA-Cts-Epi350	1.03 ± 0.05	1.31	1.26	31.3	45.6	3.2
TA-Cts-Epi500	1.05 ± 0.06	1.26	1.34	33.0	49.2	3.2

The nano titania impregnated-epichlorohydrin crosslinked chitosan beads studied in section 5.3.2 were prepared by the addition of the crosslinking agent during the bead formation stage itself, while the beads detailed here were prepared by crosslinking of the pre-formed beads. The swelling parameters were high (ESR – 200.1% and EWC – 66.6%) for the TA-Cts beads for the former as compared to the later. Addition of epichlorohydrin during the bead formation stage ensures the homogeneous distribution of the crosslinker in the pre-polymerisation solution, and hence uniform crosslinking in the bulk of the beads. Whereas, when crosslinking is performed on preformed beads, crosslinking may be confined more to the surface of the beads than the bulk. Hence, introduction of higher amounts of epichlorhydrin moieties makes the beads more hydrophilic and swellable.Thus, 100 µL of epichlorohydrin per 0.3 g of the non-crosslinked TA-Cts beads is enough for obtaining the maximum bead density and less swelling. Addition of more epichlorohydrin actually makes the beads bulkier, and more swelling, unlike the regular ion exchange resins (in regular ion exchange resins, swelling of the beads decreases with increase in crosslinking agent added [94]).

5.3.4.3.2 Cts-Epi Beads

Effect of the epichlorohydrin amount added on the physical properties of the Cts-Epi beads obtained was studied in detail. Cts-Epi beads were seen to have similar properties as the TA-Cts-Epi beads. Non crosslinked chitosan beads showed the least swollen density with maximum swelling and water uptake. Both EWC and ESR were found to increase with increase in epichlorohydrin content (Table 5.15). The similar trend in EWC and ESR among the Cts-Epi beads and TA-Cts-Epi beads shows that the chitosan component is responsible for the swelling of the TA-Cts-Epi beads as well.

Table 5.15. Physical properties of the Cts-Epi beads

Sorbent Name	**Swollen density** (g.mL^{-1})	**EWC** (%)	**ESR** (%)	**pH$_{Eq.}$**
Cts-NCL	1.14	59.4	146.3	4.7
Cts:Epi-1:1	1.32	21.6	27.6	3.3
Cts:Epi-1:2	1.30	23.5	30.7	3.3
Cts:Epi-1:5	1.32	29.1	41.1	3.1
Cts:Epi-1:10	1.28	33.1	49.4	3.2

5.3.4.4 Sorption Studies Using TA-Cts-Epi and Cts-Epi Beads

Sorption or removal of metal ions over chitosan based sorbents is dependent on the crosslinking agent used or the crosslinking density of the sorbent. The uptake capacity and the sorption kinetics were found to be affected by crosslinking. Utilisation of the functional groups responsible for the metal ion sorption by the crosslinker will reduce the metal uptake. Moreover, crosslinking will hinder the access of the metal ions to the binding sites and as a result lead to reduction in metal ion uptake by the sorbents. Any hindrance in access to the targeted binding sites will affect the kinetics of the sorption as well. Studies on the uptake of metal ions by chitosan (section 3.3.3) and Co(II)- ion imprinted chitosan (section 4.3.6) showed that uptake capacity and kinetics were largely affected by crosslinking. Studies on the effect of the crosslinker added on the sorption properties of the TA-Cts-Epi beads and Cts-Epi beads are detailed below.

5.3.4.4.1 Sorption of antimony over TA-Cts-Epi beads

Removal of antimony, as Sb(V), by the TA-Cts-Epi beads synthesised using varying amount of crosslinker were analysed in batch mode. The results obtained are given in Table 5.16. In the first set of experiments, which were done using 1 mM Sb(V) solution, and with 48 h equilibration, antimony uptake was found to increase with increase in epichlorohydrin added. Studies carried out using 5 mM Sb(V) solution, and with 5 days equilibration, showed a different trend, and indicated the need for longer equilibration time for obtaining the sorption equilibrium by the crosslinked TA-Cts-Epi beads. In the second step of experiments, Lowest Sb(V) uptake capacity (in the crosllinked TA-Cts-Epi beads) was shown by TA-Cts-Epi100 beads, and the maximum uptake capacity was shown by the TA-Cts-Epi500 beads.

Table 5.16. Results of sorption studies with TA-Cts-Epi beads: Sb(V) removal by the sorbents

Sorbent / conditions used	**10 mg to 10 mL of 1 mM Sb(V) solution ($pH_{in.}$ 5.4), 48 h**			**20 mg to 10 mL of 5 mM Sb(V) solution (pH_{in}. 5.1), 5 days**		
	Sb(V) uptake		**$pH_{Eq.}$**	**Sb(V) uptake**		**$pH_{Eq.}$**
	(µmol.g^{-1})	(%)		(µmol.g^{-1})	(%)	
TA-Cts-NCL	75	7.4	7.0	119	5.0	7.1
TA-Cts-Epi050	134	13.4	3.8	312	13.1	4.0
TA-Cts-Epi100	140	13.6	3.9	271	11.2	3.9
TA-Cts-Epi200	195	19.1	4.5	287	12.0	4.0
TA-Cts-Epi350	356	35.2	4.2	501	20.8	4.1
TA-Cts-Epi500	493	49.9	4.3	697	29.3	4.3

The uptake capacities showed by the crosslinked TA-Cts-Epi beads can be correlated with the swelling properties of the beads as; the least capacity (and minimum swelling) was observed with TA-Cts-Epi100 and the highest capacity (and maximum swelling) was observed with TA-Cts-Epi500 beads. This may be attributed to the better access to the binding sites (in more swollen beads) by antimony ions.

The least capacity shown by the non-crosslinked TA-Cts beads, even though they swell more compared to the crosslinked beads, may be due to the higher equilibrium pH obtained with the TA-Cts-NCL beads. In the case of crosslinked TA-Cts beads, equilibrium pH values were well below the pKa of chitosan amine groups and pZc of TiO_2. This provides the favourable conditions for the uptake of the Sb(V), as $[\mathrm{Sb(OH)_6}]^-$ anions, through electrostatic interaction with the positively charged surface. For non-crosslinked TA-Cts beads, equilibrium pH was above the pKa of chitosan amine groups and the sorption may occur only through the TiO_2 surface and resulted the reduced pickup of Sb(V).

5.3.4.4.2 Sorption of antimony over Cts-Epi beads

To know the effect of crosslinking agent added on the sorption properties of the chitosan beads, Sb(V) removal by the Cts-Epi beads was studied in batch mode. The results obtained are given in Table 5.17.

Table 5.17. Results of sorption studies with Cts-Epi beads: Sb(V) removal by the sorbents

Sorbent / conditions used	**10 mg to 5 mL of 1 mM Sb(V) solution (pH_{ini} 5.6), 4 days**			**20 mg to 10 mL of 5 mM Sb(V) solution ($pH_{ini.}$ 4.8), 5 days**		
	Sb(V) Uptake		**$pH_{Eq.}$**	**Sb(V) Uptake**		**$pH_{Eq.}$**
	(µmol.g^{-1})	(%)		(µmol.g^{-1})	(%)	
Cts-NCL	82	17.0	6.5	130	5.7	6.6
Cts:Epi-1:1	15	3.3	3.9	21	1.0	3.8
Cts:Epi-1:2	95	20.6	3.8	43	2.0	3.8
Cts:Epi-1:5	397	86.3	3.5	362	17.1	3.7
Cts:Epi-1:10	422	95.7	3.6	652	30.6	3.8

Despite the favourable (acidic) pH conditions for Sb(V) sorption by the Cts-Epi beads, with introduction of crosslinking, there was decrease in uptake capacity in the least crosslinker added sample (Cts-Epi-1:1) as compared to the non-crosslinked beads (Cts-NCL). Sb(V) uptake of the crosslinked Cts-Epi beads increases with the increase in crosslinker added, and follows the swelling behaviour of the Cts-Epi beads (Table 5.15), similar to the TA-Cts-Epi beads as has already been explained in the previous section.

5.3.4.5 Kinetics of Antimony Sorption over TA-Cts-Epi Beads

Sorption kinetics of metal ions over ion exchange resins or on other crosslinked matrices largely depends upon the nature of the crosslinking agent and the crosslinking density. To study the effect of crosslinker added on the sorption kinetics of TA-Cts-Epi beads, 20 mg of the TA-Cts-Epi beads were equilibrated with 10 mL of the 1 mM Sb(V) solutions in batch mode. Samples were collected at regular intervals and analysed for antimony removal with time. The results obtained are plotted in Fig. 5.19.

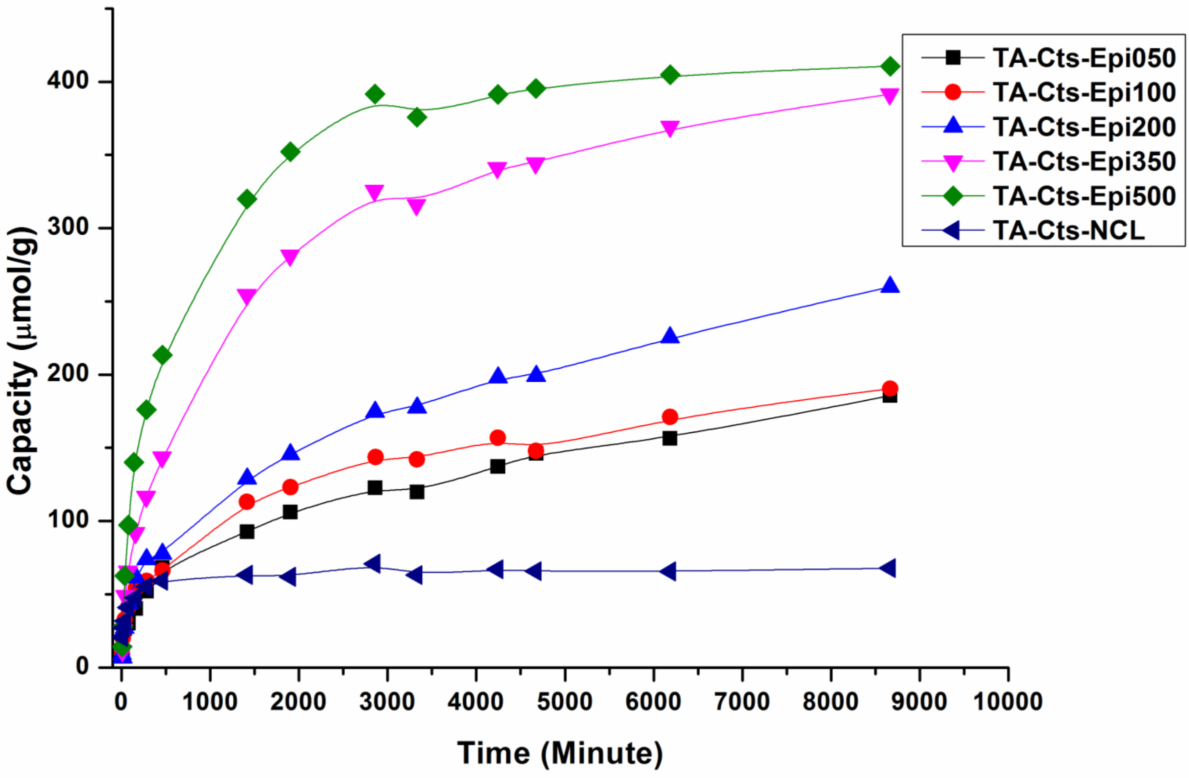

Figure 5.19.Kinetics of antimony sorption over TA-Cts-Epi beads: Antimony uptake over TA-Cts-Epi beads with time

The results showed a faster attainment of equilibrium (even though the capacity is less) for the non-crosslinked TA-Cts beads compared to the crosslinked TA-Cts-Epi beads. Crosslinking hinder the Sb(V) uptake, and the rate of Sb(V) uptake was largely affected by the crosslinker (epichlorohydrin) added. The experimental kinetic data were plotted as linearized forms of the integrated pseudo first order (Eq. 2.11) and second order kinetics rate expressions (Eq. 2.12). Sorption of antimony over the TA-Cts-Epi beads with time was found to follow the pseudo second order kinetics equation, which is characteristic of chemisorption.

The pseudo second order kinetic constant, K_2, and the theoretical equilibrium capacity, q_e, were obtained by plotting t/q versus t. The linear fit was found to be better (R^2, regression coefficient value, closer to unity) on splitting the plots into two regions. i.e., 0 to 500 and 500 to 8600 min. Non-crosslinked TA-Cts beads were found to follow the pseudo second order kinetic equation over the entire equilibration period, while crosslinked beads showed some difference (Table 5.18).

Table 5.18. Pseudo second order kinetic model parameters for Sb(V) sorption over TA-Cts-Epi Beads

Sorbent Name	**Full Range**			**0-500 minutes**			**500-8600 minutes**		
	R^2	q_e	K_2 (E-6)	R^2	q_e^I	K_2^I (E-4)	R^2	q_e^{II}	K_2^{II} (E-6)
TA-Cts-NCL	0.9988	67.6	229	0.9953	62.5	4.83	0.9966	66.7	269
TA-Cts-Epi050	0.9587	175.4	7.92	0.9606	59.2	3.05	0.9773	181.8	4.44
TA-Cts-Epi100	0.9771	185.2	9.56	0.9973	71.9	2.86	0.9895	192.3	5.14
TA-Cts-Epi200	0.9633	256.4	4.75	0.9944	90.9	1.48	0.9878	270.3	2.49
TA-Cts-Epi350	0.9925	400	4.31	0.9909	178.6	0.435	0.9977	416.7	2.62
TA-Cts-Epi500	0.9989	416.7	7.66	0.9902	270.3	0.277	0.9989	434.8	4.93

The changes are more visible in the values of q_e and K_2. K_2^I, q_e^I and K_2^{II}, q_e^{II} are the respective pseudo second order kinetic constants and the theoretical equilibrium capacities for the two regions selected. The effect of the amount of crosslinker added on the K_2 values was more prominent for the initial period of time (i.e., K_2^I), which found to decrease with increase in the crosslinker added (Fig. 5.20). K_2^I values were greater than the corresponding K_2 and K_2^{II} values, and the difference between the two K_2 values (K_2^I and K_2^{II}) were more prominent for the less crosslinker added beads.

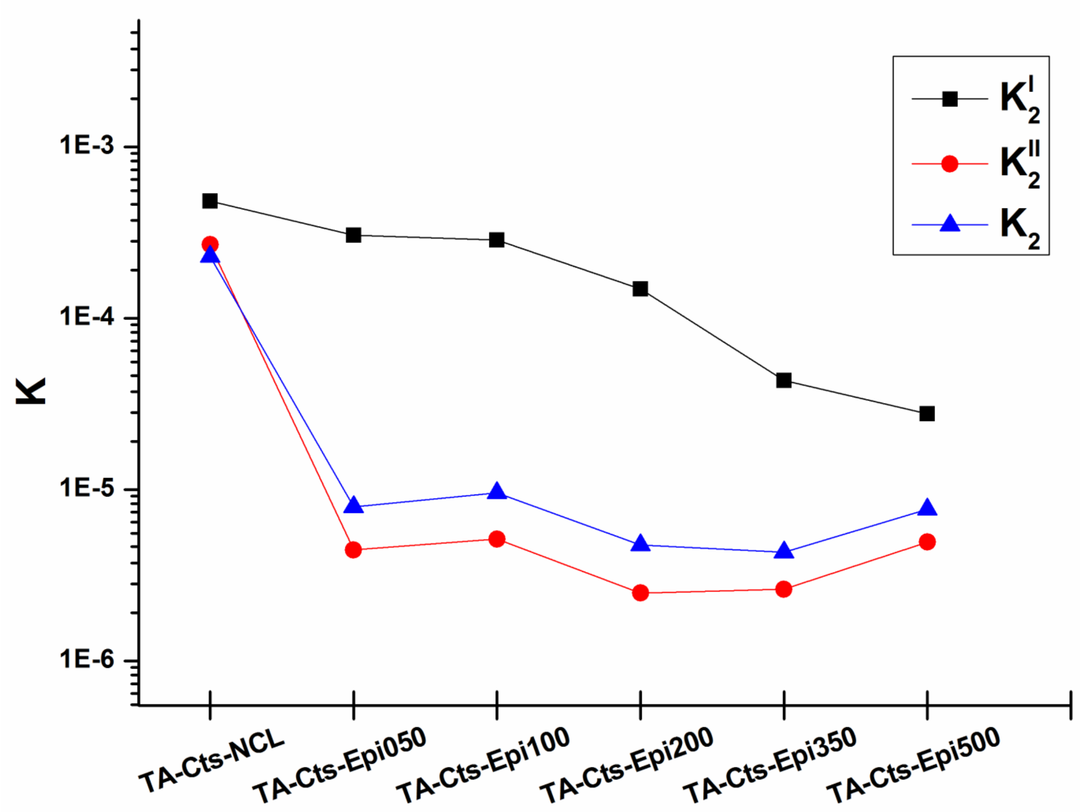

Figure 5.20.Kinetics of Sb(V) sorption over TA-Cts-Epi beads: Pseudo second order rate kinetics constants variation with epichlorohydrin added

The high ESR values for the samples having high amounts of epichlorohydrin, due to the associated increase in the ease of access to the binding sites, should lead to faster kinetics for the sorption. However, the K_2^I showed a decrease with increase in epichlorohydrin, which indicate the possibility of existence of different types of binding sites in the sorbents.

5.4 Conclusion

The comparative analysis of the six different sorbents revealed the importance of the solution pH and the antimony speciation in the solution on the antimony uptake by the sorbents. Among the six sorbents studied, titania based materials are seen to be more promising for antimony removal when both Sb(V) and Sb(III) are present in the solution, while anion resin was found to be better as a column material at relatively wider pH range for removal of antimony present as Sb(V). This study has importance in (i) nuclear industry wherein processes involving different pH conditions and either reducing or oxidising conditions are contemplated for effective removal of radioactive antimony, (ii) treating antimony containing industrial effluents, and (iii) water treatment processes for devising effective antimony removal strategies.

Nano Titania–Chitosan (TA-Cts) composite sorbent was synthesised as beads and studied for its antimony sorption properties. The beads were shown to be effective sorbent for both forms (+3 and +5) of antimony. Preparation of the sorbent in the form of beads makes it more suitable for the envisaged large scale applications. The beads were shown to be stable and suitable for column mode operation**,** with reasonably high dynamic capacity of 500 µmol of Sb per g of the TA-Cts beads.

The study has detailed an easy reproducible procedure for the preparation of nano titania impregnated – epichlorohydrin crosslinked chitosan beads of varying TiO_2 and chitosan compositions. The decrease in antimony uptake with increase in nano TiO_2 content (or decrease in chitosan content) demonstrated the importance of crosslinked chitosan in removing Sb(V) present as anionic species. TA-Cts composite beads prepared using AEROXIDE® TiO_2 P 25 was found to have similar swelling and sorption properties as the corresponding 1TA-5Cts beads, which shows the possibility of using different nano TiO_2 samples for the synthesis of the TA-Cts beads with reproducible physical and sorption properties.

Crosslinking makes the TA-Cts beads a better sorbent for antimony with increased uptake and better physical properties. TA-Cts-Epi/Cts-Epi beads with varying crosslinking density can be easily prepared. It is possible to have good control over the physical and sorption properties of the beads prepared by employing suitable conditions. The beads prepared showed good antimony sorption properties. Amount of the crosslinking agent (epichlorohydrin) added was found to affect both the antimony uptake capacity and kinetics of the TA-Cts-Epi beads. Crosslinking make the TA-Cts beads a better sorbent for antimony with increased uptake.

Chapter 6. INVESTIGATIONS ON THE SUITABILITY OF TA-Cts BEADS FOR ANTIMONY REMOVAL DURING NUCLEAR REACTOR DECONTAMINATION

6.1 Introduction

Synthesis, characterisation and the preliminary evaluation of antimony sorption properties of the nano titania impregnated-epichlorohydrin crosslinked chitosan (TA-Cts) beads has been discussed in detail in the previous chapter. Herein, studies carried out to evaluate the suitability of the TA-Cts beads for use in the Dilute Chemical Decontamination (DCD) conditions of Indian Pressurized Heavy Water Reactors (PHWRs) are discussed in detail. Detailed studies on the radiation stability of the TA-Cts beads, its selectivity for other ions under DCD conditions and the removal of antimony from typical DCD conditions, under batch and column conditions, over the TA-Cts beads are discussed in the following sections. The column experiments in particular, as would be shown below, established the suitability of the TA-Cts beads for large scale applications like DCD campaigns of NPPs.

6.2 Experimental Details

6.2.1 Evaluation of Radiation Stability

Radiation stability of the beads was evaluated under gamma irradiation. Both *in-situ* and post irradiation sorption studies were carried out. The former was carried out by irradiating the beads suspended in antimony solution for a fixed time interval. Typically, 10 mL of the 1.0 mM Sb(V) solutions was de-aerated with argon gas for 10 minutes, and then equilibrated with 50 mg of the TA-Cts beads in a gamma chamber to different doses. The irradiated samples were taken out of gamma chamber and the sorption equilibration was further continued for about 7 h to complete the sorption. The supernatants were then analysed for antimony uptake and bead decomposition using TOC.

In the second method, 100 mg of TA-Cts beads (or Tulsion® A33) was soaked in 10 mL of double distilled water, de-aerated thoroughly by passing argon and irradiated in the gamma chamber to different doses. The irradiated TA-Cts / Tulsion® A33 resin beads were then separated and dried at 60 ^{O}C, and used for antimony uptake studies. Supernatants were analysed for beads degradation using TOC.

6.2.2 Sorption Studies

Sb(V) sorption properties of the TA-Cts beads were analysed in batch and column mode. For batch sorption studies; Sb(V) solutions were made using $KSb(OH)_6$, Sb(III) solutions with potassium antimony(III) Tartarate, and $(NH_4)_2Fe(SO_4)_2$ was used as source for Fe(II). To study the selectivity of the TA-Cts beads for different ions namely, Co(II), Cu(II), Ni(II), Cr(IV) and Fe(II); 20 mg of the TA-Cts beads were treated with 10 mL of the metal ion solutions (having different compositions). Compositions of the three different solutions prepared are given in Table 6.1.

Table 6.1. Compositions of the solutions made for studying the selectvity of the TA-Cts beads

Solution	**pH$_{in.}$**	**Metal ion concentration (mM)**					
		Sb(III)	**Co(II)**	**Cu(II)**	**Ni(II)**	**Fe(II)**	**Cr(IV)**
Solution A (in ultra-pure water)	3.9	0.90	1.13	1.16	1.18	*	*
Solution B (in NAC formulation)	2.4	0.14	0.18	0.17	0.18	3.92	*
Solution C (in NAC formulation)	2.5	0.19	0.24	0.23	0.23	3.59	0.20

Desorption of the sorbed metal ions were carried out using 5 M HCl. Desorption of the metal loaded samples (20 mg) obtained with solution A was done with 5 mL of 5 M HCl, while metal loaded samples (20 mg each) obtained using solutions B &C were extracted using 2.5 mL of 5 M HCl

For column studies, sorbent column was prepared by filling a glass column of 4 mm diameter with the beads (250 mg) which were swollen overnight in ultrapure water. Typical decontamination formulation (NAC) for the column studies was prepared by dissolving 1.4 mmol NTA, 1.7 mmol ascorbic acid, and 1.4 mmol citric acid in 1 L of demineralised water. For studies using solutions containing Fe(II) ions, 275 mg magnetite powder was dissolved in the NAC solution to obtain a 3.5 mM Fe(II) concentration. Sb_2O_3 was used as the source for antimony. Concentrations obtained using the reagents/conditions used for antimony removal over TA-Cts beads column from NAC formulations were (a) 1.35 ppm Sb, 183.7 ppm Fe at flow rate: 1 mL.min.$^{-1}$(b) 1.31 ppm. Sb at flow rate: 1 mL.min.$^{-1}$ (c) 2.45 ppm Sb at flow rate: 2 mL.min.$^{-1}$ and (d) 1.76 ppm Sb, 206.5 ppm Fe at flow rate: 2 mL.min.$^{-1}$. All the solutions were prepared and kept under deaerated conditions through argon gas purging, and the argon gas flow/cover is maintained throughout the course of the column experiment.

6.3 Results and Discussions

The suitability of the TA-Cts beads for nuclear applications was investigated through detailed studies on irradiation and examination of the sorption properties from typical decontamination formulations.

6.3.1 Evaluation of Radiation Stability of the TA-Cts Beads

Radiation stability of the TA-Cts beads prepared was studied under gamma ray irradiation. The beads, suspended in antimony solution, were irradiated to various pre-determined doses followed by further equilibration without irradiation to take the sorption to completion. The sorption capacity measured was thus reflective of the ability of the beads to sustain irradiation in aqueous medium. The organics released, from possible decomposition of the beads, during irradiation was measured as change in TOC. The results (Table 6.2) clearly show that the gamma irradiation did not negatively affect the sorption, and that the increase in TOC was not significant.

Table 6.2. Sb(V) sorption over TA-Cts beads under gamma irradiation

Dose (kGy)	**pH**		**Antimony Uptake**		**ΔTOC (ppm)**
	Initial	Eq.	(μmol.g^{-1})	(%)	($TOC_{Eq.}–TOC_{In.}$)
0	5.7	3.5	154	76.4	1.6
2	5.2	3.4	167	80.3	1.0
20	5.5	3.6	186	90.3	4.9

There was, however, a noticeable increase in sorption capacity with increase in irradiation dose. The enhanced sorption capacity could be due to the increase in solution temperature associated with increase in irradiation dose.

6.3.1.1 Comparison with A Nuclear Grade Strong Base Anion Resin

Radiation stability and antimony uptake capacities of the TA-Cts beads were compared with Tulsion® A-33, a commercially available nuclear grade strong base anion resin. The evaluation was done by equilibrating antimony solution with TA-Cts beads/ Tulsion® A-33 resin which were irradiated to various doses. The results obtained on equilibration of 10 mg of the irradiated sorbents with 2 mL of 1 mM antimony solutions are given in Table. 6.3.

Table 6.3. Comparison of radiation stability of TA-Cts beads and Tulsion® A33

Dose (kGy)	**Total Organic Carbon (ppm)**		**Sb(V) Sorption**			
	TA-Cts Beads	**Tulsion® A-33**	**TA-Cts beads**		**Tulsion® A-33**	
			(μmol.g^{-1})	(%)	(μmol.g^{-1})	(%)
0	0.2	3.3	158	93.4	121	73.4
5	0.7	3.4	156	93.5	119	74.2
50	24.3	14.3	157	92.4	125	73.2

The stability of the irradiated sorbent was evaluated by measuring the TOC content of the supernatant of the irradiated solutions. The results (Table 6.3) show that the prepared beads compare favourably to the commercial nuclear grade resins in terms of sorption capacity.

There was slight colouration (from off white to pale brown) of the TA-Cts beads at 50 kGy. Nevertheless, the sorption capacity for Sb(V) indicated that the antimony removal properties of the beads were not affected by irradiation. Further, the TOC values show that the beads retained the chemical stability as well.

6.3.2 Antimony Uptake from Complexing Media: Batch Study

Antimony sorption properties of the TA-Cts beads under typical decontamination conditions were evaluated through batch sorption studies involving typical decontamination formulation (NAC) containing known amount of ferrous ions (in excess) and/or antimony. Chitosan and nano titania, the constituents of the TA-Cts beads, were also subjected to sorption studies to obtain better understanding of the sorption behaviour. Sorption results obtained on equilibration of the sorbents with NAC solutions are given in Table 6.4. The results clearly demonstrate the effect of solution conditions and antimony speciation on the sorption properties. TA-Cts beads were able to remove Sb(III) from complexing solutions (82% reduction at an initial concentration of 154 ppb), while Sb(V) pickup was found to be greatly reduced. For iron, chitosan showed maximum sorption and nano-titania the least from NAC solutions. Thus, the metal ion selectivity of the beads seems to align more with titania than chitosan. Further, it is to be noted that from NAC solution containing 303 ppb antimony and 204 ppm of iron, the beads removed 13.1% of antimony and 11.7% of iron. The preferential sorption of antimony over iron, though the latter was present in excess, demonstrates the antimony selectivity of the TA-Cts beads. The pickup of NTA, however, was significant (70 to 86%). The reduction in TOC values was more than what could be accounted for by NTA removal, which indicate the pickup of citric acid/ascorbic acid from the formulation. Nano TiO_2 showed nil or a minimal reduction in TOC indicating a reduced pickup of the complexants from the NAC formulation, which shows that the chitosan component in the TA-Cts beads is responsible for the sorption of NTA. This is in tune with our earlier results which demonstrated the ability of chitosan to remove NTA from solutions containing NTA alone or NTA and metal ions (Chapter 3).

Table 6.4. Antimony uptake from complexing media: Batch studies

Sorbent and test solution	**Sb Removal**		**Fe(II) Removal**		**pH**		**TOC analysis**[#]	
	(%)	(µmol.g^{-1})	(%)	(µmol.g^{-1})	Ini.	Eq.	**Δ TOC** (ppm)	**Reduction** (%)
10 mg TA-Cts with 10 mL Solution-I	36.8	0.4	--	--	2.6	2.6	93.8 (77.5)	28.6 (86.1)
10 mg TA-Cts with 10 mL Solution-II	81.8	1.0	--	--	2.6	2.6	87.5 (71.9)	27.0 (81.1)
10 mg TA-Cts with 10 mL Solution-III	52.1	1.3	--	--	2.7	2.6	90.9 (63.6)	27.9 (70.5)
2 mg Nano TiO_2 with 10 mL Solution-III	37.6	4.1	--	--		2.7	3.6 (0.7)	1.1 (0.8)
4 mg Chitosan with 5 mL Solution-III	6.4*	0.2*	--	--		2.9	-285.2*	-87.6*
10 mg TA-Cts with 10 mL Solution-IV	13.1	0.3	11.7	185	2.5	2.5	64.7 (1.6)	19.4 (1.6)
2 mg Nano TiO_2 with 10 mL Solution-IV	17.6	2.1	1.4	111		2.4	26.4 (BDL)	7.9 (BDL)
4 mg Chitosan with 5 mL Solution-IV	5.4	0.2	16.2	312		2.6	67.9 (BDL)	20.3 (BDL)

[#] NTA was estimated spectrophotometrically and TOC reduction attributable to NTA removal is given in brackets

* Negative values are due to the dissolution of chitosan (at low equilibrium pH), which leads to increase in TOC value on equilibration

BDL: Below detectable level

Solution-I: 146 ppb Sb(V) in NAC formulation

Solution-II: 154 ppb Sb(III) in NAC formulation

Solution-III: 285 ppb Sb (Sb(III)+Sb(V)) in NAC formulation

Solution-IV: 303 ppb Sb (Sb(III)+Sb(V)) and 203.7 ppm Fe(II) in NAC formulation

The pickup of complexants from the NAC formulation by the TA-Cts beads is not favourable for the online application of the TA-Cts beads in recirculating mode during decontamination campaigns. However, the results show that there was a marked reduction in NTA pickup in presence of Fe(II). As a typical decontamination involves presence of Fe(II) in similar concentrations, this makes it a promising material for use in online decontamination campaigns. This aspect was further studied (section 6.3.4) through experiments involving sorption studies in column mode.

6.3.3 Competitive Sorption and Desorption of Metal Ions: Selectivity Studies

To evaluate the ability of the TA-Cts beads to remove antimony from solutions containing other metal ions, which are found during typical PHWR decontaminations, competitive batch sorption experiments were carried out. The batch sorption studies were carried out by equilibrating 20 mg TA-Cts beads with 10 ml of solutions of different compositions (Table 6.1).

The results obtained (Table 6.5) show that the sorbent selectively removes antimony from solutions containing other competitor ions. From the solution A, which contain around 1 mM each of Sb, Cu, Co and Ni in water, the K_d values obtained for each metal ion demonstrate the high selectivity of TA-Cts beads towards antimony over Co^{2+}, Cu^{2+}, and Ni^{2+}. The selectivity against these ions was retained in the NAC formulation as well (Solution B & C), though iron showed K_d values comparable to that of antimony.

Further, to evaluate the possibility of reuse of the sorbent, elution studies were carried out in batch mode using 5 M HCl as the eluent. It was found that by using 5 or 2.5 mL of the eluent, quantitative extraction of the total metal ions sorbed over 20 mg of the beads was feasible (Table 6.5). The relatively lower amount of extraction of antimony from sorbent equilibrated with NAC formulation could be attributed to the very low level of antimony available for removal from the sorbent. This demonstrates the possibility of reuse of the sorbent material.

Table 6.5. Competitive sorption and desorption of metal ions by TA-Cts beads: Selectivity studies

Solutions/conditions Used and Results Obtained			*Solution A*	*Solution B*	*Solution C*
$pH_{Eq.}$			4.1	2.5	2.5
Sb	Sorption	Uptake ($mg.g^{-1}$)	47.18	1.48	1.54
		K_d ($L.g^{-1}$)	429.4×10^{-2}	10.2×10^{-2}	7.8×10^{-2}
	Desorption (%)	1 h	81.0	53.2	49.3
		18 h	84.2	78.1	80.4
Co	Sorption	Uptake ($mg.g^{-1}$)	0.07	0.05	0.13
		K_d ($L.g^{-1}$)	0.1×10^{-2}	0.4×10^{-2}	1.0×10^{-2}
	Desorption (%)	1 h	BDL	BDL	BDL
		18 h	BDL	BDL	BDL
Cu	Sorption	Uptake ($mg.g^{-1}$)	12.64	0.12	0.15
		K_d ($L.g^{-1}$)	26.6×10^{-2}	1.1×10^{-2}	1.0×10^{-2}
	Desorption (%)	1 h	95.9	65.7	59.1
		18 h	97.1	73.2	62.3
Ni	Sorption	Uptake ($mg.g^{-1}$)	0.20	0.02	0.03
		K_d ($L.g^{-1}$)	0.3×10^{-2}	0.2×10^{-2}	0.2×10^{-2}
	Desorption (%)	1 h	BDL	BDL	BDL
		18 h	BDL	BDL	BDL
Fe	Sorption	Uptake ($mg.g^{-1}$)	--	20.14	20.80
		K_d ($L.g^{-1}$)	--	11.4×10^{-2}	13.1×10^{-2}
	Desorption (%)	1 h	--	98.8	93.6
		18 h	--	100	97.2
Cr	Sorption	Uptake ($mg.g^{-1}$)	--	--	0.50
		K_d ($L.g^{-1}$)	--	--	5.4×10^{-2}
	Desorption (%)	1 h	--	--	88.6
		18 h	--	--	97.1

A. *Solution A ($pH_{In.}$: 3.9)*: 0.90 mM – Sb, 1.13 mM – Co, 1.16 – Cu and 1.18 – Ni in ultrapure water
B. *Solution B ($pH_{In.}$: 2.4)*: NAC formulation containing 0.14 mM – Sb, 0.18 mM – Co, 0.17 mM – Cu, 0.18 mM – Ni and 3.92 mM – Fe
C. *Solution C ($pH_{In.}$: 2.5)*: NAC formulation containing 0.19 mM – Sb, 0.24 mM – Co, 0.23 mM – Cu, 0.23 mM – Ni, 3.59 mM – Fe and 0.20 mM – Cr

6.3.4 Removal of Antimony from Simulated Decontamination Formulations: Column Study

To know the usability of the TA-Cts beads prepared for large scale applications, antimony removal properties of the TA-Cts beads prepared were studied under simulated PHWR DCD conditions in column mode. Thoroughly deaerated NAC formulation containing iron and/or Sb(III) was passed through the column at constant flow rates. TA-Cts beads were able to remove antimony from the decontamination formulations both in presence and absence of iron. Antimony removal was found to decrease with time (Fig. 6.1). The decrease was prominent in the absence of iron. Presence of iron was found to enhance the pickup of antimony. More than 40% reduction in antimony concentration was observed (at the outlet) at a flow rate of 2mL.min.$^{-1}$ even after 8 h of continuous operation. While with Sb-NAC alone solutions, the reduction dropped to 6% over the same time span. Decrease in flow rate was found to increase the Sb pickup, both in presence and absence of iron ions, which implies the relatively slow kinetics of antimony pickup by the TA-Cts beads.

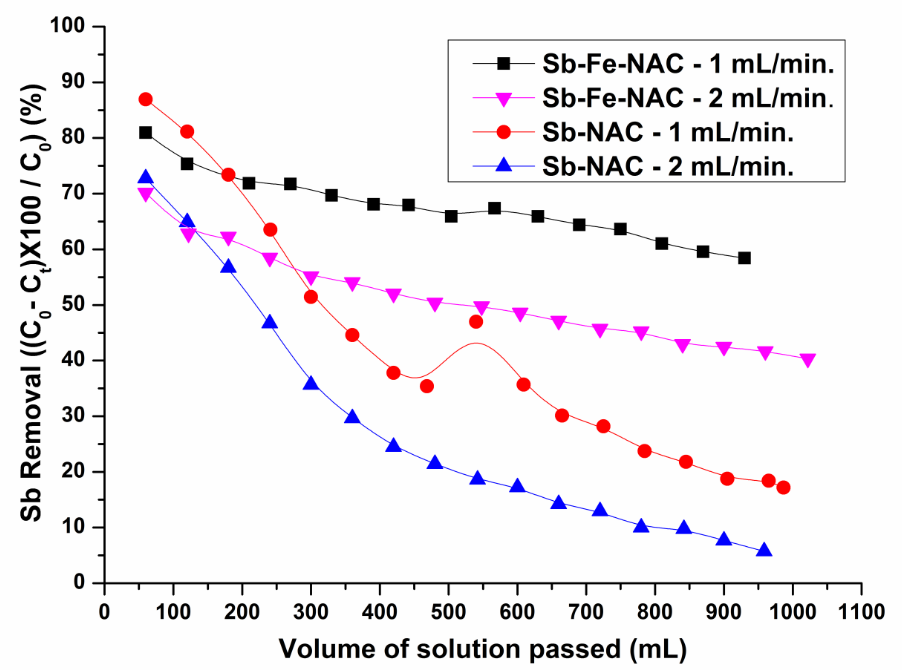

Figure 6.1. Column performance of the TA-Cts beads under simulated DCD conditions: Antimony removal over the TA-Cts beads column

Iron removal was observed only during the initial periods (Figure 6.2(i)), while the antimony sorption continued. Though a stoichiometric correlation between NTA and Fe(II) pickup over the TA-Cts beads was not established, there is a corresponding decrease in NTA removal along with decrease in Fe(II) removal (Figure 6.29(ii)). The removal of NTA (and other organics) is further exemplified in reduced effluent TOC values (Figure 6.2(iv)).

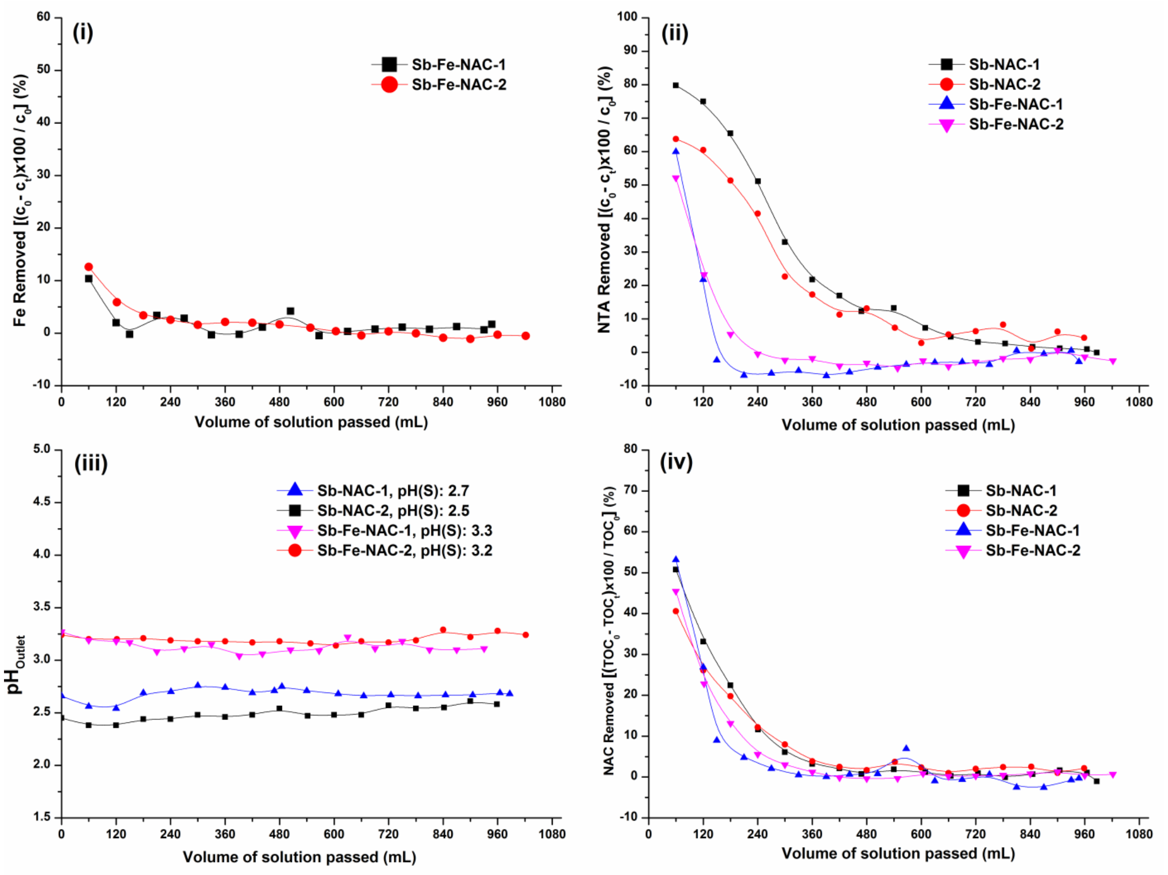

Figure 6.2. Column performance of the TA-Cts beads under simulated DCD conditions: (i) Removal of Fe(II); (ii) Removal of NTA; (iii) pH of the effluent; and (iv) Removal of NAC formulation over the TA-Cts beads column.

Effluent concentrations of both Fe(II) and NTA reached saturation simultaneously. This implies that iron is predominantly present, and removed, as its NTA complex. Further, in the absence of Fe(II), there was significant reduction in removal of antimony. This may be attributed to the unavailability of free Sb(III) ions due to its complexation with NTA. Thus, presence of Fe(II) keeps the NTA in solution as Fe(II)-NTA, which enhances the availability, and hence the pickup, of free Sb(III) ions. TOC values obtained during batch studies also point to a similar trend involving predominant removal of the complexants over the TA-Cts beads in the absence of Fe(II) ions. The outlet pH was found to be close to the inlet pH indicating negligible influence of sorption on the solution pH (Figure 6.2(iii)).

6.3.5 Estimation of Rate Constants for the Sb(V) Sorption by the TA-Cts Column

Based on the results obtained from the column study, rate constants for the sorption process were calculated using Thomas model (Eq.2.9) and Yoon-Nelson model (Eq.2.10), the two widely used adsorption models. Antimony removal over the TA-Cts beads column was found to follow both Thomas and Yoon-Nelson models. Fig. 6.3 shows the plots derived using the lineraised forms of these models. The rate constants (obtained from the slope) and the respective model parameters derived from the linear fit are tabulated in Table 6.6.

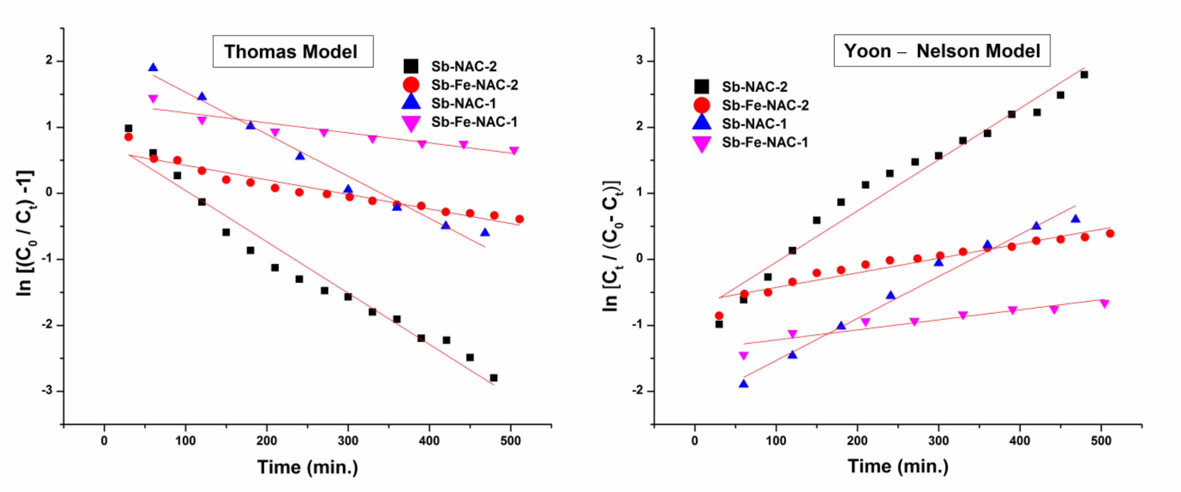

Figure 6.3. Plots generated using Thomas model and Yoon-Nelson model for antimony sorption by TA-Cts beads during the column experiments

Linear correlation was better for sorption of antimony from Sb-NAC solutions than for Sb-Fe-NAC solutions. Maximum (Thomas) adsorption capacity, q_T was found to increase with increase in flow rate with Sb-NAC solutions. Yoon-Nelson rate constants were found to increase with increase in flow rate, while the time required for 50 % sorbate breakthrough (τ) decreased. Sorption of iron was found to be not fitting with both the models.

Table 6.6.Antimony removal over the TA-Cts beads column: Thomas model and Yoon-Nelson model parameters

Name	**Flow rate** (mL.min^{-1})	**C_0** (mg.L^{-1})	**W** (g)	**Thomas model**			**Yoon-Nelson model**		
				R^2	**K_T** (x 10^{-3}) (mL.mg^{-1}.min^{-1})	**q_T** (mg.g^{-1})	**R^2**	**K_{YN}** (x 10^{-3}) (min^{-1})	**τ** (min.)
Sb-NAC-1	1	1.31	0.30	0.978	4.85	1480.8	0.978	6.4	341
Sb-NAC-2	2	2.45	0.25	0.961	3.17	2054.1	0.961	7.8	105
Sb-Fe-NAC-1	1	1.35	0.26	0.858	1.13	4749.2	0.858	1.5	903
Sb-Fe-NAC-2	2	1.76	0.25	0.922	1.25	4085.1	0.922	2.2	292

6.4 Conclusion

The results obtained in this study demonstrates that the nano titania impregnated-epichlorohydrin crosslinked chitosan beads can remove antimony, in presence of large excess of iron, from typical decontamination formulations. The results further show that the TA-Cts beads have immense potential for use in regular decontamination campaigns, wherein selective removal of Sb(III) in presence of large excess of Fe(II) ions is needed. High antimony uptake, favourable selectivity, and radiation stability that are comparable to that of commercial nuclear grade resins make the TA-Cts beads a potential antimony sorbent for using in nuclear industry. These beads can be incorporated as a separate column for removing antimony, in series, along with regular ion exchange columns [5] that are currently used in the decontamination campaigns.

Chapter 7. REMOVAL OF ARSENIC OVER NANO TITANIA IMPREGNATED CHITOSAN (TA-Cts) AND CHITOSAN (Cts) BEADS

7.1 Introduction

Arsenic poisoning due to arsenic contamination of ground water is a worldwide health problem. High arsenic groundwater areas have been identified in many parts of the world including Argentina, Chile, Mexico, China, Hungary, West Bengal (India), Bangladesh and Vietnam [185]. Studies conducted by School of Environmental Studies (SOES), Jadavpur University, Kolkata cautions on the alarming situation of arsenic contamination over a good portion of Ganga-Meghna-Brahmaputra plain that covers an area 569,749 km^2 and risking a population over 500 million [186]. 12 districts were identified as affected by arsenic in West Bengal alone by September 2006.

Arsenic can exist in oxidation states of –3, 0, +3 and +5, and may be present in earth crust as sulphides, metal arsenides or arsenates. In water, it is mostly present in arsenate (+5) form, while under anaerobic conditions, it may be present in arsenite (+3) forms. The Provisional guideline value set by WHO for arsenic in drinking water is 10 $\mu g.L^{-1}$. [187]. Most of the arsenic treatment processes can be classified into four categories, which includes ion exchange, membrane process, adsorption, and chemical precipitation [20, 188, 189]. Of these; adsorption and chemical precipitation processes were identified as cheap and cost effective processes for efficient removal of arsenic [20, 190].

Chitosan [191, 192] and TiO_2 [147, 169, 193, 194] had been reported, in neat, immobilised [195] or composites formats [196], as sorbent material for arsenic. Combining nano TiO_2 and chitosan offers a new type of material with the combined properties of both [49, 157, 178, 197, 198]. Removal of Arsenic by non-crosslinked chitosan-titania beads has been reported in the literature [156, 157]. But their instability in acidic solutions makes it necessary to introduce crosslinks in the chitosan chain backbone in order to make it suitable to use in acidic solutions as well. Arsenic removal properties of the nano TiO_2 impregnated-epichlorohydrin crosslinked chitosan beads and the crosslinked chitosan beads (discussed already) are reported in this chapter.

7.2 Experimental Details

7.2.1 Sorption Studies

To know the effect of sorbent to solution ratio and solution concentration of arsenic on the arsenic removal, known amount of the TA-Cts beads were equilibrated with different volumes of the test solutions having varying concentrations for 48 h. To know the effect of solution pH (initial) on the arsenic removal, 20 mg of the TA-Cts beads were equilibrated with 10 mL of the respective arsenic solutions. To know the effect of sorbent composition on the arsenic removal, 10 mg of the sorbents having varying chitosan to nano TiO_2 ratio had been equilibrated with 10 mL of 1.17 ppm As(V) solutions having pH 6.7 for 3 days. To know the effect of crosslinker concentration used in the preparation of the beads on their As removal properties, 10 mg of the respective sorbents were treated with 10 mL of the As(V) solution ($pH_{in.}$ 6.5) having a concentration of 1.23 ppm As(V) (for TA-Cts-Epi) or 1.20 ppm As(V) (for Cts-Epi beads) for 4 days.

7.3 Results and Discussions

7.3.1 Effect of Sorbent to Solution Ratio and Solution Concentration Used on As(V) Removal

Studies using different solution concentration of As(V) showed that the TA-Cts beads were able to remove As(V) effectively from solutions having concentrations as low as 145 ppb and its capacity is high enough to to remove As(V) quantitatively from solutions having concentration as high as 14 ppm (Table 7.1).

Table 7.1.Effect of sorbent to solution ratio and solution concentration used on As(V) removal over TA-Cts beads

Conditions Used	**As(V) removal**	
	(μmol.g^{-1})	(%)
10 mg TA-Cts beads to 10 mL of 145 ppb As(V)	1.8	94.2
10 mg TA-Cts beads to 1 mL of 14.04 ppm As(V)	17.9	97.3
10 mg TA-Cts beads to 2 mL of 14.04 ppm As(V)	36.2	96.6

7.3.2 Effect of Solution pH (Initial) on Arsenic Removal

TA-Cts beads showed good pickup of As(V) from its solutions having different initial solution pH (Table 7.2). Equilibrium pH was found to shift towards the acidic region for both neutral and basic solution used. More than 99 % removal of As(V) was observed in all the conditions studied.

Table 7.2. Effect of solution pH (initial) on the As(V) removal by TA-Cts beads

Conditions Used	**pH**		**As(V) Removal**	
	Initial	Eq.	(μmol.g^{-1})	(%)
20 mg TA-Cts beads to 10 mL of 1.92 ppm As(V) solution	3.2	3.9	12.5	99.6
20 mg TA-Cts beads to 10 mL of 1.52 ppm As(V) solution	6.4	4.2	10.1	99.6
20 mg TA-Cts beads to 10 mL of 1.86 ppm As(V) solution	10.7	5.5	12.3	99.2

7.3.3 Effect of Sorbent Composition on Arsenic Removal: Chitosan to Nano TiO_2 Ratio Variation

To study the effect of composition of the TA-Cts beads on As(V) removal, arsenic removal by TA-Cts beads having varying ratio of chitosan to nano TiO_2 was investigated. Crosslinked chitosan beads as well as the TA-Cts beads prepared using Aeroxide® TiO_2 p 25 were also studied. All the TA-Cts beads studied showed almost complete removal of As(V) even at an equilibrium pH of 6.1 (Table 7.3). Crosslinked chitosan beads and 1p25-5Cts beads also showed good uptake of As(V) even though it is less compared to the TA-

Cts beads which used locally sourced nano TiO_2. This gives a clear indication about the role of nano TiO_2 used on the uptake of As(V) by the TA-Cts beads.

Table 7.3.Effect of sorbent composition on arsenic removal: Chitosan to nano TiO_2 ratio variation

Sorbent	**$pH_{Eq.}$**	**As (V) Removal**	
		(μmol.g^{-1})	(%)
1TA-5Cts	3.6	15.4	100
2TA-4Cts	3.8	15.3	100
3TA-3Cts	3.8	15.0	100
4TA-2Cts	6.1	14.7	100
1p25-5Cts	3.6	13.9	95.9
Cts-CL	3.7	12.4	85.6

7.3.4 Effect of the Sorbent Composition on As(V) Removal: Variation of Crosslinker Concentration

7.3.4.1 Nano TiO_2- Epichlorhydrin Crosslinked Chitosan (TA-Cts-Epi) Beads

Epichlorohydrin crosslinked chitosan-nano titania beads, having varying amounts of crosslinking agents, were investigated for their ability to remove arsenic from its aqueous solutions containing 1.23 ppm As(V). Results are tabulated in Table. 7.4. TA-Cts-Epi beads showed good arsenic sorption properties even after crosslinking. All the samples showed similar and good arsenic uptake over the TA-Cts-Epi beads. Saturation capacities of the TA-Cts-Epi beads may not have been attained as solutions of very low concentrations of As(V) were used unlike in the case of studies with Sb(V) solutions (Section 5.3.4.3.1, Table 5.16). Hence, the effect of the crosslinker added on the capacity of the sorbent for As(V) uptake my not be visible with solutions of very low As(V) concentrations.

7.3.4.2 Epichlorhydrin Crosslinked Chitosan (Cts-Epi) Beads

Epichlorohydrin crosslinked chitosan (Cts-Epi) beads, having varying amounts of crosslinking agents, were studied for their ability to remove arsenic from its aqueous solutions containing 1.20 ppm As(V). Results are given in Table. 7.5. Chitosan beads showed good removal of As(V). Highest pickup of As(V) was observed with the least cross linker added (i.e., 1:1-Cts-Epi bead) sample. As(V) capacities were found to decrease with increase in crosslinker added. The lower capacity of non-crosslinked chitosan beads may be because of the comparatively higher equilibrium pH, which in turn reduces number of protonated amine functional groups present over the beads. Even though the equilibrium pH values are comparable and favourable for anion removal, As(V) uptake capacities of Cts-Epi beads, unlike TA-Cts-Epi beads, were found to decrease with increase in crosslinker added.

Table 7.4. Effect of sorbent composition on As(V) removal: TA-Cts-Epi beads (Variation of crosslinker concentration)

Sorbent	**As (V) Removal**		**pH$_{Eq.}$**
	(μmol.g^{-1})	(%)	
TA-Cts-NCL*	15.4	96.1	6.6
TA-Cts-Epi050	15.1	95.8	3.8
TA-Cts-Epi100	15.6	95.4	3.8
TA-Cts-Epi200	14.9	95.8	3.9
TA-Cts-Epi350	15.8	97.9	4.1
TA-Cts-Epi500	15.8	97.7	4.0

* 5 mg to 5 mL solution

Table 7.5. Effect of sorbent composition on As(V) removal: Cts-Epi beads (Variation of crosslinker concentration)

Sorbent	**pH$_{Eq.}$**	**As (V) Removal**	
		(μmol.g^{-1})	(%)
Cts-NCL	5.2	11.4	71.3
1:1-Cts:Epi	3.9	12.5	80.3
1:2-Cts:Epi	3.8	12.2	78.6
1:5-Cts:Epi	3.7	10.5	70.0
1:10-Cts:Epi	3.7	10.0	64.7

Titania containing TA-Cts-Epi beads were found to be more efficient in removing As(V) compared to the Cts-Epi beads. The higher As(V) uptake by the TA-Cts-Epi beads compared to Cts-Epi beads indicates the active participation of nano TiO_2 in arsenic removal.

7.4 Conclusion

Both crosslinked chitosan and nano titania impregnated-crosslinked chitosan were found to be effective sorbents for As(V). Nano titania impregnated-crosslinked chitosan beads were found to be better option for complete removal of As(V) as compared to the crosslinked chitosan beads. The complete removal of As(V), even at an equilibrium pH conditions of 6.1, by the 4TA-2Cts beads shows this to be an ideal solution for treating the ground water arsenic contamination.

Chapter 8. Conclusion and Future Directions

The study reported here reveals the new sorbents prepared for the removal of cobalt and antimony during dilute chemical decontaminations of nuclear power plants and the complexities involved in it. Selective removal of Co(II) by chitosan is possible through metal ion imprinting and by the careful selection of solution conditions. Nano titania-chitosan composite can be utilised for the selective removal of antimony during the dilute chemical decontamination of NPPs

The biosorbent chitosan, due to its ability to remove both metal ions and complexing agents, can act like a mixed bed resin. The metal ion uptake and the uptake mechanisms that operate under different conditions are dependent upon the solution nature and pH. For non complexing solutions, sorption of the metal ions occurs through metal chelation and the uptake increases with increase in solution pH. For complexing solutions, sorption of metal ions and/or ligands occur either through chelation or through electrostatic interactions between the protonated amine groups of chitosan and the negatively charged ligands/metal complexes, at optimum pH conditions. The sorption studies carried out on chitosan under different solution conditions reveals that, chitosan selectivity for a particular metal ion can be varied according to the solution nature and pH. The fast uptake of metal ions and the complexants by the chitosan makes it a potential replacement for the mixed bed organic resin, which is used towards the end of the decontamination campaign for removing the complexing agents and the remaining complexed/uncomplexed metal ions.

In this thesis, it has been demonstrated that the selectivity of the biosorbent chitosan can be reversed through metal ion imprinting. The retention of cobalt selectivity even from solutions having very low concentration of Co(II), and in presence of large excess of Fe(II), make the Co(II)-ion imprinted chitosan a promising sorbent for use in nuclear related applications such as DCD campaigns, where the active Co(II) ions are present in very low concentration levels and non-active Fe(II) ions are in large excess. Fast and easy regeneration of the imprinted chitosan makes it suitable for reuse without any significant loss in capacity or selectivity. The long contact time needed for obtaining the saturation capacity may limit the use of the Co-chitosan MIP under (online) column operations. However, it can be used for offline batch mode operations. In order to be able to use the imprinted chitosan in column mode, in online processes such as DCD of NPPs, the uptake kinetics needs to be improved, and complete Fe(II) exclusion by the MIPs has to be realized. Both can possibly be addressed through the Co(II) ion imprinting of functionalized chitosans such as N,N′-dicarboxymethylchitosan.

The comparative analysis of the six different antimony sorbents revealed the importance of antimony speciation and the solution pH on antimony uptake by the sorbents. Among the six sorbents studied, titania based materials were found to be more suitable for antimony removal when both Sb(V) and Sb(III) are present in the solution, while anion resins were found to be better as a column material at relatively wider pH range for removal of antimony present as Sb(V). It is possible to combine nano TiO_2 with chitosan without compromising on the former’s sorption properties and with the added advantages of obtaining the sorbent in a format suitable for large scale column applications. Nano titania-Chitosan (TA-Cts) composite sorbent was synthesized in bead format and studied for its antimony sorption properties under batch and column mode of operations. The beads were shown to be effective sorbent for antimony in both +3 and +5 forms. It is possible to have good control over the properties of the beads prepared through rational choice of composition of the constituents in the pre-polymerisation mixture during preparation of the beads, and by employing suitable solution conditions during sorption. The composition and the crosslinker amount added play an important role in deciding the physical and sorption properties of the composite beads. The decrease in antimony uptake with increase in nano TiO_2 content (or decrease in chitosan content) of the TA-Cts beads having varying TiO_2 and chitosan compositions demonstrate the importance of crosslinked chitosan in the Sb(V) pickup. TA-Cts-Epi / Cts-Epi beads with varying crosslinker, epichlorohydrin, concentrations were prepared, and the amount of the crosslinking agent added was found to affect both the antimony uptake capacity and kinetics of the TA-Cts-Epi /Cts-Epi beads prepared.

TA-Cts beads have immense potential for use in regular decontamination campaigns, wherein online selective removal of antimony ions in presence of large excess of Fe(II) ions is needed. High antimony uptake, favourable selectivity, and radiation stability that are comparable to that of commercial nuclear grade resins make the TA-Cts beads a potential antimony sorbent for the nuclear industry.

Nano TiO_2 – chitosan beads have good potential in general drinking water treatment processes as well due to its favourable arsenic sorption properties. Both crosslinked chitosan and nano titania impregnated-epichlorohydrin crosslinked chitosan beads were found to be effective in removal of As(V). Nano titania impregnated-epichlorohydrin crosslinked chitosan beads were found to be the better option for complete removal of As(V) in comparison to crosslinked chitosan beads. 4TA-2Cts beads, which remove arsenic even at an equilibrium pH of 6, have high potential to use as an arsenic removal agent for treating arsenic contaminated groundwater. The possibilities, and difficulties if any, of employing this material for onsite application for treating ground water for arsenic removal is to be explored in coordination with local authorities in the regions affected by arsenic contamination. Further, the TA-Cts beads, due to the known photocatalytic activity of TiO_2, have high potential for use as a material that could remove, and decompose metal chelating agents and other organic pollutants. This aspect is to be explored in detail in the future studies.

REFERENCES

[1] S.S. Bajaj, A.R. Gore, The Indian PHWR, *Nuclear Engineering and Design*, 236 (**2006**) 701-722.

[2] M. Kiran Kumar, K. Gaonkar, S. Ghosh, V. Kain, M. Bojinov, T. Saario, Optimisation of the hot conditioning of carbon steel surfaces of primary heat transport system of Pressurized Heavy Water Reactors using electrochemical impedance spectroscopy, *Journal of Nuclear Materials*, 401 (**2010**) 46-54.

[3] Decontamination Handbook (*TR-112352*), EPRI, Palo Alto, CA: **July 1999**.

[4] Velmurugan, A.L. Rufus, V.S. Sathyaseelan, V.K. Mittal, S. Veena, S.V. Narasimhan, Experience with Dilute Chemical Decontamination in Indian Pressurized Heavy Water Reactors, *Energy Procedia*, 7 (**2011**) 645-649.

[5] A. Bhaskarapillai, N.V. Sevilimedu, B.r. Sellergren, Synthesis and Characterization of Imprinted Polymers for Radioactive Waste Reduction, *Industrial & Engineering Chemistry Research*, 48 (**2009**) 3730-3737.

[6] IUPAC. Compendium of Chemical Terminology, 2nd ed. (the "Gold Book"). Compiled by A. D. McNaught and A. Wilkinson. Blackwell Scientific Publications, Oxford (**1997**). http://goldbook.iupac.org *Last update*: 24th February 2014, doi:10.1351/goldbook.S05769, *Last accessed on* 24th August 2016.

[7] G. Crini, P.-M. Badot, Sorption processes and pollution: conventional and non-conventional sorbents for pollutant removal from wastewaters, Presses universitaires de Franche-Comté, Besançon, **2010**.

[8] M. Fomina, G.M. Gadd, Biosorption: current perspectives on concept, definition and application, *Bioresource Technology*, 160 (**2014**) 3-14.

[9] K. Chojnacka, Biosorption and bioaccumulation – the prospects for practical applications, *Environment International*, 36 (**2010**) 299-307.

[10] F. Veglio, F. Beolchini, Removal of metals by biosorption: a review, *Hydrometallurgy*, 44 (**1997**) 301-316.

[11] B. Volesky, Biosorption and me, *Water Research*, 41 (**2007**) 4017-4029.

[12] J. Wang, C. Chen, Biosorbents for heavy metals removal and their future, *Biotechnology Advances*, 27 (**2009**) 195-226.

[13] U. Farooq, J.A. Kozinski, M.A. Khan, M. Athar, Biosorption of heavy metal ions using wheat based biosorbents – A review of the recent literature, *Bioresource Technology*, 101 (**2010**) 5043-5053.

[14] T.A.H. Nguyen, H.H. Ngo, W.S. Guo, J. Zhang, S. Liang, Q.Y. Yue, Q. Li, T.V. Nguyen, Applicability of agricultural waste and by-products for adsorptive removal of heavy metals from wastewater, *Bioresource Technology*, 148 (**2013**) 574-585.

[15] M. Rinaudo, Chitin and chitosan: Properties and applications, *Progress in Polymer Science*, 31 (**2006**) 603-632.

[16] C. Gerente, V.K.C. Lee, P.L. Cloirec, G. McKay, Application of Chitosan for the Removal of Metals From Wastewaters by Adsorption—Mechanisms and Models Review, *Critical Reviews in Environmental Science and Technology*, 37 (**2007**) 41-127.

[17] M. Vakili, M. Rafatullah, B. Salamatinia, A.Z. Abdullah, M.H. Ibrahim, K.B. Tan, Z. Gholami, P. Amouzgar, Application of chitosan and its derivatives as adsorbents for dye removal from water and wastewater: A review, *Carbohydrate Polymers*, 113 (**2014**) 115-130.

[18] A. Nour, H. Lahading, R. Yunus, Chitosan Based Adsorbent for Removal of Oil from Industrial Wastewater: Chitosan; Production of Chitosan; Palm Oil Mill Effluent (POME); Effect of Adsorbent Dosage; Effect of Agitation Rate, Lambert Academic Publishing, **2011**.

[19] I. Younes, M. Rinaudo, Chitin and Chitosan Preparation from Marine Sources. Structure, Properties and Applications, *Marine Drugs*, 13 (**2015**).

[20] D. Mohan, C.U. Pittman Jr, Arsenic removal from water/wastewater using adsorbents—A critical review, *Journal of Hazardous Materials*, 142 (**2007**) 1-53.

[21] Zbigniew Hubicki, Monika Wawrzkiewicz, Grzegorz Wójcik, Dorota Kołodyńska and Anna Wołowicz (**2015**). Ion Exchange Method for Removal and Separation of Noble Metal Ions, Ion Exchange - Studies and Applications, Prof. Ayben Kilislioglu (Ed.), InTech, DOI: 10.5772/60597. *Available from:* http://www.intechopen.com/books/ion-exchange-studies-and-applications/ion-exchange-method-for-removal-and-separation-of-noble-metal-ions; *Last accessed on* 8th August 2016.

[22] Zbigniew Hubicki and Dorota Kołodyńska (**2012**). Selective Removal of Heavy Metal Ions from Waters and Waste Waters Using Ion Exchange Methods, Ion Exchange Technologies, Prof. Ayben Kilislioglu (Ed.), InTech, DOI: 10.5772/51040. *Available from:* http://www.intechopen.com/books/ion-exchange-technologies/selective-removal-of-heavy-metal-ions-from-waters-and-waste-waters-using-ion-exchange-methods *Last accessed on* 8th August 2016.

[23] J. Ramkumar, T. Mukherjee, Principles of Ion Exchange Equilibria, in: Inamuddin, M. Luqman (Eds.) Ion Exchange Technology I: Theory and Materials, Springer Netherlands, Dordrecht, **2012**, pp. 41-49.

[24] S.D. Alexandratos, Ion-Exchange Resins: A Retrospective from Industrial and Engineering Chemistry Research, *Industrial & Engineering Chemistry Research*, 48 (**2009**) 388-398.

[25] A.N. Pustam, S.D. Alexandratos, Engineering selectivity into polymer-supported reagents for transition metal ion complex formation, *Reactive and Functional Polymers*, 70 (**2010**) 545-554.

[26] J. Matsui, H. Kubo, T. Takeuchi, Design and Preparation of Molecularly Imprinted Atrazine-Receptor Polymers: Investigation of Functional Monomers and Solvents, *Analytical Sciences*, 14 (**1998**) 699-702.

[27] G.Z. Kyzas, D.N. Bikiaris, N.K. Lazaridis, Selective separation of basic and reactive dyes by molecularly imprinted polymers (MIPs), *Chemical Engineering Journal*, 149 (**2009**) 263-272.

[28] F. Shen, X. Ren, Covalent molecular imprinting made easy: a case study of mannose imprinted polymer, *RSC Advances*, 4 (**2014**) 13123-13125.

[29] J.W. Michael, K. Nicole, The Semi-Covalent Approach, in: Molecularly Imprinted Materials, CRC Press, **2004**, pp. 93-122.

[30] Q. Osmani, H. Hughes, P. McLoughlin, Probing the recognition of molecularly imprinted polymer beads, *Journal of Materials Science*, 47 (**2011**) 2218-2227.

[31] H. Chen, S. Son, F. Zhang, J. Yan, Y. Li, H. Ding, L. Ding, Rapid preparation of molecularly imprinted polymers by microwave-assisted emulsion polymerization for the extraction of florfenicol in milk, *Journal of Chromatography B*, 983–984 (**2015**) 32-38.

[32] T. Kazuhiko, Y. Kai Yu, O. Yoshihisa, M. Tohru, M. Mizuo, T. Makoto, Surface Imprinting: Preparation of Metal Ion-Imprinted Resins by Use of Complexation at the Aqueous-Organic Interface, in: Molecular and Ionic Recognition with Imprinted Polymers, American Chemical Society, **1998**, pp. 251-263.

[33] X. Ding, P.A. Heiden, Recent Developments in Molecularly Imprinted Nanoparticles by Surface Imprinting Techniques, *Macromolecular Materials and Engineering*, 299 (**2014**) 268-282.

[34] M. Meng, Y. Feng, M. Zhang, Y. Ji, J. Dai, Y. Liu, P. Yu, Y. Yan, Optimization of surface imprinted layer attached poly(vinylidene fluoride) membrane for selective

separation of salicylic acid from acetylsalicylic acid using central composite design, *Chemical Engineering Journal*, 231 (**2013**) 132-145.

[35] P. Metilda, K. Prasad, R. Kala, J.M. Gladis, T.P. Rao, G.R.K. Naidu, Ion imprinted polymer based sensor for monitoring toxic uranium in environmental samples, *Analytica Chimica Acta*, 582 (**2007**) 147-153.

[36] C.R. Preetha, J.M. Gladis, T.P. Rao, G. Venkateswaran, Removal of Toxic Uranium from Synthetic Nuclear Power Reactor Effluents Using Uranyl Ion Imprinted Polymer Particles, *Environmental Science & Technology*, 40 (**2006**) 3070-3074.

[37] V.E. Pakade, E.M. Cukrowska, J. Darkwa, G. Darko, N. Torto, L. Chimuka, Simple and efficient ion imprinted polymer for recovery of uranium from environmental samples, *Water Science and Technology*, 65 (**2012**) 728-736.

[38] D.K. Singh, S. Mishra, Synthesis and characterization of UO_2^{2+}-ion imprinted polymer for selective extraction of UO_2^{2+}, *Analytica Chimica Acta*, 644 (**2009**) 42-47.

[39] P. Metilda, J.M. Gladis, G. Venkateswaran, T. Prasada Rao, Investigation of the role of chelating ligand in the synthesis of ion-imprinted polymeric resins on the selective enrichment of uranium(VI), *Analytica Chimica Acta*, 587 (**2007**) 263-271.

[40] D. James, J.M. Gladis, A.K. Pandey, G.R.K. Naidu, T. Prasada Rao, Design of two-dimensional biomimetic uranyl optrode and its application to the analysis of natural waters, *Talanta*, 74 (**2008**) 1420-1427.

[41] P.E. Hande, A.B. Samui, P.S. Kulkarni, Highly selective monitoring of metals by using ion-imprinted polymers, *Environmental Science and Pollution Research*, 22 (**2015**) 7375-7404.

[42] M. Shamsipur, H.R. Rajabi, Flame photometric determination of cesium ion after its preconcentration with nanoparticles imprinted with the cesium-dibenzo-24-crown-8 complex, *Microchimica Acta*, 180 (**2013**) 243-252.

[43] F.F. He, H.Q. Wang, Y.Y. Wang, X. F Wang, H.S. Zhang, H.L. Li, J.H. Tang, Magnetic Th(IV)-ion imprinted polymers with salophen schiff base for separation and recognition of Th(IV), *Journal of Radioanalytical and Nuclear Chemistry*, 295 (**2013**) 167-177.

[44] E. Zambrzycka, B. Godlewska-Żyłkiewicz, A new ion imprinted polymer based on Ru(III)-thiobarbituric acid complex for solid phase extraction of ruthenium(III) prior to its determination by ETAAS, *Microchimica Acta*, 181 (**2014**) 1019-1027.

[45] Y. Liu, X. Meng, M. Luo, M. Meng, L. Ni, J. Qiu, Z. Hu, F. Liu, G. Zhong, Z. Liu, Y. Yan, Synthesis of hydrophilic surface ion-imprinted polymer based on graphene oxide

for removal of strontium from aqueous solution, *Journal of Materials Chemistry A*, 3 (**2015**) 1287-1297.

[46] F. Shakerian, S. Dadfarnia, A.M. Haji Shabani, M. Nili Ahmad abadi, Synthesis and characterisation of nano-pore antimony imprinted polymer and its use in the extraction and determination of antimony in water and fruit juice samples, *Food Chemistry*, 145 (**2014**) 571-577.

[47] L. Xu, Y.-A. Huang, Q.-J. Zhu, C. Ye, Chitosan in Molecularly-Imprinted Polymers: Current and Future Prospects, *International Journal of Molecular Sciences*, 16 (**2015**).

[48] K. Li, Q. Gao, G. Yadavalli, X. Shen, H. Lei, B. Han, K. Xia, C. Zhou, Selective Adsorption of Gd^{3+} on a Magnetically Retrievable Imprinted Chitosan/Carbon Nanotube Composite with High Capacity, *ACS Applied Materials & Interfaces*, 7 (**2015**) 21047-21055.

[49] Q. Li, H. Su, T. Tan, Synthesis of ion-imprinted chitosan-TiO_2 adsorbent and its multi-functional performances, *Biochemical Engineering Journal*, 38 (**2008**) 212-218.

[50] C.-Y. Chen, C.-Y. Yang, A.-H. Chen, Biosorption of Cu(II), Zn(II), Ni(II) and Pb(II) ions by cross-linked metal-imprinted chitosans with epichlorohydrin, *Journal of Environmental Management*, 92 (**2011**) 796-802.

[51] A.-H. Chen, C.-Y. Yang, C.-Y. Chen, C.-Y. Chen, C.-W. Chen, The chemically crosslinked metal-complexed chitosans for comparative adsorptions of Cu(II), Zn(II), Ni(II) and Pb(II) ions in aqueous medium, *Journal of Hazardous Materials*, 163 (**2009**) 1068-1075.

[52] Y. Lu, J. He, L. Wu, G. Luo, Relationship between breakthrough curve and adsorption isotherm of Ca(II) imprinted chitosan microspheres for metal adsorption, *Chinese Journal of Chemical Engineering*, 24 (**2016**) 323-329.

[53] J. He, Y. Lu, G. Luo, Ca(II) imprinted chitosan microspheres: An effective and green adsorbent for the removal of Cu(II), Cd(II) and Pb(II) from aqueous solutions, *Chemical Engineering Journal*, 244 (**2014**) 202-208.

[54] F. Liu, Y. Liu, Y. Xu, L. Ni, X. Meng, Z. Hu, G. Zhong, M. Meng, Y. Wang, J. Han, Efficient static and dynamic removal of Sr(II) from aqueous solution using chitosan ion-imprinted polymer functionalized with dithiocarbamate, *Journal of Environmental Chemical Engineering*, 3 (**2015**) 1061-1071.

[55] M. Monier, D.A. Abdel-Latif, Y.G. Abou El-Reash, Ion-imprinted modified chitosan resin for selective removal of Pd(II) ions, *Journal of Colloid and Interface Science*, 469 (**2016**) 344-354.

[56] B. Liu, W. Chen, X. Peng, Q. Cao, Q. Wang, D. Wang, X. Meng, G. Yu, Biosorption of lead from aqueous solutions by ion-imprinted tetraethylenepentamine modified chitosan beads, *International Journal of Biological Macromolecules*, 86 (**2016**) 562-569.

[57] M.E.H. Ahamed, X.Y. Mbianda, A.F. Mulaba-Bafubiandi, L. Marjanovic, Selective extraction of gold(III) from metal chloride mixtures using ethylenediamine N-(2-(1-imidazolyl)ethyl) chitosan ion-imprinted polymer, *Hydrometallurgy*, 140 (**2013**) 1-13.

[58] L. Zhang, J. Xue, X. Zhou, X. Fei, Y. Wang, Y. Zhou, L. Zhong, X. Han, Adsorption of molybdate on molybdate-imprinted chitosan/triethanolamine gel beads, *Carbohydrate Polymers*, 114 (**2014**) 514-520.

[59] R.P. Dhakal, T. Oshima, Y. Baba, Planarity-recognition enhancement of N-(2-pyridylmethyl)chitosan by imprinting planar metal ions, *Reactive and Functional Polymers*, 68 (**2008**) 1549-1556.

[60] L. Zhou, C. Shang, Z. Liu, G. Huang, A.A. Adesina, Selective adsorption of uranium(VI) from aqueous solutions using the ion-imprinted magnetic chitosan resins, *Journal of Colloid and Interface Science*, 366 (**2012**) 165-172.

[61] B. Liu, D. Wang, H. Li, Y. Xu, L. Zhang, As(III) removal from aqueous solution using α-Fe_2O_3 impregnated chitosan beads with As(III) as imprinted ions, *Desalination*, 272 (**2011**) 286-292.

[62] C.X. Li, J.M. Pan, J. Gao, Y.S. Yan, G.Q. Zhao, An ion-imprinted polymer supported by attapulgite with a chitosan incorporated sol–gel process for selective separation of Ce(III), *Chinese Chemical Letters*, 20 (**2009**) 985-989.

[63] Q. Li, H. Su, J. Li, T. Tan, Studies of adsorption for heavy metal ions and degradation of methyl orange based on the surface of ion-imprinted adsorbent, *Process Biochemistry*, 42 (**2007**) 379-383.

[64] Y. Ren, X. Wei, M. Zhang, Adsorption character for removal Cu(II) by magnetic Cu(II) ion imprinted composite adsorbent, *Journal of Hazardous Materials*, 158 (**2008**) 14-22.

[65] C. Li, J. Gao, J. Pan, Z. Zhang, Y. Yan, Synthesis, characterization, and adsorption performance of Pb(II)-imprinted polymer in nano-TiO_2 matrix, *Journal of Environmental Sciences*, 21 (**2009**) 1722-1729.

[66] Y. Liu, X. Cao, Z. Le, M. Luo, W. Xu, G. Huang, Pre-concentration and determination of trace uranium (VI) in environments using ion-imprinted chitosan resin via solid phase extraction, *Journal of the Brazilian Chemical Society*, 21 (**2010**) 533-540.

[67] Y. Liu, X. Cao, R. Hua, Y. Wang, Y. Liu, C. Pang, Y. Wang, Selective adsorption of uranyl ion on ion-imprinted chitosan/PVA cross-linked hydrogel, *Hydrometallurgy,* 104 (**2010**) 150-155.

[68] A. Chen, G. Zeng, G. Chen, X. Hu, M. Yan, S. Guan, C. Shang, L. Lu, Z. Zou, G. Xie, Novel thiourea-modified magnetic ion-imprinted chitosan/TiO_2 composite for simultaneous removal of cadmium and 2,4-dichlorophenol, *Chemical Engineering Journal*, 191 (**2012**) 85-94.

[69] X. Song, C. Li, R. Xu, K. Wang, Molecular-Ion-Imprinted Chitosan Hydrogels for the Selective Adsorption of Silver(I) in Aqueous Solution, *Industrial & Engineering Chemistry Research,* 51 (**2012**) 11261-11265.

[70] Y. Cai, L. Zheng, Z. Fang, Selective adsorption of Cu(II) from an aqueous solution by ion imprinted magnetic chitosan microspheres prepared from steel pickling waste liquor, *RSC Advances*, 5 (**2015**) 97435-97445.

[71] P.E. Hande, S. Kamble, A.B. Samui, P.S. Kulkarni, Chitosan-Based Lead Ion-Imprinted Interpenetrating Polymer Network by Simultaneous Polymerization for Selective Extraction of Lead(II), *Industrial & Engineering Chemistry Research*, 55 (**2016**) 3668-3678.

[72] J.F. Barry, The cross section of the ^{58}Ni(n, p)^{58}Co reaction for neutrons in the energy range 1.6 to 14.7 MeV, *Journal of Nuclear Energy. Parts A/B. Reactor Science and Technology*, 16 (**1962**) 467-472.

[73] P.-L. Frattini, D.-M. Wells, S.-E. Garcia, K. Richard, R. Asay, L. Yengoyan, Sequestration Resins for Accelerating Removal of Radioactive Contaminants, in: *NPC 2012: Nuclear Plant Chemistry Conference*, International Conference on Water Chemistry of Nuclear Reactor Systems, France, **2012**.

[74] M. Filella, N. Belzile, Y.-W. Chen, Antimony in the environment: a review focused on natural waters: I. Occurrence, *Earth-Science Reviews*, 57 (**2002**) 125-176.

[75] B.S. Tomar, S. Kumar, T.P. Chaturvedi, V.K. Manchanda, Gamma spectrometric measurements on PHT and Moderator systems of PHWRs, *IANCAS Bulletin*, Vol. VII. No.2 (**2008**) 138-143.

[76] K.-H. Neeb, The Radiochemistry of Nuclear Power Plants With Light Water Reactors, Walter De Gruyter, **1997**.

[77] S. Osváth, Z. Molnár, J. Groska, N. Vajda, Determination of ^{125}Sb in nuclear power plant wastes, *Journal of Radioanalytical and Nuclear Chemistry*, 307 (**2016**) 761-764.

[78] V.K. Mittal, S. Bera, S. Velmurugan, V.S. Narasimhan, Studies on Sorption of Antimony on Carbon Steel Surface in Chemical Decontamination Medium, *Journal of Nuclear Science and Technology*, 48 (**2011**) 256-262.

[79] R. Watkins, D. Weiss, W. Dubbin, K. Peel, B. Coles, T. Arnold, Investigations into the kinetics and thermodynamics of Sb(III) adsorption on goethite (α-FeOOH), *Journal of Colloid and Interface Science*, 303 (**2006**) 639-646.

[80] D.G. Miller, D.A. Guzonas, R. Laporte, T.A. Dereski, R.A. Speranzini, Controlling radiation fields in CANDU reactors using chemical decontamination technologies *(AECL-11852, COG-97-472-I)*, AECL, Chalk River, Ontario, Canada, **1997**.

[81] Y. Dundar, Odar, S., Steit, K., Allsop, H., Guzonas, D., Application of KWU Antimony Removal Process at Gentilly-2 *(AECL–11663)*, 7th International Conference on Water Chemistry of Nuclear Reactor Systems, British Nuclear Energy Society, Bournemouth, U.K, **1996**.

[82] S. Velmurugan, Mittal, Vinit K., Kumbhar, A.G., Narasimhan, S.V., Bhat, H.R., Krishna Rao, K.S., Upadhyay, S.K., & Jain, A.K., Experience with antimony activity removal process in Indian PHWRs, *OPENWAC-2008: symposium on operational and environmental issues concerning use of water as a coolant in power plants and industries*, Department of Atomic Energy, Mumbai, India, Kalpakkam, India, **2008**, pp. 86-90.

[83] IUPAC. Compendium of Chemical Terminology, 2nd ed. (the "Gold Book"). Compiled by A. D. McNaught and A. Wilkinson. Blackwell Scientific Publications, Oxford (**1997**). http://goldbook.iupac.org *Last update:* 24th February 2014, DOI: 10.1351/goldbook.P04440. *Last accessed on* 22nd August 2016.

[84] K.Y. Foo, B.H. Hameed, Insights into the modeling of adsorption isotherm systems, *Chemical Engineering Journal*, 156 (**2010**) 2-10.

[85] G. Limousin, J.P. Gaudet, L. Charlet, S. Szenknect, V. Barthès, M. Krimissa, Sorption isotherms: A review on physical bases, modeling and measurement, *Applied Geochemistry*, 22 (**2007**) 249-275.

[86] H.C. Thomas, Heterogeneous Ion Exchange in a Flowing System, *Journal of the American Chemical Society*, 66 (**1944**) 1664-1666.

[87] Y.H. Yoon, J.H. Nelson, Application of Gas Adsorption Kinetics I. A Theoretical Model for Respirator Cartridge Service Life, *American Industrial Hygiene Association Journal*, 45 (**1984**) 509-516.

[88] S. Ayoob, A.K. Gupta, Sorptive response profile of an adsorbent in the defluoridation of drinking water, *Chemical Engineering Journal*, 133 (**2007**) 273-281.

[89] F. Rozada, M. Otero, A.I. García, A. Morán, Application in fixed-bed systems of adsorbents obtained from sewage sludge and discarded tyres, *Dyes and Pigments*, 72 (**2007**) 47-56.

[90] Z. Aksu, F. Gönen, Biosorption of phenol by immobilized activated sludge in a continuous packed bed: prediction of breakthrough curves, *Process Biochemistry*, 39 (**2004**) 599-613.

[91] K.V. Kumar, Linear and non-linear regression analysis for the sorption kinetics of methylene blue onto activated carbon, *Journal of Hazardous Materials*, 137 (**2006**) 1538-1544.

[92] Y.S. Ho, G. McKay, A Comparison of Chemisorption Kinetic Models Applied to Pollutant Removal on Various Sorbents, *Process Safety and Environmental Protection*, 76 (**1998**) 332-340.

[93] T.R. Raj Singh, P.A. McCarron, A.D. Woolfson, R.F. Donnelly, Investigation of swelling and network parameters of poly(ethylene glycol)-crosslinked poly(methyl vinyl ether-co-maleic acid) hydrogels, *European Polymer Journal*, 45 (**2009**) 1239-1249.

[94] C.E. Harland, Ion Exchange: Theory and Practice, Royal Society of Chemistry, **1994**.

[95] S.N. Bhattacharyya, K.P. Kundu, Spectrophotometric determination of EDTA, *Talanta*, 18 (**1971**) 446-449.

[96] R.A.A. Muzzarelli, Potential of chitin/chitosan-bearing materials for uranium recovery: An interdisciplinary review, *Carbohydrate Polymers*, 84 (**2011**) 54-63.

[97] A.J. Varma, S.V. Deshpande, J.F. Kennedy, Metal complexation by chitosan and its derivatives: a review, *Carbohydrate Polymers*, 55 (**2004**) 77-93.

[98] R.A.A. Muzzarelli, O. Tubertini, Radiation resistance of chitin and chitosan applied in the chromatography of radioactive solutions, *Journal of Radioanalytical Chemistry*, 12 (**1972**) 431-440.

[99] A. Bhatnagar, M. Sillanpää, Applications of chitin- and chitosan-derivatives for the detoxification of water and wastewater — A short review, *Advances in Colloid and Interface Science*, 152 (**2009**) 26-38.

[100] R.-S. Juang, F.-C. Wu, R.-L. Tseng, Adsorption removal of copper(II) using chitosan from simulated rinse solutions containing chelating agents, *Water Research*, 33 (**1999**) 2403-2409.

[101] P.-J. Lu, W.-W. Hu, T.-S. Chen, J.-M. Chern, Adsorption of copper–citrate complexes on chitosan: Equilibrium modeling, *Bioresource Technology*, 101 (**2010**) 1127-1134.

[102] O. Gylienė, R. Binkienė, R. Butkienė, Sorption of Cu(II) complexes with ligands tartrate, glycine and quadrol by chitosan, *Journal of Hazardous Materials*, 171 (**2009**) 133-139.

[103] J. Guzman, I. Saucedo, J. Revilla, R. Navarro, E. Guibal, Copper sorption by chitosan in the presence of citrate ions: influence of metal speciation on sorption mechanism and uptake capacities, *International Journal of Biological Macromolecules*, 33 (**2003**) 57-65.

[104] O. Gylienė, O. Nivinskienė, I. Razmutė, Copper(II)–EDTA sorption onto chitosan and its regeneration applying electrolysis, *Journal of Hazardous Materials*, 137 (**2006**) 1430-1437.

[105] O. Gylienë, O. Nivinskienë, Electrochemical regeneration of chitosan after Ni (II)–citrate complex sorption, *Chemija*, 16 (**2005**) 7-14.

[106] C. Jeon, K. Ha Park, Adsorption and desorption characteristics of mercury(II) ions using aminated chitosan bead, *Water Research*, 39 (**2005**) 3938-3944.

[107] V.E. Tikhonov, L.A. Radigina, Y.A. Yamskov, Metal-chelating chitin derivatives via reaction of chitosan with nitrilotriacetic acid, *Carbohydrate Research*, 290 (**1996**) 33-41.

[108] A. Bernkop-Schnürch, Chitosan and its derivatives: potential excipients for peroral peptide delivery systems, *International Journal of Pharmaceutics*, 194 (**2000**) 1-13.

[109] Y. Liu, J. Gao, C. Li, J. Pan, Y. Yan, J. Xie, Synthesis and Adsorption Performance of Surface-Grafted Co(II)-Imprinted Polymer for Selective Removal of Cobalt, *Chinese Journal of Chemistry*, 28 (**2010**) 548-554.

[110] E. Metwally, S.S. Elkholy, H.A.M. Salem, M.Z. Elsabee, Sorption behavior of ^{60}Co and $^{152+154}$Eu radionuclides onto chitosan derivatives, *Carbohydrate Polymers*, 76 (**2009**) 622-631.

[111] J. Mizera, G. Mizerová, V. Machovič, L. Borecká, Sorption of cesium, cobalt and europium on low-rank coal and chitosan, *Water Research*, 41 (**2007**) 620-626.

[112] E. Guibal, Interactions of metal ions with chitosan-based sorbents: a review, *Separation and Purification Technology*, 38 (**2004**) 43-74.

[113] A. Domard, pH and c.d. measurements on a fully deacetylated chitosan: application to Cu^{II}—polymer interactions, International *Journal of Biological Macromolecules*, 9 (**1987**) 98-104.

[114] L. Dambies, C. Guimon, S. Yiacoumi, E. Guibal, Characterization of metal ion interactions with chitosan by X-ray photoelectron spectroscopy, *Colloids and Surfaces A: Physicochemical and Engineering Aspects*, 177 (**2001**) 203-214.

[115] R. Navarro, J. Guzmán, I. Saucedo, J. Revilla, E. Guibal, Recovery of Metal Ions by Chitosan: Sorption Mechanisms and Influence of Metal Speciation, *Macromolecular Bioscience*, 3 (**2003**) 552-561.

[116] J.R. Rangel-Mendez, R. Monroy-Zepeda, E. Leyva-Ramos, P.E. Diaz-Flores, K. Shirai, Chitosan selectivity for removing cadmium (II), copper (II), and lead (II) from aqueous phase: pH and organic matter effect, *Journal of Hazardous Materials*, 162 (**2009**) 503-511.

[117] I.M.N. Vold, K.M. Vårum, E. Guibal, O. Smidsrød, Binding of ions to chitosan–selectivity studies, *Carbohydrate Polymers*, 54 (**2003**) 471-477.

[118] A.-H. Chen, S.-C. Liu, C.-Y. Chen, C.-Y. Chen, Comparative adsorption of Cu(II), Zn(II), and Pb(II) ions in aqueous solution on the crosslinked chitosan with epichlorohydrin, *Journal of Hazardous Materials*, 154 (**2008**) 184-191.

[119] I.S. Lima, C. Airoldi, A thermodynamic investigation on chitosan–divalent cation interactions, *Thermochimica Acta*, 421 (**2004**) 133-139.

[120] M. Rhazi, J. Desbrières, A. Tolaimate, M. Rinaudo, P. Vottero, A. Alagui, M. El Meray, Influence of the nature of the metal ions on the complexation with chitosan.: Application to the treatment of liquid waste, *European Polymer Journal*, 38 (**2002**) 1523-1530.

[121] K. Swayampakula, V.M. Boddu, S.K. Nadavala, K. Abburi, Competitive adsorption of Cu(II), Co(II) and Ni(II) from their binary and tertiary aqueous solutions using chitosan-coated perlite beads as biosorbent, *Journal of Hazardous Materials*, 170 (**2009**) 680-689.

[122] C.K.S. Pillai, W. Paul, C.P. Sharma, Chitin and chitosan polymers: Chemistry, solubility and fiber formation, *Progress in Polymer Science*, 34 (**2009**) 641-678.

[123] W.S. Wan Ngah, C.S. Endud, R. Mayanar, Removal of copper(II) ions from aqueous solution onto chitosan and cross-linked chitosan beads, *Reactive and Functional Polymers*, 50 (**2002**) 181-190.

[124] A. Webster, M.D. Halling, D.M. Grant, Metal complexation of chitosan and its glutaraldehyde cross-linked derivative, *Carbohydrate Research*, 342 (**2007**) 1189-1201.

[125] B. Sellergren, Molecularly Imprinted Polymers: Man-Made Mimics of Antibodies and their Application in Analytical Chemistry, Elsevier Science, **2000**.

[126] H. Minamisawa, H. Iwanami, N. Arai, T. Okutani, Adsorption behavior of cobalt(II) on chitosan and its determination by tungsten metal furnace atomic absorption spectrometry, *Analytica Chimica Acta*, 378 (**1999**) 279-285.

[127] T. Tianwei, H. Xiaojing, D. Weixia, Adsorption behaviour of metal ions on imprinted chitosan resin, *Journal of Chemical Technology & Biotechnology*, 76 (**2001**) 191-195.

[128] P. Baroni, R.S. Vieira, E. Meneghetti, M.G.C. da Silva, M.M. Beppu, Evaluation of batch adsorption of chromium ions on natural and crosslinked chitosan membranes, *Journal of Hazardous Materials*, 152 (**2008**) 1155-1163.

[129] F.A. Cotton, G. Wilkinson, Advanced inorganic chemistry: a comprehensive text, Mei Ya Publications, Incorporated, **1971**.

[130] Y. Baba, T. Oshima, S. Kanemaru, A Quantitative Consideration for Template Effect of Palladium(II) Using N-[Pyridylmethyl] Chitosan, *Solvent Extraction and Ion Exchange*, 29 (**2011**) 509-517.

[131] A. Bhaskarapillai, S. Chandra, N.V. Sevilimedu, B. Sellergren, Theoretical investigations of the experimentally observed selectivity of a cobalt imprinted polymer, *Biosensors and Bioelectronics*, 25 (**2009**) 558-562.

[132] A.L. Rufus, S. Velmurugan, V.S. Sathyaseelan, S.V. Narasimhan, Comparative study of nitrilo triacetic acid (NTA) and EDTA as formulation constituents for the chemical decontamination of primary coolant systems of nuclear power plants, *Progress in Nuclear Energy*, 44 (**2004**) 13-31.

[133] D. Amarasiriwardena, F. Wu, Antimony: Emerging toxic contaminant in the environment, *Microchemical Journal*, 97 (**2011**) 1-3.

[134] S.D. Richardson, T.A. Ternes, Water Analysis: Emerging Contaminants and Current Issues, *Analytical Chemistry*, 86 (**2014**) 2813-2848.

[135] M. He, X. Wang, F. Wu, Z. Fu, Antimony pollution in China, *Science of The Total Environment*, 421–422 (**2012**) 41-50.

[136] P. Westerhoff, P. Prapaipong, E. Shock, A. Hillaireau, Antimony leaching from polyethylene terephthalate (PET) plastic used for bottled drinking water, *Water Research*, 42 (**2008**) 551-556.

[137] P.A. Riveros, J.E. Dutrizac, R. Lastra, A Study Of The Ion Exchange Removal Of Antimony(III) And Antimony(V) From Copper Electrolytes, *Canadian Metallurgical Quarterly*, 47 (**2008**) 307-316.

[138] Antimony in Drinking-water (Background document for development of WHO Guidelines for Drinking-water Quality): *WHO/SDE/WSH/03.04/74* (English only);

http://www.who.int/water_sanitation_health/water-quality/guidelines/chemicals/antimony.pdf, *Last accessed on* 24th August 2016.

[139] National Primary Drinking Water Regulations; Table of Regulated Drinking Water Contaminants: https://www.epa.gov/your-drinking-water/table-regulated-drinking-water-contaminants#Inorganic, *Last accessed on* 24th August 2016.

[140] M. Filella, N. Belzile, Y.-W. Chen, Antimony in the environment: a review focused on natural waters: II. Relevant solution chemistry, *Earth-Science Reviews*, 59 (**2002**) 265-285.

[141] A. Anjum, Adsorptive Removal of Antimony (III) Using Modified Montmorillonite: A Study on Sorption Kinetics, *Journal of Analytical Sciences, Methods and Instrumentation*, 02 (**2012**) 167-175.

[142] P. Navarro, J. Simpson, F.J. Alguacil, Removal of antimony (III) from copper in sulphuric acid solutions by solvent extraction with LIX 1104SM, *Hydrometallurgy*, 53 (**1999**) 121-131.

[143] Z. Wu, M. He, X. Guo, R. Zhou, Removal of antimony (III) and antimony (V) from drinking water by ferric chloride coagulation: Competing ion effect and the mechanism analysis, *Separation and Purification Technology*, 76 (**2010**) 184-190.

[144] M. Kang, T. Kamei, Y. Magara, Comparing polyaluminum chloride and ferric chloride for antimony removal, *Water Research*, 37 (**2003**) 4171-4179.

[145] M. Kang, M. Kawasaki, S. Tamada, T. Kamei, Y. Magara, Effect of pH on the removal of arsenic and antimony using reverse osmosis membranes, *Desalination*, 131 (**2000**) 293-298.

[146] T. Saito, S. Tsuneda, A. Hirata, S.y. Nishiyama, K. Saito, K. Saito, K. Sugita, K. Uezu, M. Tamada, T. Sugo, Removal of Antimony (III) Using Polyol-Ligand-Containing Porous Hollow-Fiber Membranes, *Separation Science and Technology*, 39 (**2004**) 3011-3022.

[147] M. Pena, X. Meng, G.P. Korfiatis, C. Jing, Adsorption Mechanism of Arsenic on Nanocrystalline Titanium Dioxide, *Environmental Science & Technology*, 40 (**2006**) 1257-1262.

[148] J.-K. Yang, S.-M. Lee, EDTA effect on the removal of Cu(II) onto TiO2, *Journal of Colloid and Interface Science*, 282 (**2005**) 5-10.

[149] W.S. Wan Ngah, L.C. Teong, M.A.K.M. Hanafiah, Adsorption of dyes and heavy metal ions by chitosan composites: A review, *Carbohydrate Polymers*, 83 (**2011**) 1446-1456.

[150] A. Pavlík, M. Semelová, J. John, K. Černochová, F. Šebesta, Treatment of spent NTA-based decontamination solutions, *Czechoslovak Journal of Physics*, 56 (**2006**) D673-D680.

[151] X. Guan, J. Du, X. Meng, Y. Sun, B. Sun, Q. Hu, Application of titanium dioxide in arsenic removal from water: A review, *Journal of Hazardous Materials*, 215–216 (**2012**) 1-16.

[152] U.G. Akpan, B.H. Hameed, Parameters affecting the photocatalytic degradation of dyes using TiO_2-based photocatalysts: a review, *Journal of Hazardous Materials*, 170 (**2009**) 520-529.

[153] D.S. Han, A. Abdel-Wahab, B. Batchelor, Surface complexation modeling of arsenic(III) and arsenic(V) adsorption onto nanoporous titania adsorbents (NTAs), *Journal of Colloid and Interface Science,* 348 (**2010**) 591-599.

[154] B. Mukhopadhyay, S. Lahiri, Adsorption of ^{125}Sb on alumina and titania surfaces, *Journal of Radioanalytical and Nuclear Chemistry*, 273 (**2007**) 423-426.

[155] H. Su, Q. Li, T. Tan, Double-functional characteristics of a surface molecular imprinted adsorbent with immobilization of nano-TiO_2, *Journal of Chemical Technology & Biotechnology*, 81 (**2006**) 1797-1802.

[156] S.M. Miller, M.L. Spaulding, J.B. Zimmerman, Optimization of capacity and kinetics for a novel bio-based arsenic sorbent, TiO_2-impregnated chitosan bead, *Water Research*, 45 (**2011**) 5745-5754.

[157] S.M. Miller, J.B. Zimmerman, Novel, bio-based, photoactive arsenic sorbent: $TiO_{(2)}$-impregnated chitosan bead, *Water Research*, 44 (**2010**) 5722-5729.

[158] X. Zhang, X. Zhao, H. Su, Degradation characteristic of TiO_2-chitosan adsorbent on Rhodamine B and purification of industrial wastewater, *Korean Journal of Chemical Engineering*, 28 (**2011**) 1241-1246.

[159] O.A.C. Monteiro Jr, C. Airoldi, Some studies of crosslinking chitosan–glutaraldehyde interaction in a homogeneous system, *International Journal of Biological Macromolecules*, 26 (**1999**) 119-128.

[160] H. Jonassen, A.-L. Kjøniksen, M. Hiorth, Stability of Chitosan Nanoparticles Cross-Linked with Tripolyphosphate, *Biomacromolecules*, 13 (**2012**) 3747-3756.

[161] F.-C. Wu, R.-L. Tseng, R.-S. Juang, A review and experimental verification of using chitosan and its derivatives as adsorbents for selected heavy metals, *Journal of Environmental Management*, 91 (**2010**) 798-806.

[162] E. Mirzaei B, A. Ramazani S. A, M. Shafiee, M. Danaei, Studies on Glutaraldehyde Crosslinked Chitosan Hydrogel Properties for Drug Delivery Systems, *International Journal of Polymeric Materials and Polymeric Biomaterials*, 62 (**2013**) 605-611.

[163] D. Reichenberg, D.J. McCauley, Properties of ion-exchange resins in relation to their structure. Part VII. Cation-exchange equilibria on sulphonated polystyrene resins of varying degrees of cross-linking, *Journal of the Chemical Society* (Resumed), (**1955**) 2741-2749.

[164] I.L. Jones, G. Carta, Ion exchange of amino acids and dipeptides on cation resins with varying degree of crosslinking. 2. Intraparticle transport, *Industrial & Engineering Chemistry Research*, 32 (**1993**) 117-125.

[165] N. Li, R.K. Thomas, A.R. Rennie, Effect of pH, surface charge and counter-ions on the adsorption of sodium dodecyl sulfate to the sapphire/solution interface, *Journal of Colloid and Interface Science*, 378 (**2012**) 152-158.

[166] U.Y. Özer, R.F. Bogucki, Equilibrium studies of antimony(III) chelates in aqueous solution, *Journal of Inorganic and Nuclear Chemistry*, 33 (**1971**) 4143-4153.

[167] B. Lothenbach, M. Ochs, H. Wanner, M. Yui, Thermodynamic Data for the Speciation and Solubility of Pd, Pb, Sn, Sb, Nb and Bi in Aqueous Solution (*JNC TN8400 99-01 1*), Japan Nuclear Cycle Development Institute, **January, 1999**.

[168] K.H. Gayer, A.B. Garrett, The Equilibria of Antimonous Oxide (Rhombic) in Dilute Solutions of Hydrochloric Acid and Sodium Hydroxide at 25^{O}, *Journal of the American Chemical Society*, 74 (**1952**) 2353-2354.

[169] X. Guan, J. Du, X. Meng, Y. Sun, B. Sun, Q. Hu, Application of titanium dioxide in arsenic removal from water: A review, *Journal of Hazardous Materials*, 215–216 (**2012**) 1-16.

[170] S.N. Lanin, E.V. Vlasenko, N.V. Kovaleva, F.T. Zung, The adsorption properties of titanium dioxide, *Russian Journal of Physical Chemistry A, Focus on Chemistry*, 82 (**2008**) 2152-2155.

[171] M. Kosmulski, The pH-dependent surface charging and points of zero charge: V. Update, *Journal of Colloid and Interface Science*, 353 (**2011**) 1-15.

[172] M. Kosmulski, The significance of the difference in the point of zero charge between rutile and anatase, *Advances in Colloid and Interface Science*, 99 (**2002**) 255-264.

[173] J.E. Gonçalves, Y. Gushikem, S.C. de Castro, Preparation and properties of antimony (V) oxide adsorbed on silica–titania mixed oxide, *Journal of Non-Crystalline Solids*, 260 (**1999**) 125-131.

[174] P.K. Dutta, A.K. Ray, V.K. Sharma, F.J. Millero, Adsorption of arsenate and arsenite on titanium dioxide suspensions, *Journal of Colloid and Interface Science*, 278 (**2004**) 270-275.

[175] M. Tella, G.S. Pokrovski, Antimony(III) complexing with O-bearing organic ligands in aqueous solution: An X-ray absorption fine structure spectroscopy and solubility study, *Geochimica et Cosmochimica Acta*, 73 (**2009**) 268-290.

[176] F. Liu, X.C. Le, A. McKnight-Whitford, Y. Xia, F. Wu, E. Elswick, C.C. Johnson, C. Zhu, Antimony speciation and contamination of waters in the Xikuangshan antimony mining and smelting area, China, *Environmental Geochemistry and Health*, 32 (**2010**) 401-413.

[177] K.A.M. Amin, M.i.h. Panhuis, Reinforced Materials Based on Chitosan, TiO_2 and Ag Composites, *Polymers*, 4 (**2012**) 590-599.

[178] F.A. Al-Sagheer, S. Merchant, Visco-elastic properties of chitosan–titania nano-composites, *Carbohydrate Polymers*, 85 (**2011**) 356-362.

[179] Legrand C.; Delville J., *Comptes rendus hebdomadaires des séances de l'Académie des sciences*, 236 (**1953**) 944.

[180] K.C. Gupta, F.H. Jabrail, Glutaraldehyde and glyoxal cross-linked chitosan microspheres for controlled delivery of centchroman, *Carbohydrate Research*, 341 (**2006**) 744-756.

[181] J. Kumirska, M. Czerwicka, Z. Kaczyński, A. Bychowska, K. Brzozowski, J. Thöming, P. Stepnowski, Application of Spectroscopic Methods for Structural Analysis of Chitin and Chitosan, *Marine Drugs*, 8 (**2010**) 1567-1636.

[182] H.N. Cheng, D.A. Smith, 13C NMR characterization of ethylene oxide/epichlorohydrin copolymer, *Die Makromolekulare Chemie*, 192 (**1991**) 267-276.

[183] M.J. Sullivan, Industrial applications of high-resolution solid-state 13C NMR techniques, *TrAC Trends in Analytical Chemistry*, 6 (**1987**) 31-36.

[184] H.-Q. Xie, J.-S. Guo, G.-Q. Yu, J. Zu, Ring-opening polymerization of epichlorohydrin and its copolymerization with other alkylene oxides by quaternary catalyst system, *Journal of Applied Polymer Science*, 80 (**2001**) 2446-2454.

[185] P.L. Smedley, D.G. Kinniburgh, A review of the source, behaviour and distribution of arsenic in natural waters, *Applied Geochemistry*, 17 (**2002**) 517-568.

[186] M.K. Sengupta, A. Mukherjee, M.A. Hossain, S. Ahamed, M.M. Rahman, D. Lodh, U.K. Chowdhury, B.K. Biswas, B. Nayak, B. Das, K.C. Saha, D. Chakraborti, S.C. Mukherjee, G. Chatterjee, S. Pati, R.N. Dutta, Q. Quamruzzaman, Groundwater Arsenic

Contamination in the Ganga-Padma-Meghna-Brahmaputra Plain of India and Bangladesh, *Archives of Environmental Health: An International Journal*, 58 (**2003**) 701-702.

[187] WHO, Guidelines for drinking-water quality - 4th ed, World Health Organization, Switzerland, **2011**.

[188] T.S.Y. Choong, T.G. Chuah, Y. Robiah, F.L. Gregory Koay, I. Azni, Arsenic toxicity, health hazards and removal techniques from water: an overview, *Desalination*, 217 (**2007**) 139-166.

[189] N. Nicomel, K. Leus, K. Folens, P. Van Der Voort, G. Du Laing, Technologies for Arsenic Removal from Water: Current Status and Future Perspectives, *International Journal of Environmental Research and Public Health*, 13 (**2016**) 62.

[190] K.B. Vu, M.D. Kaminski, L. NuÒez, Review Of Arsenic Removal Technologies For Contaminated Groundwaters (*ANL-CMT-03/2*), Argonne National Laboratory, Argonne, IL, **April 2003**.

[191] K.C.M. Kwok, L.F. Koong, G. Chen, G. McKay, Mechanism of arsenic removal using chitosan and nanochitosan, *Journal of Colloid and Interface Science*, 416 (**2014**) 1-10.

[192] C.-C. Chen, Y.-C. Chung, Arsenic Removal Using a Biopolymer Chitosan Sorbent, *Journal of Environmental Science and Health, Part A*, 41 (**2006**) 645-658.

[193] J. Cui, J. Du, S. Yu, C. Jing, T. Chan, Groundwater arsenic removal using granular TiO_2: integrated laboratory and field study, *Environmental Science and Pollution Research*, 22 (**2015**) 8224-8234.

[194] L. Ma, S.X. Tu, Removal of arsenic from aqueous solution by two types of nano TiO_2 crystals, *Environmental Chemistry Letters*, 9 (**2011**) 465-472.

[195] A.H. Fostier, M.d.S.S. Pereira, S. Rath, J.R. Guimarães, Arsenic removal from water employing heterogeneous photocatalysis with TiO_2 immobilized in PET bottles, *Chemosphere*, 72 (**2008**) 319-324.

[196] M. Rahim, M.R.H. Mas Haris, Application of biopolymer composites in arsenic removal from aqueous medium: A review, *Journal of Radiation Research and Applied Sciences*, 8 (**2015**) 255-263.

[197] M.H. Farzana, S. Meenakshi, Synergistic Effect of Chitosan and Titanium Dioxide on the Removal of Toxic Dyes by the Photodegradation Technique, *Industrial & Engineering Chemistry Research*, 53 (**2014**) 55-63.

[198] Y. Haldorai, J.-J. Shim, Novel chitosan-TiO_2 nanohybrid: Preparation, characterization, antibacterial, and photocatalytic properties, *Polymer Composites*, 35 (**2014**) 327-333.